$5

QEX

INCLUDING:

COMMUNICATIONS QUARTERLY

Forum for Communications Experimenters

May/June 2002

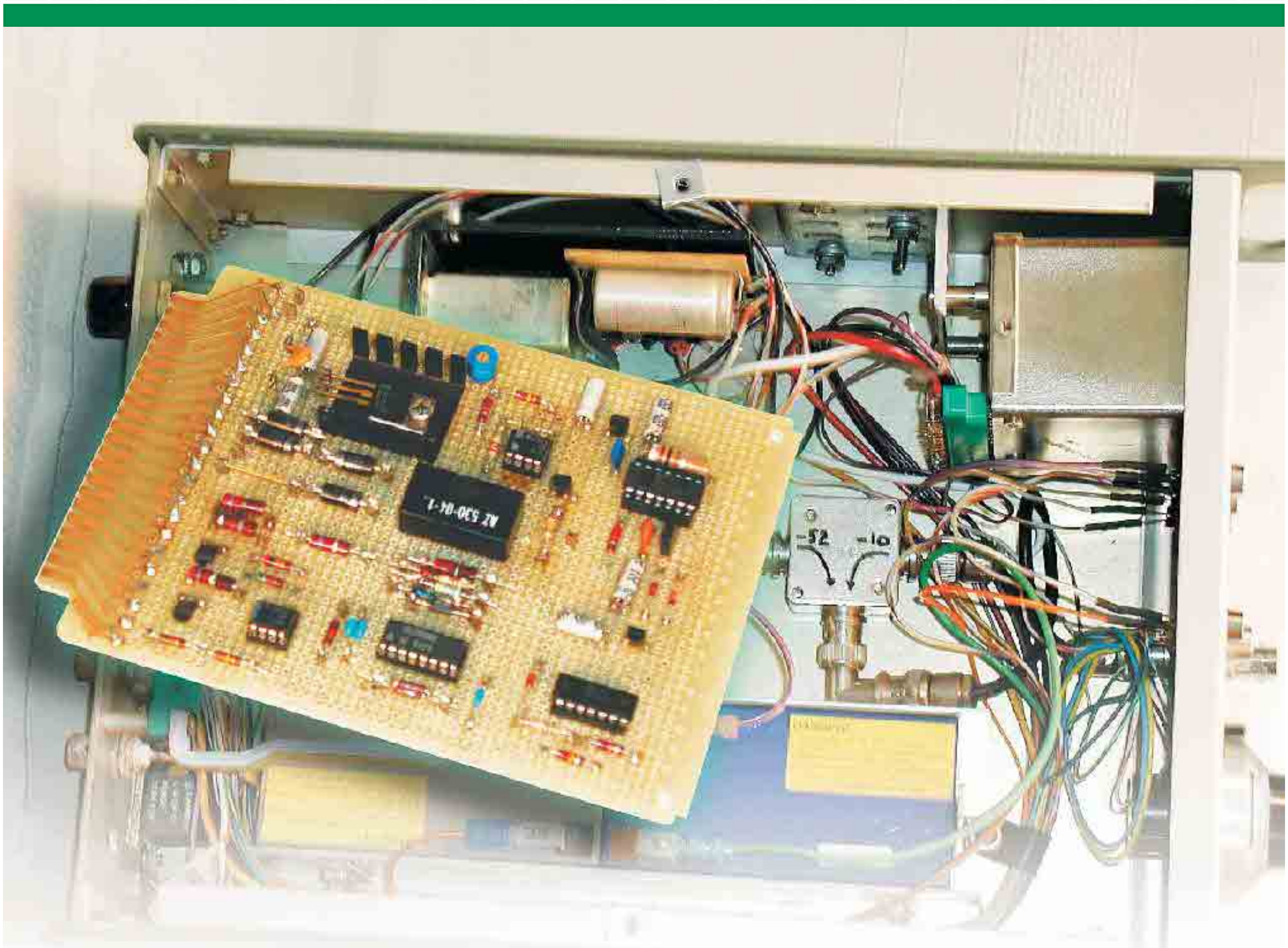

KJ6PO's 10-MHz Frequency Standard

ARRL The national association for AMATEUR RADIO

225 Main Street

Newington, CT USA 06111-1494

INCLUDING: COMMUNICATIONS QUARTERLY

QEX (ISSN: 0886-8093) is published bimonthly in January, March, May, July, September, and November by the American Radio Relay League, 225 Main Street, Newington CT 06111-1494. Yearly subscription rate to ARRL members is $24; nonmembers $36. Other rates are listed below. Periodicals postage paid at Hartford, CT and at additional mailing offices.

POSTMASTER: Send address changes to: QEX, 225 Main St, Newington, CT 06111-1494
Issue No 212

Mark J. Wilson, K1RO
Publisher

Doug Smith, KF6DX
Editor

Robert Schetgen, KU7G
Managing Editor

Lori Weinberg, KB1EIB
Assistant Editor

Peter Bertini, K1ZJH
Zack Lau, W1VT
Ray Mack, WD5IFS
Contributing Editors

Production Department

Steve Ford, WB8IMY
Publications Manager

Michelle Bloom, WB1ENT
Production Supervisor

Sue Fagan
Graphic Design Supervisor

David Pingree, N1NAS
Technical Illustrator

Joe Shea
Production Assistant

Advertising Information Contact:

John Bee, N1GNV, *Advertising Manager*
860-594-0207 direct
860-594-0200 ARRL
860-594-0259 fax

Circulation Department

Debra Jahnke, *Manager*
Kathy Capodicasa, N1GZO, *Deputy Manager*
Cathy Stepina, *QEX Circulation*

Offices

225 Main St, Newington, CT 06111-1494 USA
Telephone: 860-594-0200
Telex: 650215-5052 MCI
Fax: 860-594-0259 (24 hour direct line)
e-mail: qex@arrl.org

Subscription rate for 6 issues:

In the US: ARRL Member $24, nonmember $36;

US by First Class Mail: ARRL member $37, nonmember $49;

Elsewhere by Surface Mail (4-8 week delivery): ARRL member $31, nonmember $43;

Canada by Airmail: ARRL member $40, nonmember $52;

Elsewhere by Airmail: ARRL member $59, nonmember $71.

Members are asked to include their membership control number or a label from their *QST* wrapper when applying.

In order to ensure prompt delivery, we ask that you periodically check the address information on your mailing label. If you find any inaccuracies, please contact the Circulation Department immediately. Thank you for your assistance.

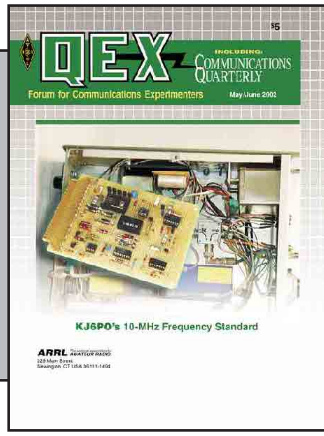

About the Cover

KJ6PO's wiring board floats above the chassis that normally contains it. The article begins on p 13.

Features

Columns

May/June 2002 *QEX* Advertising Index

Empirical Outlook

Freedom of Speech: An Awesome Responsibility

Many of us place a very high value on what we view as our inherent human rights to freedom of speech and of the press. While the framers of the US Constitution may have had certain ideas of what constituted speech, our Supreme Court has decided our rights extend to many different forms of expression.

One idea behind ensuring freedom of speech is to encourage people to discuss government openly and to get involved in governing themselves. Along with that goes an inherent right to be heard: due process. When it comes to radio regulations, you have many chances to exercise your free-speech and due-process rights and another chance is apparently about to present itself as I write this.

In a *Petition for Rulemaking* filed March 22, the ARRL asks the FCC to revise its Amateur Radio Service rules according to the modified Novice-band "refarming" plan approved by the League's Board of Directors in January. ARRL adoption of the plan followed the recommendations of the ARRL Novice Spectrum Study Committee, who surveyed the amateur community last year on the subject. We view this move as critical toward alleviating crowded conditions on 40 and 80 m and to efficient use of some of our HF spectrum. Reassignment of the 80, 40 and 15-m Novice CW bands is in the request.

If approved, the plan would expand the phone segments on 80 and 40 m by 25 kHz for Advanced and Extra license-holders and by 50 kHz for Generals. On 15 m, Advanced and Extra operators would not see any expansion but Generals would pick up an additional 25 kHz. No phone-segment changes are proposed for the other HF bands.

One important justification for expansion of phone bands is to make room for digital voice and video modes. The *Petition* also asks that current Novice and Tech-Plus license-holders be allowed to operate on 80, 40, 15 and 10-m General-class CW allocations at up to 200 W output power. Such a move would allow more room for popular, narrow-band modes such as PSK31.

We encourage you to make yourselves heard by filing comments in favor of the *Petition* during the open comment period. You may file comments on this and other petitions via the FCC's Electronic Comment Filing System (**www.fcc.gov/e-file/ecfs.html**). A complete copy of the ARRL *Petition* is available on our Web site at **www.arrl.org/announce/regulatory/refarm/**.

Yours truly will moderate a Digital Voice Forum at the Dayton Hamvention this year on Sunday, May 19. For details of that and other interesting Hamvention activities, visit **www.hamvention.org**. Be there—you haven't lived until you've been to Dayton!

In This Issue

Bob Kopski, K3NHI, brings us his improvements on a wattmeter design that first appeared in the June, 2001 *QST*. Tony Lymer, GM0DHD, has some notes about how to tune your antenna without creating too much QRM.

Randy Evans, KJ6PO, describes a precise 10-MHz reference source. Warren Bruene, W5OLY, took us seriously when we stated that theory needed to be supported by measurement. Warren writes about some new tries at measuring the source impedance of an HF tuned power amplifier. Bill Young, WD5HOH, delivers a combination of two popular technologies in his regenerative superheterodyne receiver project.

Peter Chadwick, G3RZP, initiates some informed discussion of receiver dynamic range by asking, "How much do we need?" He then uses real operating conditions to answer the question, illustrating some limitations of traditional dynamic-range specifications along the way.

Paul Wade, W1GHZ, returns with another neat microwave antenna system involving passive reflectors. Tom Cefalo, Jr, W1EX, contributes a bias-tee design. The tee is handy for supplying power through your coax to things like remotely mounted preamplifiers.

Apologies to those of you who looked hard for the review of the AADE L/C Meter model II B in the last issue! It is here this time in Ray Mack, WD5IFS's *Out of the Box*. In *Tech Notes*, Peter Bertini, K1ZJH, brings us Rudy Severns, N6LF's follow-on notes about RF current on flat conductors. In *RF*, Zack Lau, W1VT shows how to cobble up some nifty tuning knobs in a machine shop–*73, Doug Smith, KF6DX;* **kf6dx@arrl.org**.

An Advanced VHF Wattmeter

A few modifications greatly increase the utility of a popular QST *project*

By Bob Kopski, K3NHI

This homebrew instrument is based on the RF power meter project by Wes Hayward, W7ZOI and Bob Larkin, K7PUA that appears in *QST*, June 2001. The reference article presented a simple instrument for the homebrewer to measure RF power well through VHF. I decided to build it but with some personalization and enhancements to better suit my needs and interests. When I sent a thank-you note to the designers for the original article along with some information about mine, Wes encouraged me to do this write-up. "Go for it!" were his words.

If you compare this version with the original, the first thing you'll see is that this box has a lot more stuff on the front panel (see Fig 1). There are now two meters and more controls. Almost all these additions are associated with the instrument's low-frequency signal processing or "support" circuitry. Except for the inclusion of a convenient 20-dB slide-switch attenuator, the original RF section is unchanged.

The reference instrument incorporated a built-in analog meter and provision to connect an external DVM. It also utilized a conversion chart to relate meter readings to RF power. I wanted both digital and analog displays built in for both an accurate, high-resolution numeric power readout and a trend indicator at the same time. I also wanted to avoid using a calibration chart if possible.

All that's needed to accomplish these goals is a custom face for the analog meter plus some circuitry for the scaling and level-shifting of internal signals. This signal processing results in direct dBm readings on both meters—no conversion chart is needed. The DVM also displays the correct polarity sign. There's neither rocket science nor smoke and mirrors here folks: It's all done simply with op amps and resistors! The schematic tells all (See Fig 2).

In the process of designing these basic circuit functions, it occurred to me that other simple additions would add a lot to the utility of the instrument. Thus, the project grew "on the fly." One of these extras is a gain-change option that includes an external OFFSET control for the analog display.

This enhancement switches the ana-

25 West End Dr
Lansdale, PA 19446

log meter reading from 10 dB to 1 dB per major division. The panel mounted OFFSET control allows any readable input power level to be brought into the analog meter's range. It's really a "slide-back" function. Thus, this meter can change from a display calibrated in dBm to a relative-dB reading. At the same time, the DVM continues to read the absolute power level in dBm. It's the best of both worlds, I think. Since the analog panel meter responds reasonably quickly, it's like a "souped-up" trend meter, good for tuning filters and such.

Another addition is the incorporation of a separate signal output scaled to 10 mV/dB. This permits easy, calibrated swept displays. Thus, one could sweep filters, for example, and have a very usable scope display with a known, convenient log-scale response.

In conjunction with this last feature, I included a switched output-bandwidth filter as shown. This was done with the speculation that such a feature might be useful with varying sweep speeds. I've yet to fully exercise this feature; but while I was drilling panel holes, I drilled for this too!

In hindsight, I realize now I might also have included a battery-check switch to monitor the two internal 9-V batteries via the analog meter, since it's there anyway. (The DVM can't measure it's own 9-V battery supply.) Oh well—I'm sure some of you can think of other things that you might like to add for your own interests, as well.

Construction

I do not have high ambient RF levels and so I do not need a cast metal enclosure. I used a standard 3×4×5-inch Minibox instead. This has enough room for the panel, internal circuits and two 9-V batteries (see Fig 3).

My RF subassembly is shown in Fig 4. I used the original "dead-bug" technique on PC-board material. You can incorporate the 20-dB attenuator, some other operational feature or just simply follow the reference article. In any case, I suggest you stick with the original design details immediately surrounding the AD8307 IC. I did and all works well.

The signal-processing circuitry can be built in almost any way you prefer, including the original dead-bug or "ugly" way. I like to use PC "hole-board" for this sort of thing (see Fig 5). I've included the layout of this assembly for those who'd like to try it (see Figs 6 and 7). Here are a few tips to go with it.

The board is cut from RadioShack (#276-168). This hole-board has a pre-etched IC pattern and buses on it. The addition of some wire jumpers makes it a complete custom circuit board ready for the components. Please note that two wire jumpers pass *under* the IC socket. Be sure to install these *before* the 14-pin socket goes in. Probably the most important assembly guidance I can offer is to carefully study the layout for parts placement and *count holes*!

When your board assembly is done, carefully remove the flux, and inspect it thoroughly with a magnifying lens for short circuits. This step helps keep smoke levels under control for me. I prefer to dress the lead wires through some strain-relieving insulated wire loops through unused holes in the board, as shown in Fig 5. I also prefer to twist together multiple wires that go to a particular panel part such as switches.

I suggest you do some simple open and short checks on the completed subassembly with an ohmmeter before powering it up and connecting the reasonably expensive AD8307 on the RF subassembly.

I generally lay out instrument panels with a drawing program and print them using an inkjet printer on good-quality paper. I stick the paper to the metal box with rub-on glue stick. Not

Fig 1—The advanced VHF power meter includes a digital panel meter for accurate, high-resolution power readings plus an analog meter for trend information. The instrument bottoms out around –76 dBm but calibration very good above –70 dBm.

Fig 2 (right)—A schematic of the VHF power meter. All resistors are 1/4 W, 5% carbon components unless otherwise indicated. All capacitors are ceramic unless otherwise indicated.

C1—15 pF
C2—0.01 µF
C3-C6—0.1 µF
C7—1000 pF
C8-C10—10 µF, 16 V, tantalum
C11—0.012 µF
C12—150 pF
C13—1 µF, 35 V, tantalum
D1, D3—1N4148 diode
D2—LED, as preferred
IC1—AD8307 log amplifier, (Kanga, 3521 Spring Lake Dr, Findlay OH 45840)
IC2—LM324 quad op amp
IC3—78L05 5-V regulator
M1—200 mV DVM (PM-128 panel meter from Circuit Specialists, Hosfelt or as preferred)
M2—0-1 mA meter (JAMECO 171897 or as preferred)
R1, R3—61 Ω, selected
R2—248 Ω, selected
R4—53 Ω, selected
R5—470 Ω
R6—6.8 Ω
R7, R27, R28—5.6 kΩ
R8—1 kΩ trimmer (Digi-Key 36G13-ND or equivalent)
R9—3.6 kΩ
R10—1 kΩ
R11, R20—3.3 kΩ
R12—22 kΩ
R13—820 Ω
R14—200 Ω trimmer (Digi-Key 36G22-ND or equivalent)
R15—47 kΩ
R16—750 Ω
R17, R24—100 Ω trimmer (Digi-Key 36G12-ND or equivalent)
R18—100 k Ω trimmer (Digi-Key 36G15-ND or equivalent)
R19—68 kΩ
R21, R25—3.9 kΩ
R22—5 kΩ 10-turn potentiometer (Mouser 594-53411502 or equivalent)
R23—220 Ω
R26—2 kΩ trimmer (Digi-Key 36G23-ND or equivalent)
SW1, SW3—DPDT mini-toggle
SW2—SPDT mini-toggle switch
SW4—DPDT slide switch (Digi-Key SW333-ND or equivalent)
BNC connector
Phono jack
Box—3×4×5-inch Minibox
9 V—Eveready 522 or equivalent
9 V—6 AA cells and holder
Battery connectors (2)
PC Board-double sided
Holeboard RadioShack #276-168
14-pin IC socket

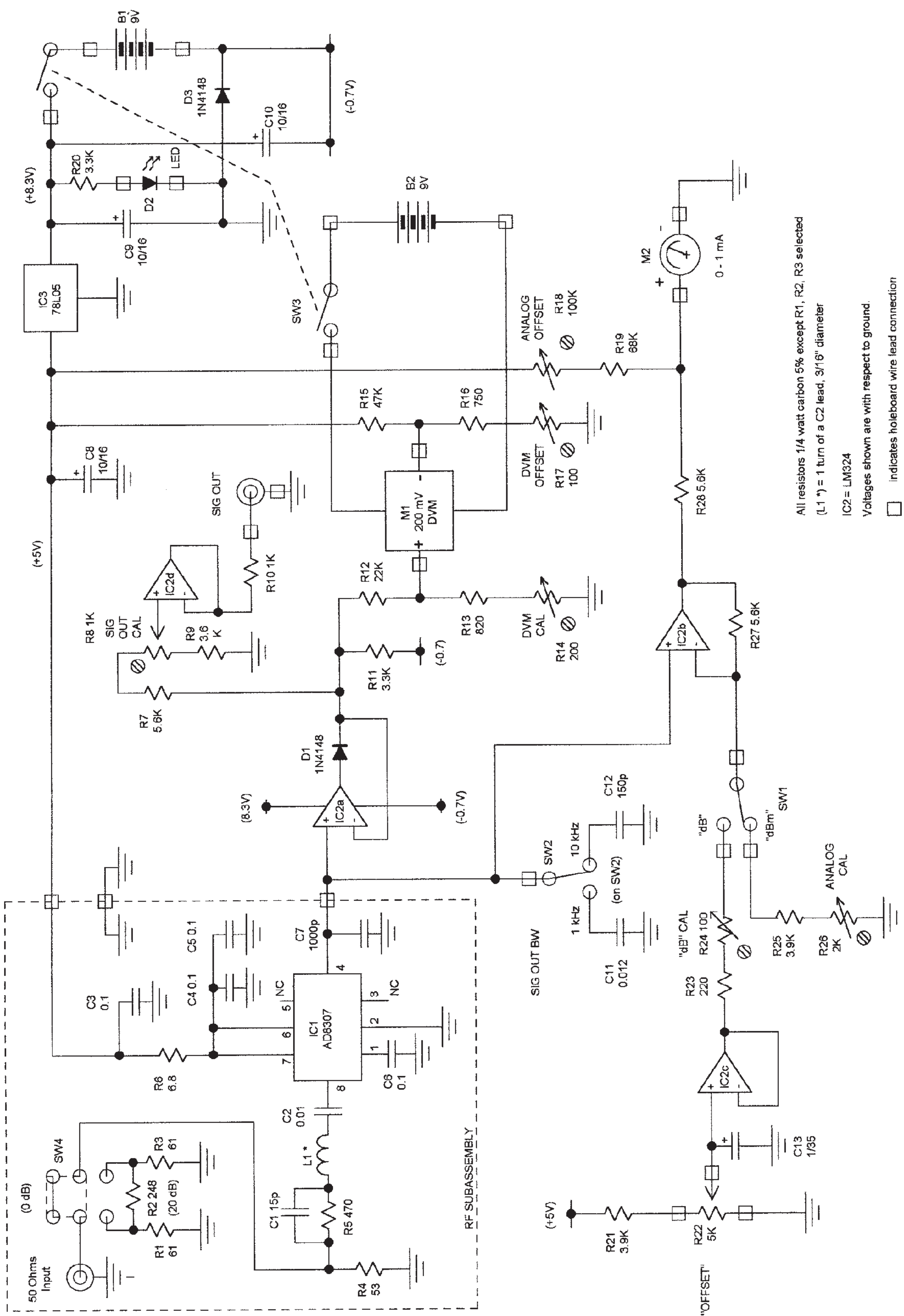
All resistors 1/4 watt carbon 5% except R1, R2, R3 selected
(L1 *) = 1 turn of a C2 lead, 3/16" diameter
IC2 = LM324
Voltages shown are with respect to ground.
Indicates holeboard wire lead connection
RF SUBASSEMBLY
SIG OUT BW
50 Ohms Input

all glue sticks work well for this. I do this process twice.

The first printout—an expendable template—includes the drill centers and other mechanical details. I use it as a drill and cutout guide. When all this heavy-duty work is done, I remove the paper by soaking in water. Some drying, deburring and solvent-cleaning of the Minibox readies it for the second and final panel paper.

The second paper is printed with the nice-looking panel details but without the construction markings. Once this paper is glued in place, I overlay it with Contact-brand clear film for durability. The final task is to cut away the overlay papers where the metalwork holes are; that is easily done with an X-acto knife and a #11 blade. The result is as you see it. It looks good, don't you think? By the way, the analog meter scale is drawn and printed the same way (see Fig 8).

I use *TurboCad* in both my electronic and R/C aeromodeling hobbies; but I think other drawing programs should be usable as well. You can also download a useable demo version of *TurboCad* from **www.turbocad.com**.

Calibration and Operation

I suggest you review the discussion in the reference article concerning RF sources for calibration of your power meter. Once you have a suitable known source, start by calibrating the DVM. Trimmer R14 sets the gain so that an x-dB change in input power results in an x-mV change in DVM reading; that is, so that 1 mV = 1 dB. Trimmer R14 locates this result in the right place. In other words, R17 makes the DVM read the power level correctly while R14 makes changes in power level read correctly.

This same idea holds for the analog panel meter, as well. With switch SW1 in dBm mode, R26 sets the rate of change of the display while R18 makes a given power level read correctly. When all is done properly, both digital and analog meters display both the same power level and the same changes in power level.

Incidentally, these adjustments are usually iterative in nature. Expect to go back and forth a few times between each cal and offset trimmer pair until convergence occurs and the respective meter reads correctly across its full range.

As above, trimmer R24 sets the gain for the analog meter in the decibel mode. In this case, though, there is no associated offset trimmer. Rather, the panel mounted OFFSET pot is used as needed in the application of the instrument. In use, it is adjusted to establish a reference reading on the analog face (usually "0") for *any* useable in-

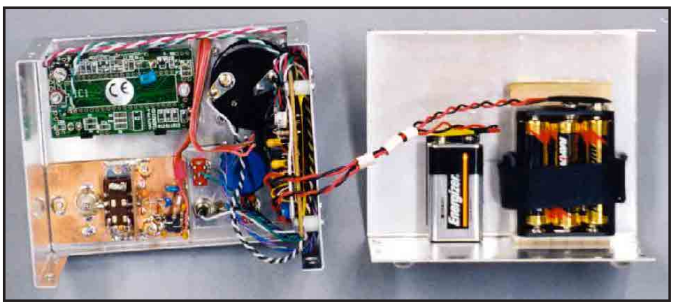

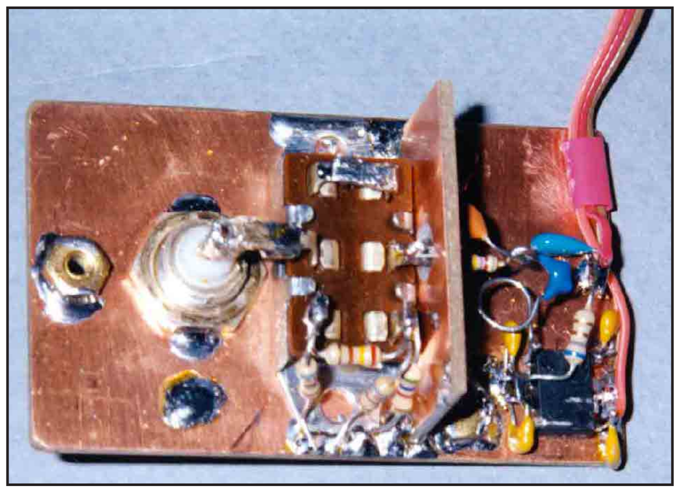

Fig 3 (above)—What's inside the 3×4×5-inch Minibox: A 9-V battery for the DVM, six AA cells power everything else. The batteries are held in place with hook and loop tape.

Fig 4(right)—The RF subassembly uses dead-bug construction and includes a 20-dB step attenuator. It is held against case front inside by three screws. A three-wire cable connects it to the signal-processing board.

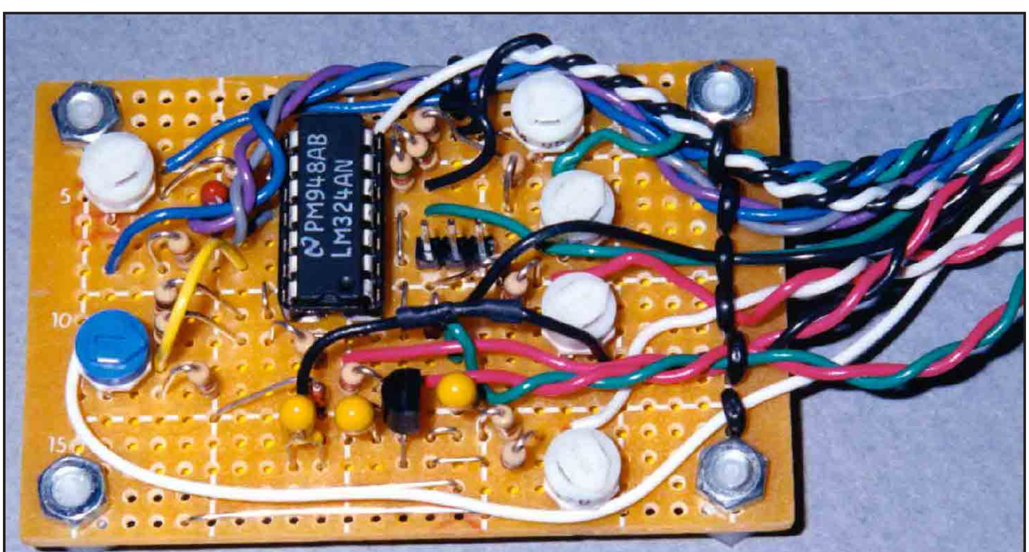

Fig 5—The signal-processing board is based on a RadioShack printed hole board. Notice the centrally located three-pin connector used to interface with the RF subassembly.

put power. Thus in this mode, the decibel readings of the analog meter are no longer referenced to a milliwatt (dBm), but it can accurately display power changes in decibels OFFSET control. In effect, it becomes an expanded-scale meter. Because this pot must accommodate a very wide signal range, a multiturn pot is highly recommended. Mine is a three-turn component, but 10 turns would be better, and such components are more readily available.

Trimmer R7 calibrates the output signal to the design value of 10 mV/dB—it's another gain trim. Notice that this signal output rests on a non-offsetable dc value. That is usually of no consequence in application. If you'd prefer to ac-couple this output (0.1 µF should do the trick), or add an offset-control circuit, feel free to do so.

Conclusion

Notice how it's possible to expand upon one basic project and customize it for your own needs and interests. It's funny how some would call that bashing! Now it's your turn to duplicate or customize your own rendition of this VHF wattmeter. Maybe there's a published homebrew item you'd like to embellish or simplify. As the man said, "Go for it!"

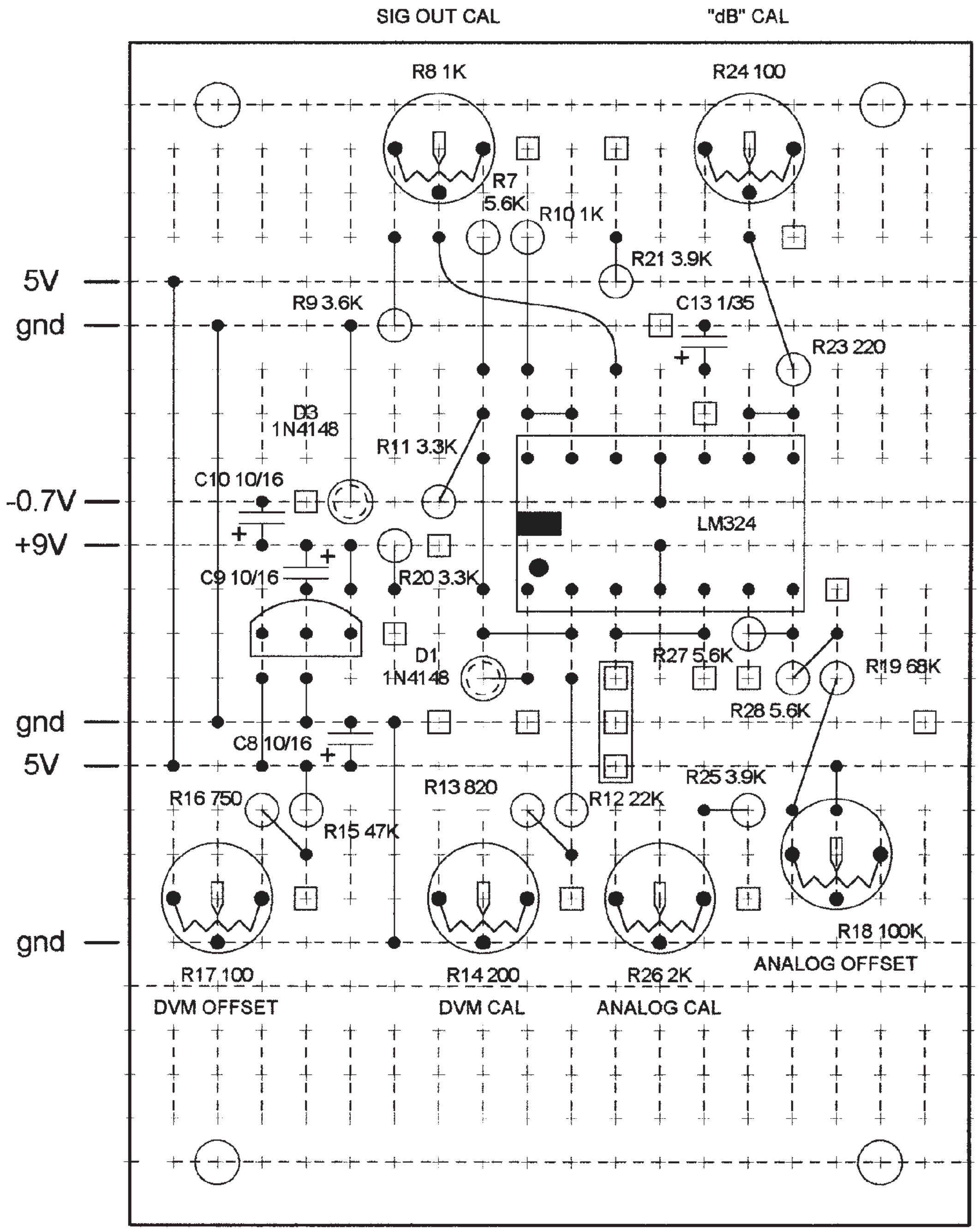

Fig 6—Component placement diagram for the signal processing board. This view is from the component side with the printed-circuit traces and lands from the other side shown dotted.

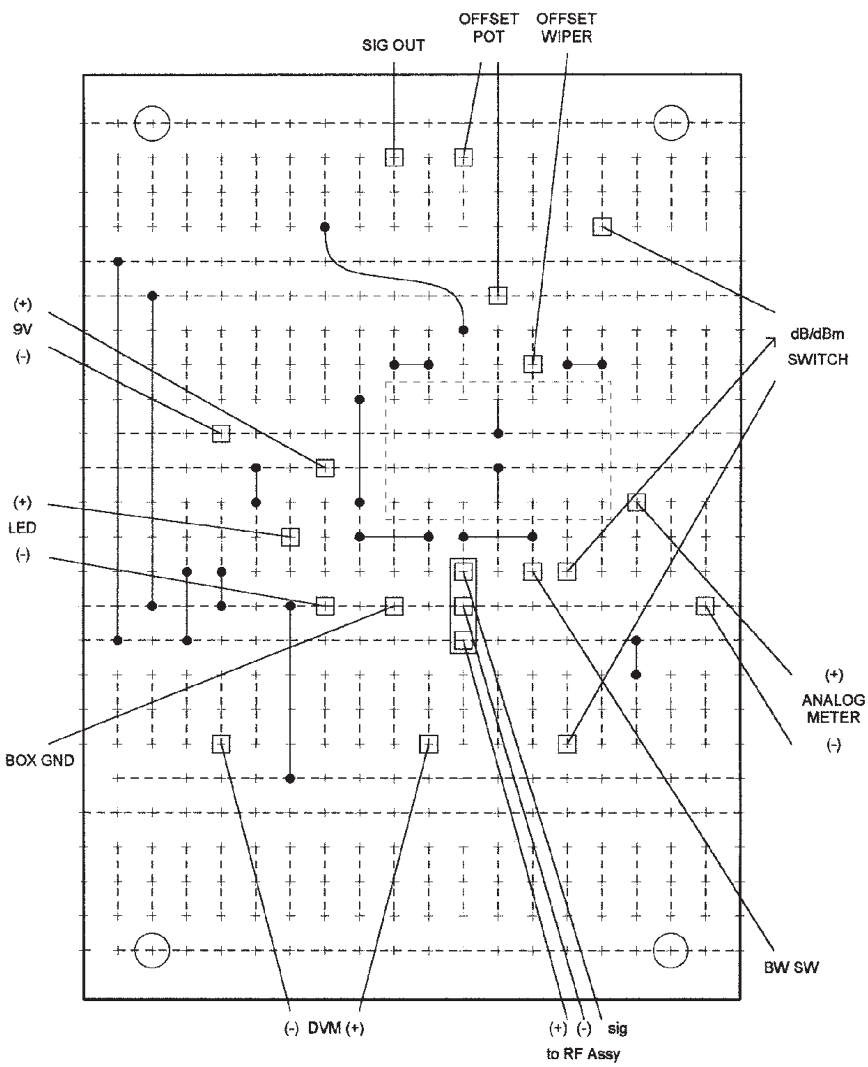

Fig 7—Wiring and jumper diagram for the signal-processing board. This view is from the component side with the printed-circuit traces and lands from the other side shown dotted.

Fig 8—The original 0-1 mA meter scale has been replaced with an eye-catching and functional power-meter scale. The replacement scale was made using a drawing program and an inkjet printer.

I'd be happy to correspond with *QEX* readers. Please include a SASE with any correspondence for which you'd like a reply.

Bob is a recently retired Senior Design Engineer with a major defense contractor. He holds BSEE and BSEP degrees from Lehigh University.

As a life-long electronics, ham and aeromodeling hobbyist, he routinely combines all three pursuits for the fun of it. His Technician ticket dates to about 1959, at which time he wanted to homebrew 6-meter radio-control equipment for R/C aeromodels. He still routinely flies on six and has operated fixed and mobile stations on six. He has published an original six-meter H-T. His broadly based aeromodeling interest dates to the early 1950s, but he has specialized in electrically powered R/C models for over 25 years. He has been a Contributing Editor to Model Aviation magazine for over 19 years with a monthly column devoted to the electric flying specialty Additionally, he has published many construction articles covering both model aircraft design and aeromodeling related electronics. He enjoys it all! □□

A Quiet Antenna Tuner

This idea adapts the common directional-coupler/ power-meter method for quiet tuning of antennas.

By Tony Lymer, GM0DHD

This SWR meter allows antenna tuning to take place with less radiated power than a conventional meter. The power radiated during tune-up is reduced to less than a hundredth of the original value, while the sensitivity of the reflected-power measurement is not reduced. As by-products, the transmitter is presented with an excellent match during the tune-up process and the antenna tuner's components are subjected to considerably less stress during the tuner-adjustment procedure than they would be with a conventional design.

When resonating or adjusting the match of an antenna, most operators reduce the output of their transmitter to a level that is just enough to measure the SWR accurately. They do this because they know that a signal will be radiated from the antenna during the adjustment. The signal may well interfere with other users of the band, so it is undesirable RF pollution. A typical low-power setting on the power meter of many antenna-tuning units (ATUs) is about 5 W. Below this power, the reflected-power measurement becomes less accurate because the meter sometimes cannot be fully deflected. But 5 W can go a long way! I have personally contacted over a hundred countries with 5 W on CW, some in each of the continents. So even adjustments at low power have the potential to interfere.

There are many ways to measure an RF impedance with less applied RF power; it is just that people don't always use them. The reflection coefficient of an antenna system can be measured with about 1-mW and a laboratory-grade network analyzer, but not many hams own one of those. It can also be measured with a milliwatt or two of pink noise. This has the advantage that it causes little obvious interference, as the radiated power is of low spectral density and may be indistinguishable from other noise in the victim's receiver. A third alternative might be to use a sensitive RF power meter and a directional coupler in the conventional manner. If the power meter can measure, say, –20 dBm full scale, then with a 20-dB coupler, only 1 mW is required at the antenna. Again, it would be uncommon

16, Gerson Park, Greendykes Rd
Broxburn, West Lothian
Scotland EH526PL UK
tony_lymer@agilent.com

for radio amateurs to own such equipment.

One common way of adjusting an ATU, or even a newly built antenna, is to radiate the full carrier power and adjust for minimum reflected power on the SWR meter. While this is not recommended, it is certainly quite common and can be heard every day on the HF bands.[1] When I operated with a W3EDP antenna (an 85-foot end-fed wire and a 17-foot counterpoise), I found that I had to retune the ATU for every band change. Furthermore, the ATU was in a different room than the radio, and it took a little while to complete the matching process. I must admit to feeling a little guilty at radiating a strong carrier close to the QRP calling frequencies, so I set out to find a technical improvement that would reduce the radiated power during tuning.

The method presented uses a common form of SWR meter, and simply swaps two of the connections. The principle was first described by Underhill and Lewis in 1979 (see Reference 1). They were mainly interested in avoiding detection while tuning antennas in military situations. They wanted to reduce the power radiated from the antenna during tuning operations. Their article suggests using the receiver to measure very low levels of reflected power, instead of a diode detector and moving-coil meter. This is an excellent idea, but it would not work with many amateur transceivers, where the transmitter and receiver cannot both be used at the same time. Part of their solution can be used by radio amateurs, though, and it is described below.

Details

Fig 1 shows the conventional method of measuring SWR on a transmission line between the transmitter and an antenna or ATU. The diagram shows power levels for a 20-dB coupler. A transmitter with an output of 100 W will provide the antenna with 99 W and 1 W will be coupled to a power detector circuit. This circuit would typically be a diode detector and a moving-coil meter. The power detector must have a resistor, matching the system's characteristic impedance, to terminate the output port of the direction coupler. This resistor is typically 50 or 75 Ω.

If the antenna reflects any power, it will be measured on a similar power detector connected to the other dual-directional-coupler port. The problems with this arrangement are that interference is caused during the tune-up process, and the transmitter may be affected by the power reflected from the antenna. Many modern transmitters begin to reduce the output power to protect the PA devices when the SWR rises above about 3:1. The reflected power has a maximum value of 0.99 W (99 W attenuated by the coupling factor).

Fig 2 shows the arrangement suggested by Underhill and Lewis. The transmitter and reflected power detector have been swapped. The transmitter still has 100 W output, but 99% of this power is dissipated in the dummy load. Only 1W is applied to the antenna. Any reflected power returns to the reflected power detector without attenuation, so the detector measures 1 W maximum for an infinite SWR. The sensitivity of the measurement has not altered, but only 1 W was applied to the antenna in the second case. The radiated interference has been reduced by the coupling factor—in this case, 20 dB. Furthermore, if the antenna has infinite SWR, the transmitter is protected since only 1/10,000 of the 100 W is reflected back to the transmitter in the ideal case.

Various circuits for SWR meters have been popular over the years; not all are suitable for quiet tuning. One by David Stockton, GM4ZNX, is popular with constructors in the UK because it is simple and has good accuracy. This power meter is based on a dual directional coupler, so it is ideal for modification as a quiet tuner. The coupling factor is determined by the number of turns on the transformers. With a ferrite core and reasonably compact layout, the number of turns is an integer equal to the number of times the wire passes through the aperture of the core, so the coupling factor is accurate and stable. Various people have adapted this design and there is a very good description of a similar coupler in *The 2000 ARRL Handbook*. Page 22.38, Fig 22.71, shows full constructional details. The schematic, Fig 22.73 on p 22.39, also shows a suitable low-power detector. The two designs differ in the number of turns on the transformers used in the coupler and in the cores used for the transformers.

Stockton used 12 turns and had a coupling factor of 21.58 dB. The ARRL design uses 40 turns and has a coupling factor of 32.04 dB. Either design can be modified to work as a quiet tuner, but the ARRL design is more suitable for power levels exceeding 100 W; both require a dummy load of adequate power rating for the full transmitter power. Either core is said to be suitable for

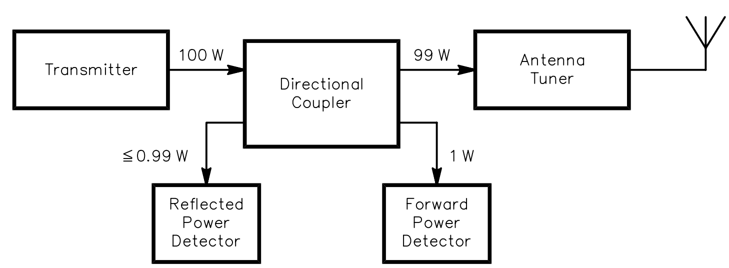

Fig 1—Conventional dual direction coupler-based on an SWR meter.

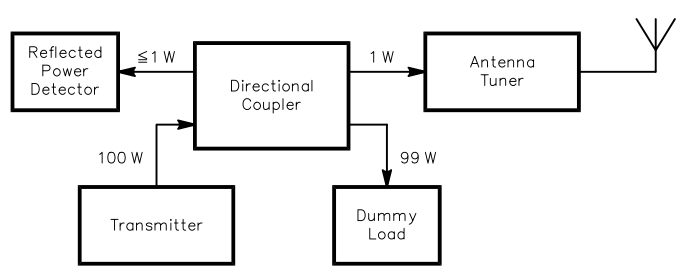

Fig 2—SWR meter converted to a quiet tuner.

[1](This is certainly *not* recommended with SWR protected transceivers that reduce output with high SWR, where minimum reflected power might coincide with minimum power output. With such equipment, the ATU is often tuned for maximum power output.—*Ed.*)

powers up to 100 W. For lower power levels, a simpler directional coupler can be made on a single "binocular" core. The construction of a miniature coupler is described below.

Construction

A quiet tuner could be built in two ways. One employs a switch or relay to swap the transmitter for the reflected power detector. Then the meter can be put into quiet mode for ATU adjustments. Otherwise, it functions as a normal through-line meter.

Another way would be to build a dedicated SWR meter for quiet tuning. In this case, the switch can be omitted and the signal will always be attenuated by the coupling factor. This would simpler to build, and would be useful for lengthy spells of adjustment such as tuning a mobile whip.

Figure 3 shows an SWR meter that can be switched between a conventional through-line power meter and a quiet tuner, although in this form it only measures reflected power.

The resistor in series with the meter could become a variable resistor. The forward power is easily measured by disconnecting the antenna. The open-circuit termination reflects the entire power incident on the antenna port. (Although, a low-inductance short-circuit would be more accurate, especially at the higher frequencies.) The variable resistor can then be adjusted for full-scale deflection on the meter.

If a continuous display of forward power is desired, a second diode detector and meter with switched gain can be connected across the dummy load.

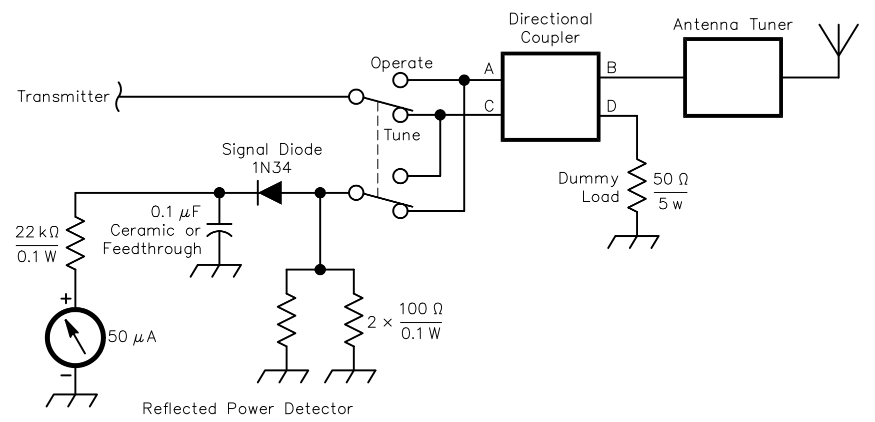

Fig 3—A schematic of the quiet tuner.

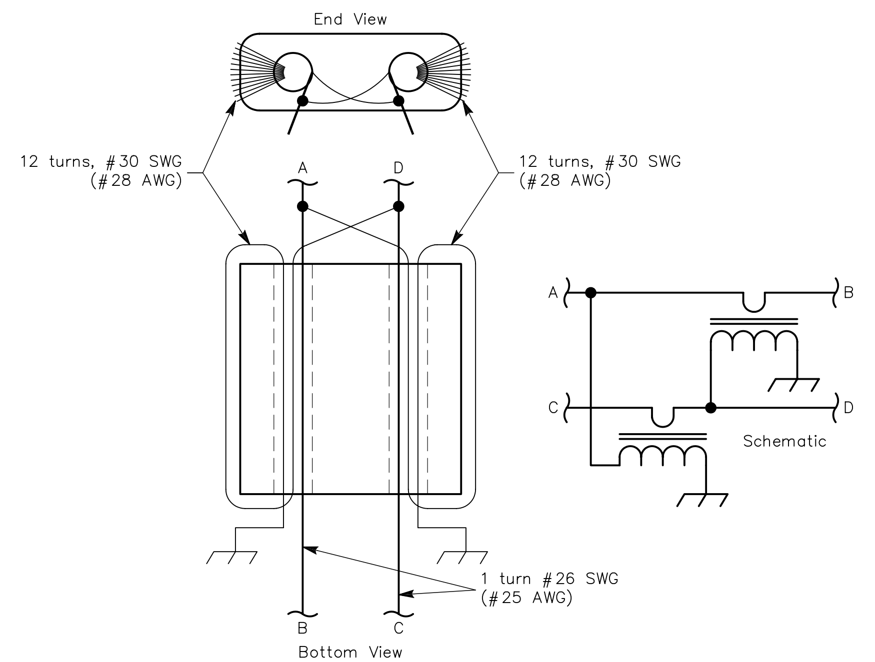

Fig 4—Construction of a directional coupler.

Directional Coupler

The directional coupler is the heart of the Quiet Tuner. This simple, small, directional coupler only uses one magnetic core. It has a wide bandwidth and adequate power handling for QRP operation.

The wire diameters are not critical. The core is a Fair-Rite 2843000302. It works happily at 5 W, but I haven't tested it above this level because I don't have a high-power transmitter. Similar cores of 43-type material ($\mu \approx 850$), or near equivalents, may be used.

Fig 4 shows the construction of a suitable low-power directional coupler. Higher-power versions can be found in References 2 and 3. Start with the two 12-turn windings of insulated wire. The number of turns is the same as the number of times the wire goes through the hole. The two single-turn windings are added next: Just slide a piece of wire through each hole. The other "half" of the turn is completed by the circuitry you connect to the coupler. A different coupling factor requires a different number of turns. The coupling factor is $20 \log_{10}(N)$, where N is the number of turns. The completed coupler is shown in Fig 5.

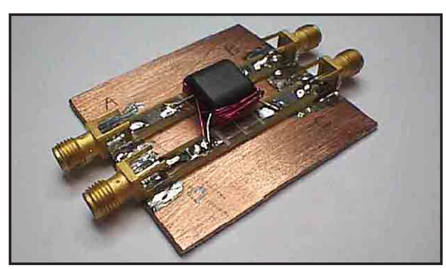

Fig 5—A completed directional coupler.

Directional-Coupler Performance Data

The measurements in Table 1 were made with an Agilent 8753C, network analyzer. The accuracy of the coupling factor is worth a mention. The directivity of a coupler is defined as follows: Directivity is the ratio (in decibels) of the power output at a coupled port, when power is transmitted in the desired direction, to the power output at the same coupled port when the same amount of power is transmitted in the opposite direction.

Table 1—Performance of the Directional Coupler

Measured Performance	*1.8 MHz*	*50 MHz*	*146 MHz*
Through path loss	0.14 dB	0.09 dB	0.12 dB
Coupling factor	–21.6	–21.7	–21.6
Directivity	31	31	17

The measured directivity drops off at 146 MHz, although useful performance is still possible up to 50 MHz. The directivity affects the accuracy of the matching of an antenna tuned for minimum reflected power. The practical limit is probably about –20 dB.

Conclusion

The quiet tuner design does not eliminate the problems of interference caused by ATU adjustments being performed at high power, but it may reduce the level of some of them. It has useful advantages in that the transmitter is matched throughout the process. The reduced transmitter power level also means that ATU components are stressed by much reduced voltages during tune-up, which should improve their reliability significantly, particularly in automatic antenna tuners.

References

1. "Quiet Tuning of Antennas," Underhill M.J. and Lewis P.A., *Electronics Letters*, 4th Jan 1979, Vol. 15, No. 1.
2. "A Bi-directional In-line Watt-meter," David Stockton, *SPRAT* 61, pp 10-13.
3. "Tandem Match," *The 2000 ARRL Handbook* (Newington, Connecticut: ARRL, 1999), p 22.38. □□

A Laboratory-Grade 10-MHz Frequency Standard

Accuracy of 1 part in 10^9 is achievable at a very reasonable cost.

By Randy Evans, KJ6PO

This article describes a laboratory-grade 10-MHz frequency standard. You can build it at relatively low cost, if you are able and willing to search for parts at flea markets or using Internet resources such as e-Bay, where I obtained many of my parts. Through judicious scrounging, I was able to build the frequency standard for less than $150.

This article may also be a guide for developing a frequency standard using different components that the builder may have available. I hope that the detailed architecture and circuits presented provide sufficient information to allow easy modification of the design. Some individuals may have no need for a frequency standard but may want to use the battery charger and protection circuits in a battery UPS system for emergency communications.

2688 Middleborough Circle
San Jose, CA 95132
randallgrayevans@yahoo.com

The key features of the frequency standard are:

- An "ovenized" 10-MHz quartz-crystal oscillator for low drift and high accuracy.
- Battery backup for at least four hours using readily available lead-acid batteries.
- A battery-disconnect circuit to prevent excessive discharge of the batteries.
- Over-voltage protection to prevent damage to the ovenized (read "expensive") oscillator in case of power-supply failure.
- Front-panel indicators that show the status of the frequency standard and its associated circuits.

Notice in Fig 1 that the frequency standard has several LED indicators and adjustment controls on the front panel. There is an AC POWER LED to indicate the presence of ac mains voltage. An OVEN ON LED indicates that the 10-MHz oscillator oven is heating up and has not yet reached its operating temperature. A lit CHARGE LED shows that the batteries are fully charged and are in the "floating" state. A POWER LOSS LED lights when ac power has been lost and battery backup is in use. A RESET push-button switch resets the POWER LOSS indicator. A VERNIER ADJUST permits very small frequency adjustments to the frequency standard. A

COARSE FREQUENCY adjustment initially sets the frequency standard, and there is a 10-MHz OUTPUT monitor jack.

Overview

Fig 2 is a block diagram of the frequency standard showing the major functional circuit elements. The frequency standard permits builders to modify the design by deleting or adding circuits as desired. This article describes each circuit in detail, so builders can understand the functioning of each stage and therefore understand the ramifications and complexity of modifying any of them.

The frequency standard is designed to work from the ac power, with a battery backup for short power outages of up to four hours. The backup time could be easily increased through minor redesign and by using larger batteries, if desired. I use two 12-V dc, 1.2-Ah lead-acid batteries. To protect the batteries from excessive discharge, I include a circuit to disconnect the batteries if their voltage drops below a certain threshold. An over-voltage protection circuit on the power-supply line to the ovenized oscillator electronics prevents catastrophic failures that would be caused by excessive voltage in case of a voltage-regulator failure.

A circuit detects the loss of ac mains power so that the user is aware of any power failures that may have occurred. A front-panel LED indicates that such a power loss has occurred. The LED remains in a latched condition until a front-panel RESET button is pushed.

An electronic fine-frequency adjustment is also provided to allow frequency adjustment down to at least 1 part in 10^{10}. The adjustment range is approximately ±1 Hz.

The output of the 10-MHz frequency standard goes to a 10-dB coupler and then to a four-way power divider. The output of the coupler goes to the front-panel monitor connector for test and calibration purposes. The output of the four-way power divider goes to rear-panel connectors for distribution to various pieces of test equipment; for example, frequency counter, signal generators and so forth.

A schematic of the entire frequency standard is shown in Fig 3. A plug-in wiring board was used to construct all the circuits for ease of modification and testing. The circuits were developed individually over time rather than all circuits being designed and tested at once. This was most efficient for me, since time was not readily available for a concentrated effort.

10-MHz Quartz Crystal Oscillator

The 10-MHz ovenized oscillator used in this project is an HP 10811A module. It uses an SC-cut crystal that achieves drift rates of less than 5 parts in 10^{10} per day. It can be easily set to an initial accuracy of around 1 part in 10^{11}. However, it is more economical to use the more readily available, albeit older, HP 10544 frequency-reference oscillator. While not quite as stable as the HP 10811, it is accurate enough for all but the most demanding applications. The pin connections, power requirements and form factor are identical to those of the HP 10811. In my case, I initially used the HP 10544A until I came across a used HP 10811A. Once one was found, it was a simple matter to replace the HP 10544A with the HP 10811A and calibrate the unit.

It is not strictly necessary that these particular HP oscillators be used. I have other 10-MHz oscillators that would work just as well, but they have different form factors, connectors and pin connections. The basic principals for the frequency standard are still applicable—only the packaging must be changed to suit other devices. I hope this article provides enough information to facilitate adaptation for other oscillator types.

Fig 1—Photo of frequency-standard front panel.

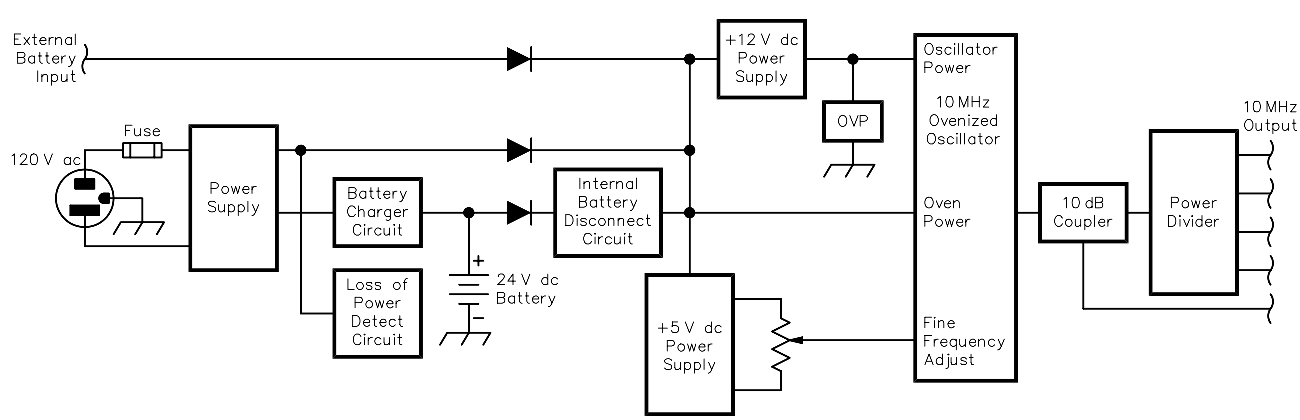

Fig 2—10-MHz frequency-standard block diagram.

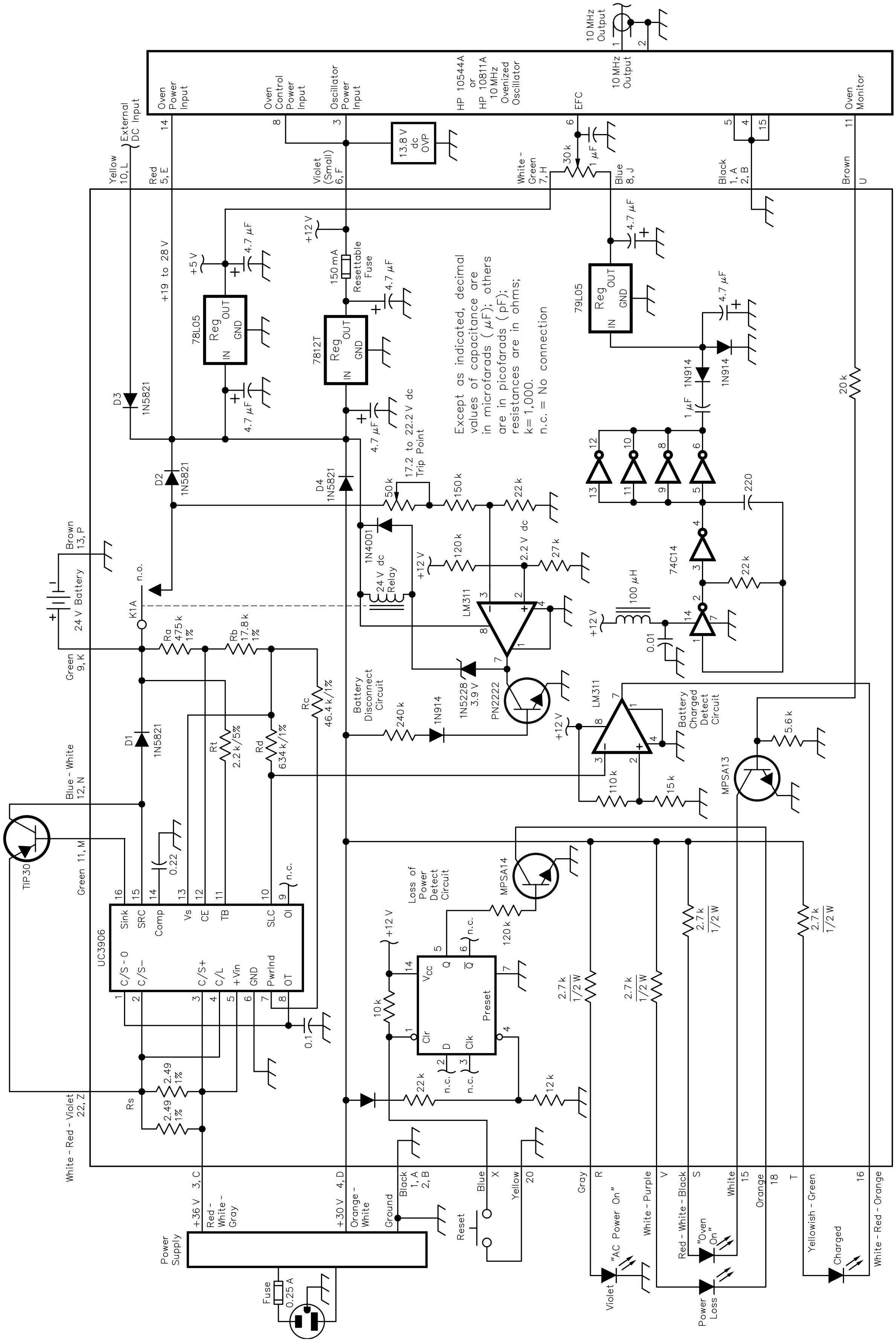

Fig 3—Frequency-standard schematic.

AC Power Supply

The power supply is a 24-V dc, 0.5-A surplus unit that was modified for 30 V dc output. The schematic with the modifications is presented in Fig 4 for those that wish to build their own. The 36-V dc output is from the unregulated filter capacitor and is used as the input to the battery charger's regulator circuit.

Alternative power-supply designs are certainly possible, perhaps using a high-voltage, three-terminal regulator for simplicity. The type of supply is not critical; what is needed is a regulated output at 29-30 V dc and an unregulated 30-36 V dc output. The highest output voltage of the battery charger is set at 28.8 V dc during the charge state. It is necessary that the regulated output of the ac power supply be at least 0.1 V greater than this to insure that the battery charger provides power only to the battery, and not to the rest of the circuit. This is the purpose of diodes D2, D3 and D4. D2 will be back-biased if the regulated power-supply output voltage is greater than the battery charger's output voltage, thus preventing any current draw from the charger circuit for the rest of the circuit.

Once the ac power is lost, diode D2 becomes forward-biased and provides power from the battery to the rest of the circuit. Schottky diodes are used to minimize the diode voltage drop; they exhibit a V_F of approximately 0.2 V dc, compared with silicon diodes that would have voltage drops in the 0.7-V dc range. This extends the battery backup time correspondingly.

12-V dc Regulator Circuit

The 12-V dc power supply is required for the electronics in the 10-MHz crystal oscillator and for the bias and monitor circuits in the frequency reference. It is a simple three-terminal linear regulator powered from the oven supply (20 to 30 V dc). The ac supply, if present, powers the oven; the battery-backup circuits power it if the ac lines fail.

An over-voltage protection circuit set at 13.8 V is used on the 12-V line, since a regulator failure could take this line up to 30 V. Such an event would be catastrophic to the 10-MHz oscillator and to my pocketbook, should it occur. I put a current-limiting device in the 12-V line to prevent an over-current condition should the over-voltage protection turn on. While a fuse would have been perfectly acceptable in this use, I used a thermally "resettable" device called a Polyswitch, which opens at around 150 mA.[1]

Bias Supply Circuits

The ovenized oscillator requires ±5 V dc to control the fine frequency adjustment using the electronic frequency control (EFC) input on the 10-MHz crystal oscillator module. The current requirements are extremely low. The +5-V dc requirement is met by a three-terminal regulator (78L05) circuit running from +12-V dc. The –5 V dc requirement is met by using a multivibrator circuit that is ac coupled to a negative voltage rectifier and doubler, followed by a three-terminal negative regulator (79L05) circuit.

Battery Charger Circuit

The battery-charger circuit is based upon a Unitrode (now Texas Instruments) UC3906 sealed lead-acid battery charger IC. The design of the charger circuit is largely based upon Unitrode application notes.[2, 3] An Excel spreadsheet that automates the design based upon the Application Note is available.[4] The results of the battery-charger-

[1]Notes appear on page 21.

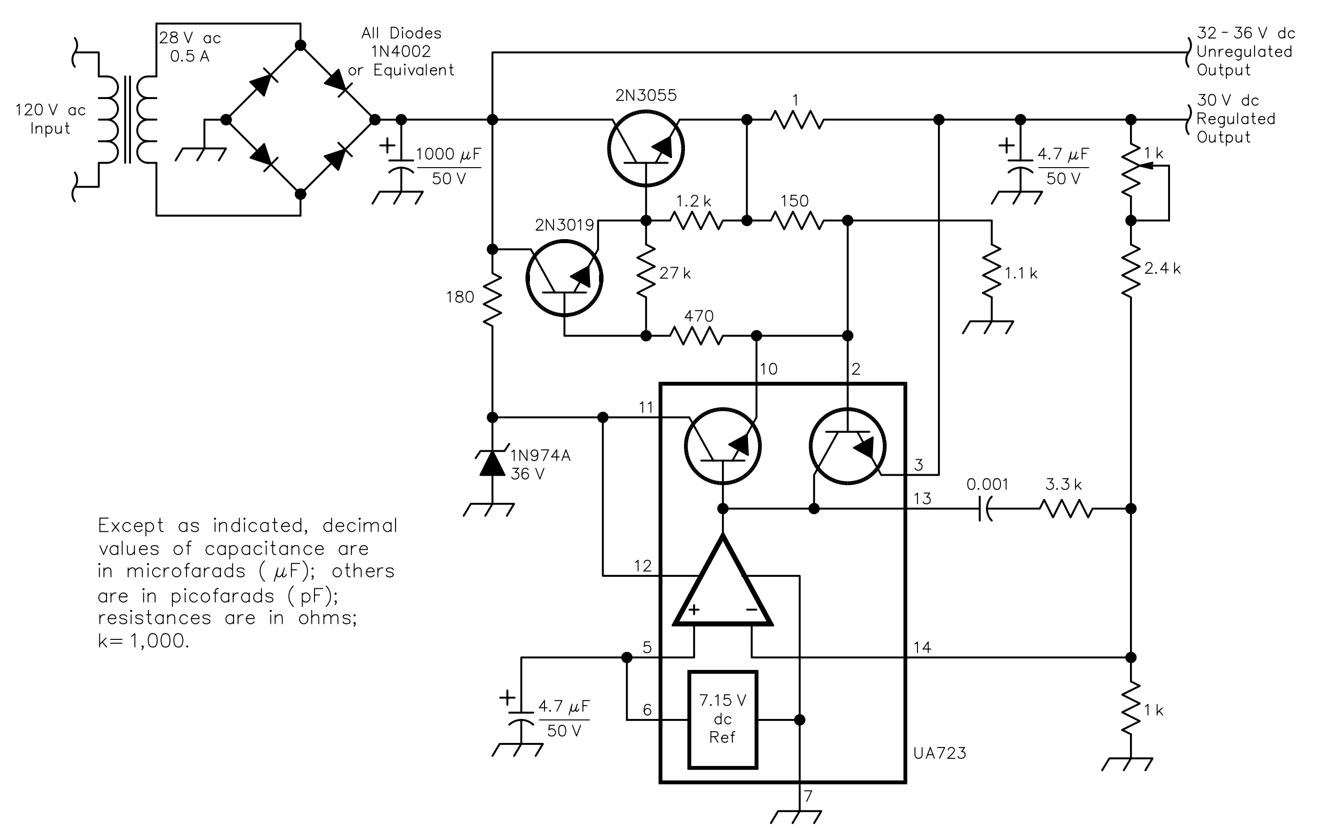

Fig 4—AC power-supply schematic.

design spreadsheet, along with all applicable formulas, are shown in Fig 5. A reference drawing of the Unitrode battery charger IC, upon which the spreadsheet is based is shown in Fig 6.

Readers should refer to the referenced Application Notes for specific design details of the UC3906 battery charger. In addition, the voltages used for the charge and float voltages, 2.4 and 2.25 V/cell, were obtained from gel-cell design manuals of the Globe Battery Division of Globe-Union.[5, 6]

The design of the battery-charger circuit shown in is based upon using two 12-V dc, 1.2 Ah lead-acid batteries in series. At a nominal current of 270 mA for the frequency-standard circuits, most drawn by the oven itself, this allows for greater than four hours of backup.

The charger IC works as shown in the state diagram shown in Fig 7. When the circuit is first switched on, the state of the IC depends upon the battery voltage and the battery-current draw. If the battery voltage is below V_t when the

From Unitrode Application note SLUS186—September 1996

Input Data:

Number of cells	N	12		
Charge voltage		2.4	Volts/cell	
Float voltage		2.25	Volts/cell	
Charge threshold voltage		1.7	Volts/cell	
Battery Capacity (C)		1.2	amp hours	
Maximum Battery Charge Rate		14.15	% of C	
Trickle Current Ratio		0.5	% of C	
Input Voltage	Vin	36	Volts	
Reference Voltage	Vref	2.3	Volts	
Transistor β, minimum	β	50		
Transistor maximum current	Icmax	1	Amp	
Divider current. Recommend 50 µA to 100 µA	Id	50	µA	when at Vf

Calculations:

Charge Threshold Voltage	Vt	20.40	Volts	N*Chrg threshold voltage
Over Charge Voltage	Voc	28.80	Volts	N*Charge Voltage
Float Voltage	Vf	27.00	Volts	N*Float Voltage
Transition Voltage from State 1 to State 2	V12	27.36	Volts	0.95Voc
Transition Voltage from State 3 to State 1	V31	24.30	Volts	0.9Vf
Maximum charge current	Imax	0.1698	Amps	C*Max Charge Rate
Over charge terminate threshold	Ioct	0.01698	Amps	Imax/10
Trickle Current	It	0.006	Amps	C*Trickle Charge Ratio

	Rc	46.0	Kohms	= Vref / Id
	Rsum	494.0	Kohms	Ra + Rb = (Vf –Vref) / Id
	Rd	631.2	Kohms	Rd = 2.3VRsum/(Voc –Vf)
	Rx	42.9	Kohms	Rx = Rc||Rd
	Ra	476.3	Kohms	Ra = (Rsum + Rx) (1 – 2.3V/
Vt)				
	Rb	17.7	Kohms	Rb = Rsum – Ra
	Rs	1.5	ohms	Rs = 0.25V/Imax
	Rt	2.18	Kohms	Rt = (Vin – Vt – 2.5V) / It
	PD of Rt	0.079	Watts	(Vin – Vt – 2.5)^2 / Rt
	Re	1690.0	ohms	(Vin – 2.2)/(Icmax/β)
	PD of Driver	119.9	mw	(Vin – Vbe)*Ib – Re* Ib^2

Notes

Battery over charge voltage is around 2.4 to 2.7 volts/cell
Battery float voltage is 2.25 to 2.30 volts/cell
Battery charge threshold voltage is typically 1.3 to 1.7 volts/cell
Imax is *bulk charge rate; e.g., C/4, range from C/20 to C/3*
Battery temperature range is nominally 0° to +50°C
Battery self discharge rate is typically 2% to 5% a month.
Diode D1 prevents reverse current flow.

Fig 5—Battery-charger design spreadsheet.

unit is turned on, the charger IC will go into state 4, the trickle-charge state. In this state, a very small current is sent through the battery until V_t is reached, at which point the IC charger goes to the bulk-charge state, state 1. Note: If the battery voltage is greater than V_t when first turned on, the charger IC goes immediately to state 1 (V_t<$V_{battery}$<V_{31}) or state 3 ($V_{battery}$>V_{31}), depending upon the initial battery voltage.

In the bulk-charge state, the IC goes into a constant-current mode at the maximum charge rate (I_{max}). Once the battery voltage reaches the over-charge voltage (V_{oc}), the IC goes to the over-charge state, state 2. In this state, the IC is in a constant-voltage mode, V_{oc}. As the battery charges, its current draw slowly drops until it reaches the current over-charge termination value, I_{oct}. At this point, the IC switches the battery charge voltage to the float voltage, V_f, and remains in this state so long as the ac supply is available. If the battery drops below V_{31} at any time, the charger IC will go back to the bulk-charge state, state 1. This should not occur unless power is lost and the battery is discharged; that is, once ac power is restored and the IC senses the battery voltage is below V_{31}.

The input section of the spreadsheet shows the parameters selected for the design. The important cell parameters are the charge voltage per cell and the float voltage per cell, which are 2.4 and 2.25 V per cell, respectively. These typical values for lead-acid batteries should maximize the battery life. The charge-threshold voltage is the voltage at which the battery should be lightly charged before bulk charging is attempted, and it is set at 1.7 V per cell. The maximum charge rate is set to approximately 14 %

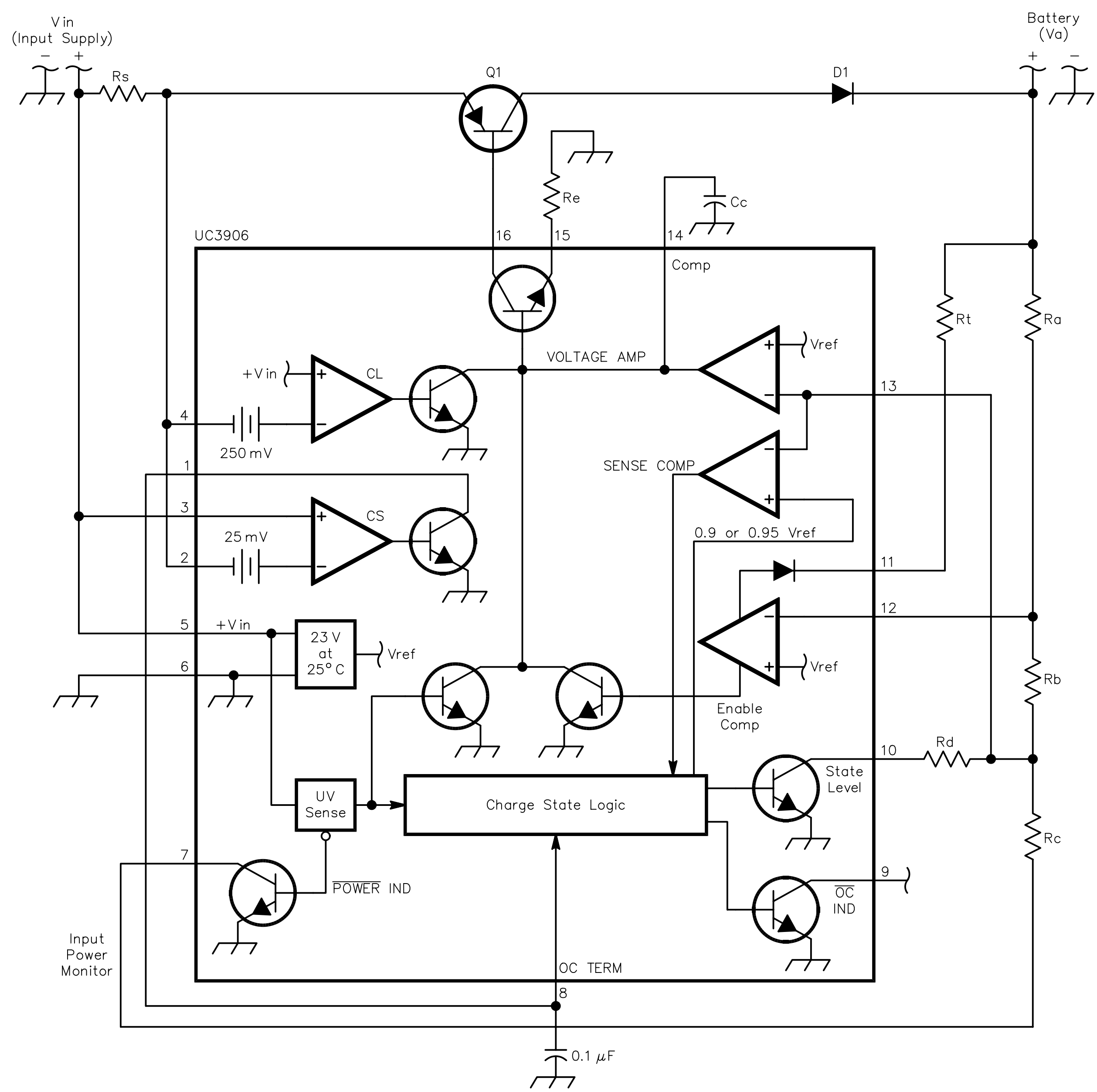

Fig 6—Unitrode UC3906 battery-charger circuit.

of the battery capacity. This was somewhat arbitrarily selected to prevent the power supply from going into current limiting while charging the battery at maximum rate and supplying current to the oscillator circuits. It is not a good idea, in any event, to rapidly charge any lead-acid battery if the battery life is to be maximized, particularly if the battery temperature is not directly monitored to prevent overcharging. The UC3906 does compensate the charging voltages for ambient temperature variations (–2.3 mV/°C per cell) but it does not have provision to directly monitor battery temperature.

Based upon a 24-V dc battery system (a 12-cell battery), the previous cell voltages reflect an overcharge voltage of 28.8 V, a float voltage of 27.0 V and a charge-threshold voltage of 20.4 V. The state level control (SLC) output (pin 10) on the UC3906 is used to detect when the battery is fully charged. That is, when the charger IC has gone into state 3, the float-charge state. The SLC pin only goes low when the charger IC is in state 3, therefore this pin is taken into the input of an LM311 comparator.

The comparator is used to detect when the SLC pin goes below approximately 1 V dc and then turns on the CHARGED LED to indicate that the battery is fully charged. Notice that an emitter resistor (R_e) shown in the Unitrode Application Note was not used in this design but is included in the spreadsheet for completeness.

Loss-of-Power Detection Circuit

The loss-of-power circuit is used to detect the loss of ac power, hence it indicates when the frequency standard has been on battery backup. A 74C74 flip-flop circuit latches the loss-of-power event. Under normal ac-powered conditions, the preset input is held high by the presence of 30 V dc, which is derived from the ac mains. The clear input is held high as long as the batteries are charged and the loss-of-power RESET button is not pushed.

Once ac power is lost, the preset input goes low because the 30 V dc is removed and the 74C74 Q output latches to the high output state. Since the 74C74 is powered by the battery, it remains in this state through the power outage and after the ac power returns. At that time, the POWER LOSS LED lights and stays on to indicate that ac power had been lost until the RESET button is pushed. Once the RESET button is pushed, the 74C74 is cleared and the LED goes off.

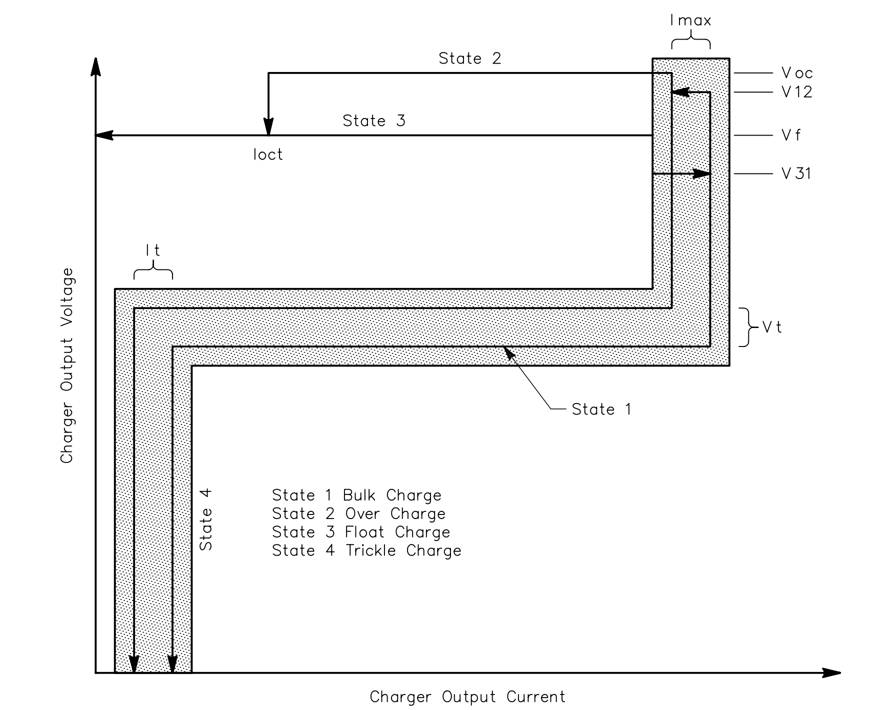

Fig 7—Battery-charger state diagram.

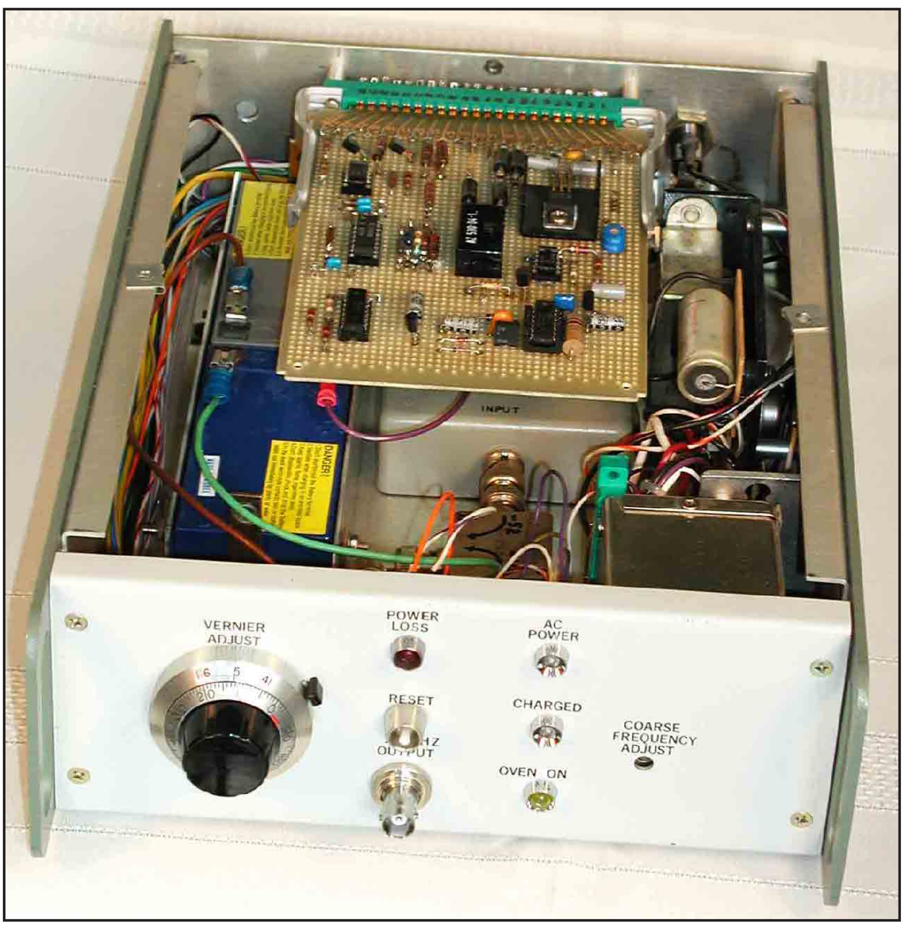

Fig 8—Top view of chassis with wiring board.

Battery-Disconnect Circuit

The battery-disconnect circuit is used to prevent excessive discharge of the battery. It monitors the battery voltage and disconnects the battery load once the voltage drops below an adjustable threshold value—around 20 V dc. Once the battery-disconnect relay opens, it cannot be closed until the ac power returns. Once the ac power returns, the power supply's +30 V dc output will switch on the PN2222 transistor, which causes the battery-disconnect relay to pull in, and the charger circuits will start charging the battery. At this point, the relay will remain pulled in until the ac power is again lost and the battery fully discharges below the threshold voltage.

Construction

The frequency standard was housed in a metal chassis that was obtained at a local flea market. The chassis used is 3.5×9×12.25 inches (HWD). A plug-in wiring board was used for most of the circuitry, as shown in Fig 8. The wiring board is a Vectorboard model 3662 (4.5×6.5 inches with 0.042-inch-diameter holes). This board mates with an industry standard 44-pin connector (0.156-inch spacing, Vector P/N R644) and uses connector-mounted card guides (Vectorboard BR27D). Most of the components were mounted and wired using mini-clips from Vector that are pushed into the Vectorboard. I used point-to-point wiring because no high frequencies are involved and parts placement and wiring is not critical.

A plug-in wiring board was used since the design was completed over a lengthy period and many circuit modifications were made before the design was finalized. A printed circuit board would have been impractical under these conditions, but one could certainly be done now if desired. A picture of the wiring board alone is shown in Fig 9. A view of the chassis without the wiring board and with all major components labeled is shown in Fig 10.

Calibration

Calibration of the 10-MHz frequency reference can be quite a challenge if the full potential of the frequency standard is to be realized. Ideally, it requires a calibration standard that is accurate to at least an order of magnitude better than the capability of the 10-MHz frequency standard. This would require a calibration standard accurate to at least 1 part in 10^{10}, which is an atomic frequency standard. Few individuals will likely have access to an atomic frequency standard.

Fortunately, there are several practical approaches to accurately calibrating the frequency reference. I built a frequency-calibration standard that uses LORAN C to achieve accuracy of 1 part in 10^{11} or better.[7] This is the primary approach I use to calibrate my frequency standard. While relatively straightforward, the LORAN C frequency calibrator becomes a project itself.[8] That approach will likely appeal only to the purists.

W4LTU describes a technique for using WWV to achieve accuracy of 1 part in 10^9 or better.[9] While this is a technique familiar to many users, it does require care to achieve an accuracy of 1 part in 10^8 or better: The frequency difference between the two standards must be less than 0.1 Hz at 10 MHz. This

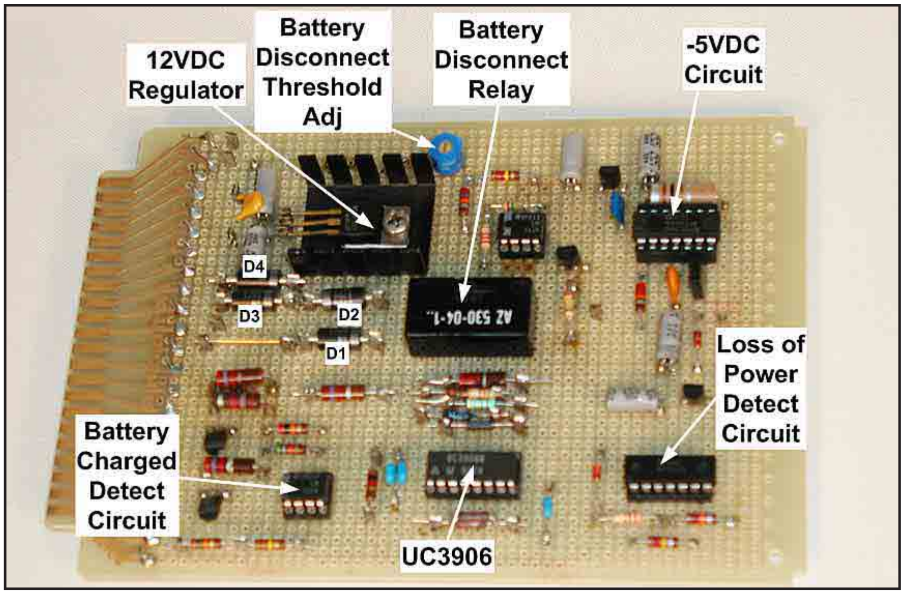

Fig 9—Wiring-board construction.

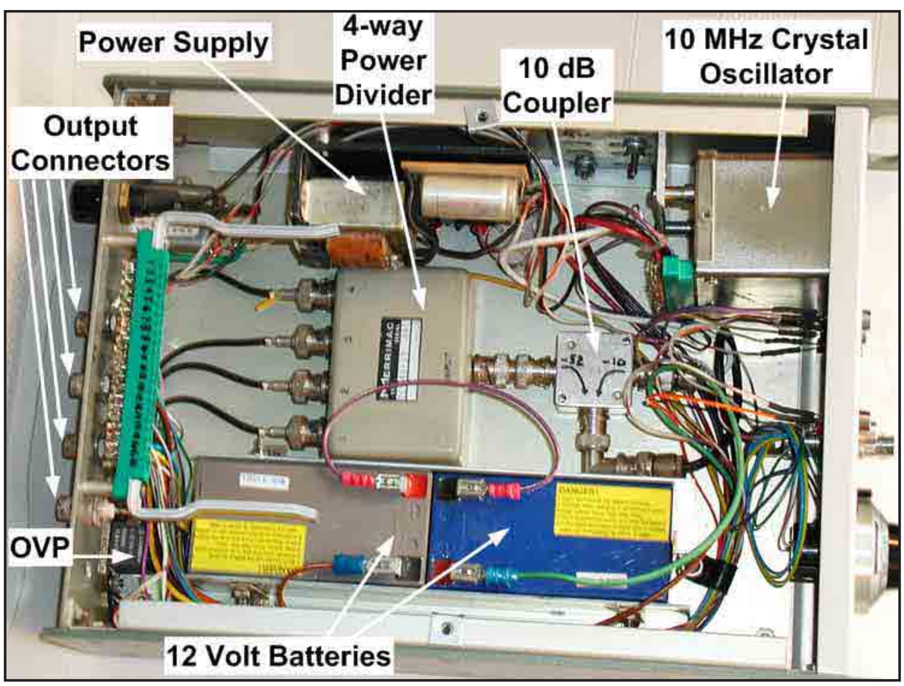

Fig 10—Chassis without wiring board.

would entail injecting the 10-MHz frequency standard output, suitably attenuated, into an AM receiver tuned to the 10-MHz WWV signal and adjusting the frequency standard while watching the signal-strength meter's beat note. The difficulty comes in separating the beat note signal strength meter variations from normal signal fading. Once the beat note goes below 10 Hz, this can become very difficult.

A better, albeit more complex, arrangement is to trigger an oscilloscope with the frequency reference and input the WWV 10-MHz signal directly to the vertical channel. The difficulty here is amplifying the WWV signal sufficiently so that it can drive the vertical channel. Use fast AGC to minimize amplitude variations. This represents a separate project, and it is a subject for a possible future article.

WWVB represents a very stable and accurate 60-kHz frequency source but requires a special receiver. It has become very popular as a time standard for wireless atomic clocks. Several references are shown for WWVB receivers that can be built relatively easily to serve as a calibration source.[10, 11, 12]

The initial drift rate was around 20 parts in 10^{10} per day. Within two weeks, it was 5 parts in 10^{10} per day, and it was down to 1 part in 10^{10} per day after a month. After two months, the drift rate settled to less than 1 part in 10^{11} per day.

Over the last three months (measurements started two months after turn-on), the frequency standard has drifted less than 0.005 Hz. All measurements were made using a GPS derived 10-MHz frequency standard that is accurate to better than 1 part in 10^{11}. At this point, the oscillator seems to have stabilized to a minimum drift rate, but further monitoring is on-going.

Notes

[1]Polyswitch devices are made by Raychem, a part of Tyco Electronics. You can download a Polyswitch catalog in PDF form at **ps.circuitprotection.com/docs/short_form_catalog.pdf**.

[2]"UC2906/UC3906 Sealed Lead Acid Battery Charger," SLUS186 September 1996, Unitrode Integrated Circuits.

[3]"Improved Charging Methods for Lead-Acid Batteries Using the UC3906," Unitrode Application Note U-104.

[4]You can download this package from the *ARRLWeb* **www.arrl.org/qexfiles/**. Look for 0205EVANS.ZIP.

[5]*Globe gel/cell Rechargeable Batteries Charging Manual*, GLOBE Battery Division, 41-2128.

[6]"Globe-Union Inc gel/cell Rechargeable Batteries and Chargers," GLOBE Battery Division, 41-2635.

[7]R. Evans, KJ6PO and D. Evans, N6UEZ, "LORAN-C Frequency Calibrator," *Communications Quarterly*, Fall 1991, pp 20-32.

[8]M. A. Lombardi, *Using LORAN-C Broadcasts for Automated Frequency Calibrations*, National Institute of Standards and Technology.

[9]W. F. Bain, W4LTU, "Simple Skywave Frequency Calibration Approaching One Part-Per-Billion," *QEX*, June 1996, pp 19-22.

[10]J. A. Cowan, W4ZPS, "Frequency Calibration using 60 kHz WWVB," *ham radio* magazine, March 1988, pp 45-46, 49, 52.

[11]D. Lancaster, "Experiment with WWVB," *Radio-Electronics*, August 1973, pp 48-51.

[12]E. P. Manly, W7LHL, "WWVB 60 kHz Frequency Comparator Receiver," *73 Magazine*, September 1972.

References

Operating & Service Manual, *10811A/B Quartz Crystal Oscillator*, Hewlett Packard 1980.

R. Valley, "IC Provides Optimal Lead-Acid Battery Charging Cycles," *EDN*, October 31, 1985, pp 163-178.

W. Dion, N1BBH, "A New Chip For Charging Gelled-Electrolyte Batteries," *QST*, June 1987, pp 26-29. ☐☐

On Measuring R_S

Here's an analysis of the load-variation method for measuring amplifier output impedance.

By Warren B. Bruene, W5OLY

It appears that measuring R_S, the output source resistance of an amplifier or generator, is as difficult as understanding just what it actually is. Unfortunately, information about the nature and magnitude of R_S is easily obfuscated. Ten years ago, I described in *QST*[1] a method of measuring the R_S of a linear RF power amplifier tube while it was delivering power. A small 50-mW test signal was injected into the amplifier output that caused very little disturbance to amplifier operation. Unfortunately, this test method requires a spectrum analyzer, so very few hams are equipped to verify these tests.

[1]Notes appear on page 25.

7805 Chattington Dr.
Dallas, TX 75248-5307

Others have proposed a "load-variation" test method,[2] also sometimes referred to as the "IEEE test method." They have presented data that they claim proved that a "conjugate match" existed at the output of a tuned RF power amplifier. I pointed out that their test method was not valid unless the phase delay of the π-output network (typically 140° to 155°) was extended to 180°.[3] It was suggested that I back up my theory with measurements to prove my point.

JB Jenkins, W5EU, offered to build an amplifier using a pair of 6146s for such a test. I accepted his offer with the hope that it would help bring closure to this debate. It used the same power amplifier components as in the Collins KWM-2 transceiver. The grid was shunted with a 50-Ω dummy load and driven by a transceiver. This eliminated the grid, neutralizing and RF feedback circuits and made the amplifier stability rock solid.

We tapped the π-network inductor to adjust the circuit Q and phase delay. An output inductor was added to convert the π network into a π-L network. The inductance was adjusted to provide a total phase delay of 180° from the tube plates through the π network and Bird directional wattmeter to the dummy load. This coil was shorted for measurements with just the normal π network.

DC and filament power was obtained from a 512F-2 power supply for the Collins KWM-2 transceiver. The 280-V screen supply was dropped to 210 V and regulated with two 105-V regulator tubes. This eliminated the effect of screen-voltage variation on R_S. Meters for measuring plate current, screen current and grid current were built into the front panel. It was a first-class construction job.

The amplifier was operated in class AB1 with the grids driven just to the verge of grid current. The tuning and loading were adjusted for the same plate current, screen current and RF power output for each test run. These were:

- 848 V dc on the plate
- 210 V dc on the screen
- 22 mA dc plate idling current
- 240 mA dc plate current
- 22 mA dc screen current
- 130 W RF power output
- 2100 Ω computed plate load resistance

All tests were performed at 4.0 MHz. An HP-8405A vector voltmeter was used to measure the phase delay from the tube plates to the dummy load. The *R1* dummy-load resistance was measured to be 50.7 Ω using a bridge. Two series-connected 300-Ω Globar resistors were switched in shunt to produce an *R2* load resistance of 46.6 Ω. The output network was always tuned into the *R1* load and left tuned that way when the load was switched to *R2*.

The phase delay of the π network using the initial inductor was 150°. A length of coax was cut to extend the phase delay to 180° for one of the tests. The π-L configuration was used for the other 180° test. Another test was made with the π inductance increased to reduce the π-network phase delay to 135° (3/8 wavelength).

To determine the values of voltage and current for use in the equation, we used the Bird directional wattmeter's forward-power reading. The reflected power could be neglected because it is only 0.25% of the forward power for the 1.1:1 SWR produced by *R2*:

$$V = \sqrt{PR} \text{ and } I = \sqrt{\frac{P}{R}} \text{ or } I = \frac{V}{R}$$

The equation for the load-variation method of computing R_{SC} at the dummy load is:

$$R_{SC} = \frac{V_1 - V_2}{I_1 - I_2} \qquad \text{(Eq 1)}$$

Unfortunately, the values of R_{SC} varied from one test to another so much that we considered the data unusable. Before abandoning this test setup, we measured R_S a different way in just the zero-signal operating condition.

A Reflected-Power Method of Measurement

The diagram of the test setup used to measure R_S with no signal present but using a large test signal is shown in Fig 1. The π-L output network with 180° phase-delay configuration was used. The power amplifier grids were left loaded with 50 Ω. A 200-W transceiver was used for the source of RF power feeding the dummy load across the power amplifier output. The 50-W slug was used in the Bird directional wattmeter to obtain good accuracy. The transceiver's power output was adjusted to show 50 W of forward power (full scale) and fed into the power amplifier under test. The reflected power was 26.5 W. The SWR computed from this ratio of reflected to forward power is 6.35:1. This means that R_S would be 6.35 times *RL* if the π-L network were loss-less. We determined that *RL* was 2100 Ω when tuned and loaded for 130 W output as before. R_S would therefore be 2100 times 6.35 or 13,335 Ω in the loss-less case.

The π-L-network percentage loss increases approximately as the resistance increases from 2100 Ω to 13,335 Ω. Assuming a network *Q* of 12 and coil *Q* of 150 results in a loss of approximately 12/150 or 8%. Increasing this percentage by 13,335/2100 gives approximately 50% loss. This leaves 50% of the real power getting to the tube plates. R_S is therefore approximately 13,335/0.50 or 26,670 Ω. The R_S/*RL* ratio is then 26,670/2100 or approximately 12.7:1.

For minimum IM distortion, the zero-signal plate current should be approximately 40 mA for the pair of tubes. It is run at 22 mA to keep plate dissipation down. This means that when driven to full power in normal operation, R_S will be less than 26,670 Ω—perhaps 18 kΩ or so.

Analysis of the Load-Variation Method of Measurement

A careful inspection of Eq 1, above, reveals the basic problem with the load-variation method. For a 10% difference in the values of *R1* and *R2*, the values of V_1 and V_2 will differ by less than 10%. (They would differ by 10% for a current source.) Therefore, an error in either V_1 or V_2 is multiplied by a factor of at least 10; that is, an error of 2% becomes an error of over 20%. If R_S/*RL* at the tube were 10 and a 180° phase delay were used, the calculated R_{SC} at the dummy load would be 10*R1* or approximately 500 Ω. This means that the difference between I_1 and I_2 would only be one-tenth of 10%, or 1%. If I_1 and I_2 were derived from *V/R*, an error in measuring the value of *R1* or *R2* also causes the same percentage error in V_1 and V_2. This extreme sensitivity to measurement error causes this test method to be useless for this application. See Appendix 1 for an example.

Fig 2 illustrates the nature of this problem. The long impedance phasor ending at the center of the small SWR circle represents the PA's RF plate load resistance, *RL*, when a 50-Ω load resistor is used. The shorter phasor ending at the SWR circle represents the plate load resistance when the load is switched to 45 Ω without retun-

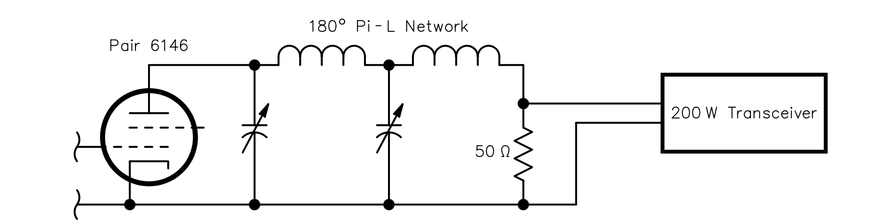

Fig 1—A diagram for measuring R_S at zero-signal operating condition.

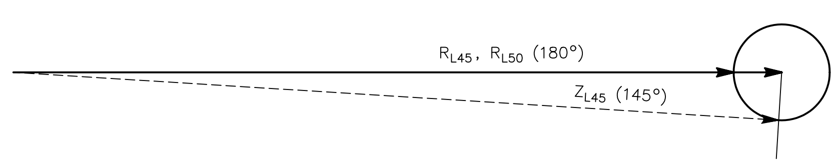

Fig 2—Diagram illustrating the small change of plate-load resistance or impedance when switching the load resistance from 50 to 45 Ω.

ing. These two phasors are in-phase when the total phase delay is 180°. The dashed phasor represents the phasor that would exist if the phase delay were 145° with the 45-Ω load. Note that the difference in magnitude between this phasor and the "50-Ω" phasor is much less than in the in-phase case. This situation causes this test method to falsely indicate that R_{SC} is less than it actually is. Increasing the phase delay to 180° eliminates that problem.

A loss-less 180° network, either a π-L or a π-plus-coax, stays in resonance when the load resistance is varied from 50 W to any other value. Also it correctly transforms resistances in either direction. When R_S is on the order of 10 times RL, the magnitude of the current change is very small (on the order of 1.5%) when switching to the 45-Ω resistor. Accurately determining the value of this small difference requires extreme accuracy in the two voltage measurements. If the current values for Eq 1 were calculated from V/R, the accuracy of the resistance values must also be on the order of 0.1% or better. This severe accuracy requirement makes this method of measurement impractical. See Appendix 1 for a numerical example.

Computer Analysis of the Load-Variation Method

For a method of measurement to be useful, it must be capable of reasonably accurate results (for example, less than ±10%) over the range of R_S, which might be encountered. I expected that the test amplifier would have an R_S on the order of 10RL. Therefore, an R_S of 20,000 Ω was used, except for one case.

A computer program was written, using HT*BASIC*, to examine this test method in detail. The computer eliminates the problem of instrument accuracy. The circuit model is shown in Fig 3. The power-amplifier tubes are represented by their Thevenin generator equivalent. The operating conditions are near those of the above-described test amplifier. Values were rounded somewhat to make it easier to evaluate changes. The total electrical length of the network plus coax was selectable to determine the effect of lengths other than 180°. The values of R_S, π-network inductor reactance, inductor Q and X_{C2} were also selectable. The reactance of X_{C2} was adjusted to produce a plate load resistance, RL, of 2000 Ω.

The program computes the reactance X_{C1} required to resonate the network and also the phase delay of the network. The length of coax in electrical degrees is then computed to produce the desired total phase delay specified. The voltage, E, is then computed to produce the specified tube RF power output.

The voltage V_1 across the 50-Ω load resistor was computed. Then the load resistor was changed to 45 Ω and V_2 was computed. From these two voltages and the two load-resistance values, the value of "output resistance" R_{SC} was computed using Eq 1. This represents the "output resistance" that this test method would give if there were no measurement errors.

The calculated output source resistance, R_{ST}, of the tube has been assumed by others to be the R_{SC} multiplied by the π-network impedance-transformation ratio—2000/50 in this example. Therefore, this method was used to determine R_{ST} in these calculations. Actually, this assumption is incorrect unless the total phase delay is 180°.

Then the program reduces voltage E to zero and computes what the output impedance, Z_{OUT}, actually is looking back into the end of the coax. Twenty-eight variables were printed out for each test run. The results of dozens of test runs are condensed to the essential data from just four runs in Table 1.

The common parameters used are:
- R_S = 20,000 or 2000 Ω
- R_L = 2000 Ω
- $R1$ = 50 Ω
- $R2$ = 45 Ω
- P = 130 W into the π-network
- $X_{L1} = j190$ Ω
- Q_{L1} = 120 or 10^6
- $X_{C2} = -j29.132$ or $-j31.375$
- $X_{C1} = -j169.459$ or $-j168.680$
- $Q_\pi = 13.5$

The alternate values of Q_{L1}, X_{C1} and X_{C2} are used for run 3, for the loss-less π-network case. The alternate value of R_S was used for run 4.

Table 1 lists the important parameters for each run. The computed value of the tube output source resistance, R_{ST}, is listed in the last column. For a valid method of measurement, R_{ST} must be the same as the value of R_S listed in the second column.

Run 1 represents the case using a typical π network that has a phase delay of 145°, a loss of 11.1% because of a coil Q of 120 and a π-network Q of 13.5. The computed R_{ST} is just a very small fraction of what it should be. The error is caused by coil loss and a phase delay that is less than 180°. Either is so large as to make this method of measurement useless.

Run 2 is for the same conditions except that a length of coax is added to bring the total phase delay to 180°. There is still a huge error, which results from coil loss only.

Run 3 removed the coil loss by assuming a coil Q of 1,000,000 (10^6). The correct value of R_{ST} is obtained, which proves that the computer program is correct.

Run 4 reduced actual R_S to 2000 Ω (providing a conjugate match), re-

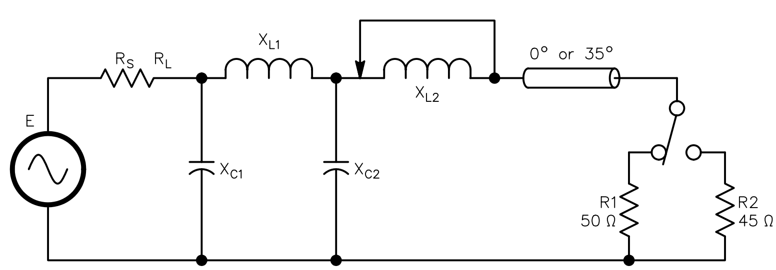

Fig 3—Schematic of a computer model for computing R_{ST}.

Table I

Run	R_S (kΩ)	Phase (°)	Loss (%)	Z_{OUT}	R_{ST}(kΩ)
1	20	145	11.1	16.1+j62.1	3.0
2	20	180	11.1	441.3+j41.7	8.5
3	20	180	0.0	500+j0.0	20
4	2	145	11.1	46.9–j4.82	1.8
5	20	135	8.9	10.6+j47.9	2.0

moved the added coax and restored the coil loss. In this special case where $R_S = RL$, the phase delay of the π network doesn't matter because the π network will transform 2000 Ω to 50 Ω just as well as it transforms 50 Ω to 2000 Ω. Nevertheless, it cannot transform any other value of R_S to 50 Ω without retuning! The error in the result is all caused by coil loss, which is greatly reduced when R_S is near the value of RL. Obtaining approximately the correct result in this special case *does not prove* that this method of measuring R_S is valid. That was clearly shown by run 1.

Run 5 is the same as run 1 except that the π-network Q is reduced from 13.5 to 10.8 by increasing X_L from $j190$ to $j231.7$. This reduces the phase delay to 135°. It also reduces the loss from 11.1% to 8.9%.

Notice that the computed R_{ST} is the same as R_L, indicating the existence of a conjugate match, whereas the actual R_S is 10 times R_L! This is caused by the 135° or 3/8 λ phase delay and is nearly independent of the actual R_S and network loss.

Conclusions

It has been shown that there are three sources of huge errors in the load-variation method of measuring R_S, any one of which is sufficient to make this method utterly useless. These are:

1. Typical values of π-network coil loss.
2. Phase delay other than 180°.
3. Requirement for voltage and resistance measurement errors of considerably less than 0.1%.

Therefore, claimed proof that a conjugate match exists by using this load-variation method is false. The method of measuring R_S that I published 10 years ago in *QST* remains the only valid published method of measurement. My measurements correlate well with values of R_S determined by an analysis of tube curves[4] published by transmitting tube manufactures.

Notes

[1]W. B. Bruene, W5OLY, "RF Power Amplifiers and the Conjugate Match," *QST*, Nov 1991, pp 31-32, 35.

[2]W. Maxwell, W2DU, "On the Nature of the Source of Power in Class-B and -C Amplifiers," *QEX*, May/Jun 2001, pp 32-44.

[3]W. B. Bruene, W5OLY, "Impedance Transformation Properties of a π-Output Network," *QEX*, Jan/Feb 2001, p 59.

[4]W. B. Bruene, W5OLY, "Plate Characteristics of a Distortion-Free Class AB RF Amplifier," *QEX*, July/Aug 2001, p 48-52.

Appendix 1: A Specific Example

This example uses the values of run 3 in Table 1 to compute R_{SC} and R_{ST} from Eq 1 and the p-network impedance-transformation ratio of 40. This run is for the case with no network loss and a phase delay of 180°. In this case, all error would be due to "meter errors."

$$R_{SC} = \frac{V_1 - V_2}{I_1 - I_2} = \frac{80.622035 - 73.225613}{1.6124407 - 1.6272358} = \frac{7.39642}{0.014795} = 499.9$$

$$R_{ST} = R_{SC}\left(\frac{2000}{50}\right) = 19{,}996\,\Omega$$

This is very close to 20,000 Ω, which is the correct answer.

Notice that the difference between I_1 and I_2 is less than 1% of either. An accurate determination of this difference with even 10% accuracy is far beyond the capability of well maintained, commonly used laboratory instruments.

Warren Bruene, W5OLY, has been licensed since 1935. Three widely used circuits he originated are tetrode neutralization, RF feedback to improve linearity and a directional wattmeter circuit. The wattmeter circuit published in April 1959 QST *is the basis for many wattmeters used by hams today. Transmitting-tube manufacturers considered him an authority on HF linear RF power amplifier design. He has been granted 22 patents. He coauthored* Single Sideband Principles and Circuits *(McGraw Hill 1964) and authored the chapter on High Power Linear Amplifiers in* HF Radio Systems and Circuits *(Noble 1998) as well as single chapters in seven engineering handbooks.*

Warren is a graduate of Iowa State University, a member of ARRL and a Life Fellow in the IEEE. His Fellow citation was for "advancing SSB radio communications." He spent 44 years with Collins Radio (Rockwell) where he designed many amateur, commercial, military and broadcast transmitters ranging from 500 W to 250 kW and from VLF to UHF. These transmitters included many "firsts" in RF-power-amplifier design, output network design and automatic tuning systems. Several are now collector's items. He spent another six years with Electrospace Systems before retiring to part-time consulting. He is listed in Who's Who in Engineering *and in* Who's Who in America. □□

A Homebrew Regenerative Superheterodyne Receiver

Come check out this flexible "old-tech" receiver for 4 to 15 MHz

By Bill Young, WD5HOH

My regenerative superhet is a single-conversion, crystal or VFO controlled high-frequency radio receiver with a two-stage (one stage tunable) regenerative intermediate-frequency amplifier. It is built on a homemade 18-gauge galvanized steel chassis divided into five compartments. Each amplifier stage is shielded from its neighbors. I recall hearing or reading that some early vacuum-tube receivers were built this way, and I wanted to try the technique.

I have not been disappointed. The gain can be cranked way up and the receiver is stable. The cost of components (bought new) for the regenerative superhet totaled about $260 including the sheet steel. The regenerative superhet has 10 JFETs, nine diodes (including the rectifier bridge) and 10 ICs. Refer to the block diagram of Fig 1 for an overview of the regenerative superhet.

343 Forrest Lake Dr
Seabrook, TX 77586
blyoung@hal-pc.org

Circuit Description

There are two tuned radio-frequency amplifier stages (Figs 2 and 3) between the antenna and the mixer. There is a crystal oscillator circuit (borrowed from a ham magazine years ago) that drives a source follower, which in turn is source-coupled to the mixer (Fig 4). The mixer drives a low-pass filter (Fig 5) designed to remove everything above the IF. There is what amounts to an untuned buffer amplifier (first IF, Fig 6) between the filter and the regenerative second IF amplifier (Fig 7). The second IF amplifier is transformer-coupled to a diode-bridge detector. A low-pass filter (Fig 8) between the detector and the audio amplifier removes everything above about 47.5 kHz. This allows plenty of room for high audio frequencies to pass, but it removes RF.

The audio stage is a conventional LM386 circuit (Fig 9) driving a pair of modified RadioShack stereo headphones connected in parallel at the jack to give an audio frequency impedance of about 4 Ω. An outboard passive high-pass filter with a 490-Hz cutoff (Fig 10) can be switched in and out. Lately, I added a pair of Zenith speakers driven by a homebrew LM380 stereo amplifier with the amplifier inputs

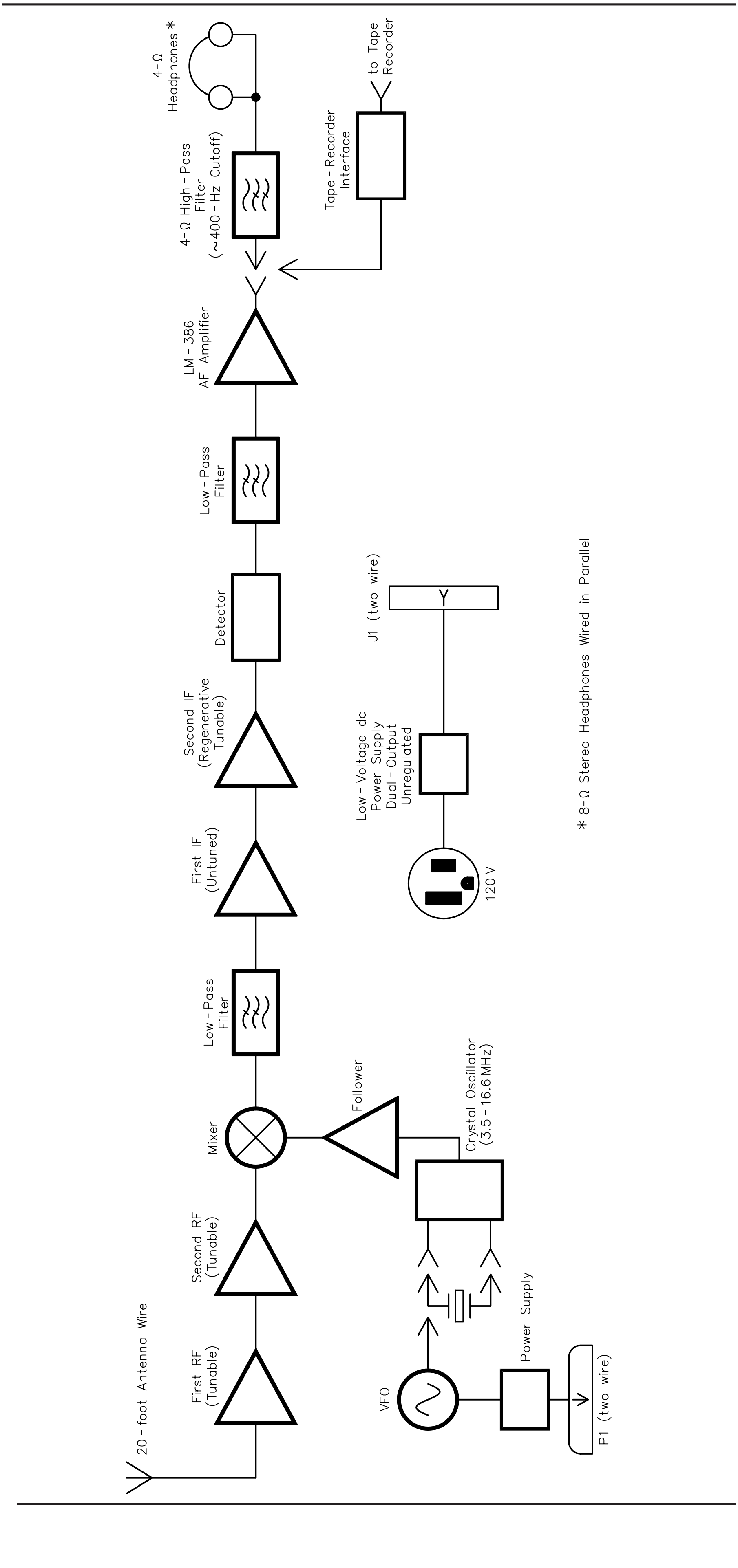

tied together. I have begun recording from the regenerative superhet using the output of a homebrew L-pad attenuator fed into the microphone jack of a RadioShack tape recorder (Fig 11).

The regenerative superhet does not have a 50-Ω input (antenna) impedance. There is another way to couple an antenna to a receiver's input and that is the high-impedance way: an electrically short wire antenna capacitance-coupled to the first parallel-resonant circuit. Electrically short wire antennas are worth looking at again. They fit nicely into a small urban lot. Some old radio books (I had access to some of them when I was young) sometimes showed the antenna capacitance-coupled to the first tuned circuit without an RF transformer. What I noticed about that configuration was that it invariably resulted in greater signal strength than the transformer configuration. Of course, it also resulted in poor selectivity. Cascading two tuned stages seems to help a lot. Of course then you have to tune both stages by hand, individually.

Two-handed tuning is archaic. It also means that the operator, in effect, realigns all the tuned stages at each received frequency. Old radio texts also state clearly that short vertical antennas are subject to noise pickup more than, for example, a half-wave dipole with a coaxial or even a twisted-pair transmission line. That is true, but I have found that although the regenerative superhet does pick up every click and pop from appliance switches, it can also receive very weak, distant signals. In addition, a high-impedance antenna does not demand a low-impedance earth ground.

The regenerative superhet has an untuned crystal-controlled oscillator. This allows the receiver IF to tune sum and difference frequencies of incoming signals and crystal-oscillator or VFO harmonics, as well as fundamental frequencies. This takes some getting used to, and it places all the responsibility for rejecting out-of-band signals on the tuned RF stages. That's why there are two of them—independently tuned.

The second RF stage's inductive load (a 1.2-mH choke) was determined "by guess and by golly" to result in reasonably sharp tuning from about 8 to about 15 MHz. The inductive reactance of this choke was then calculated to be about 75 kΩ at 10 MHz. A 2.7-mH inductance was then chosen as a load for the first RF stage to have the same inductive

Fig 1—A block diagram of the regenerative superhet.

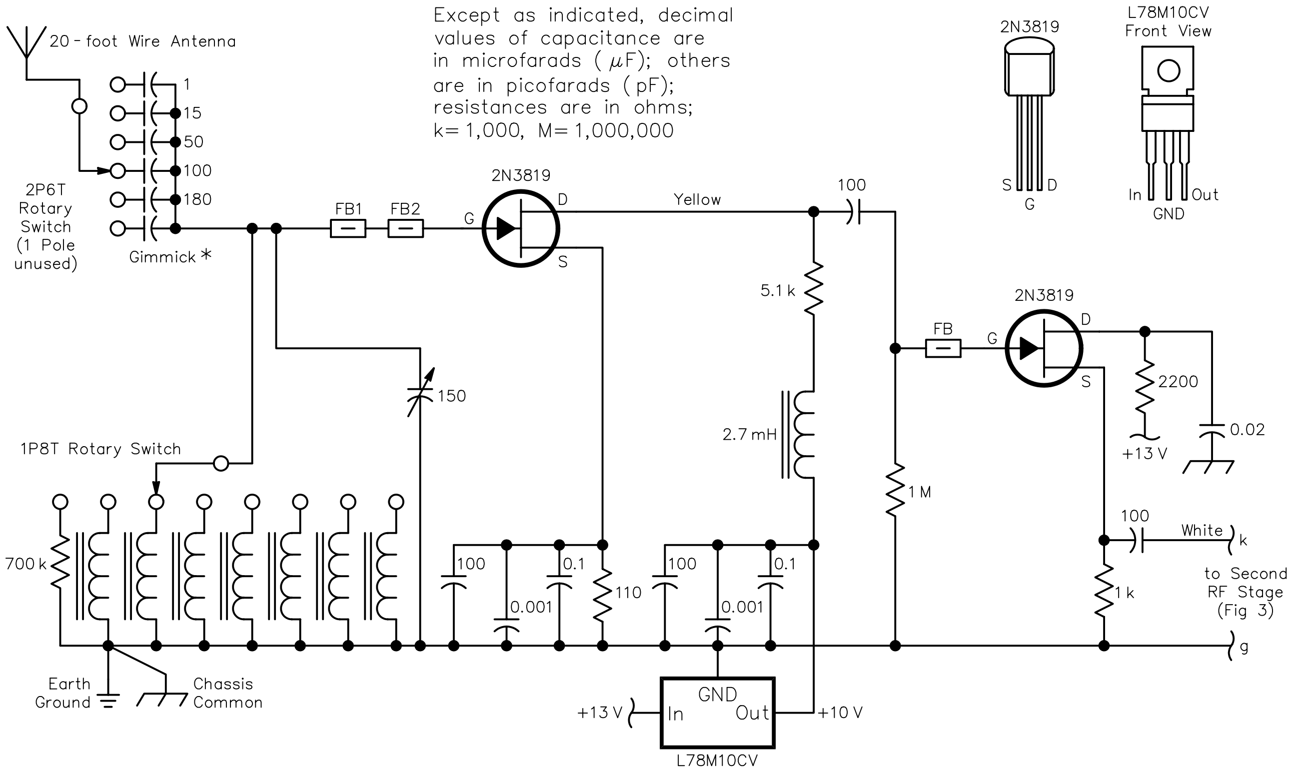

Fig 2—Schematic of first RF stage and "follower" amplifier. The seven gate-circuit inductors are #24 AWG enameled wire wound on Amidon powdered-iron toroid cores. See Table 1 for winding details.

FB1—Ferrite bead for 40-200 MHz (Mouser 542-FB43-110)

FB2—Ferrite bead for 200 MHz and above (Mouser 542-FB64-110)

Gimmick—capacitor made by four turns of twisted wire. Begin with 4 or 5 inches of #22 or #24 AWG wire.

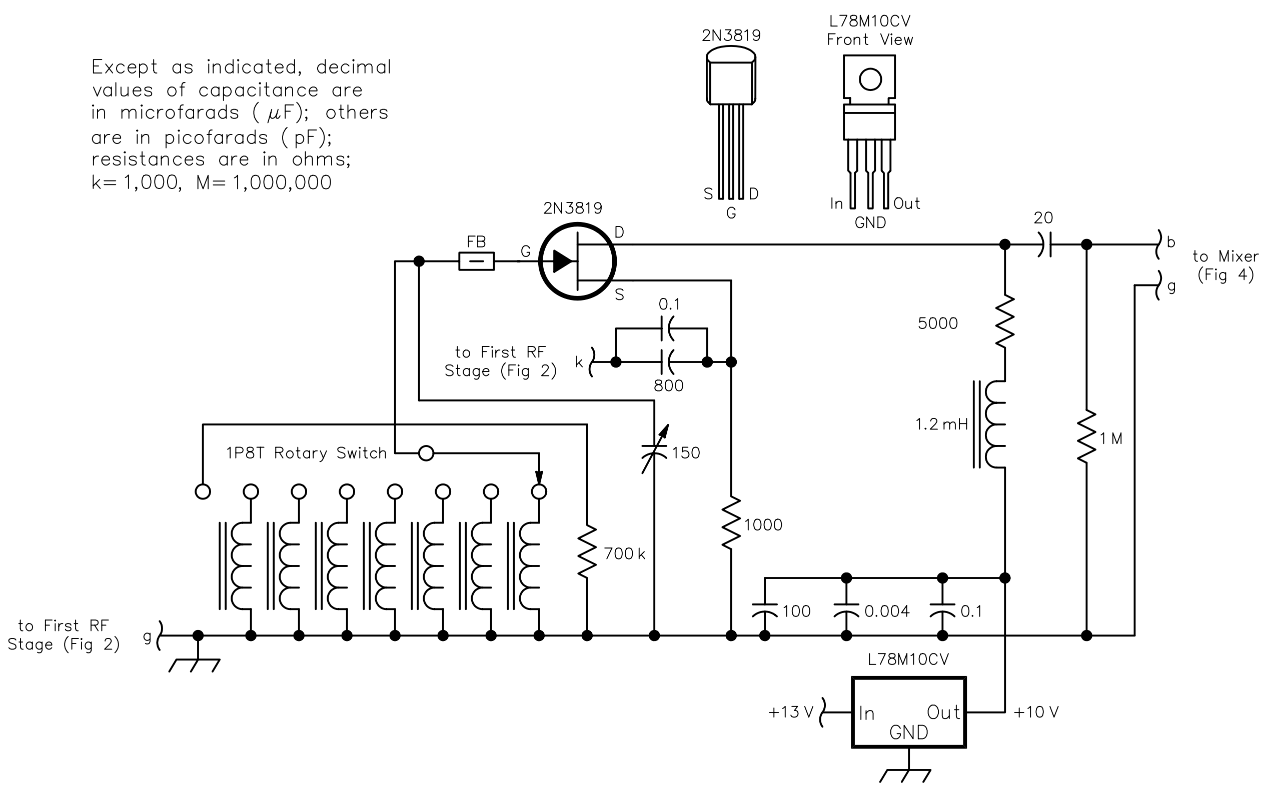

Fig 3—A schematic diagram of the second RF-amplifier stage. The seven gate-circuit inductors are #24 AWG enameled wire wound on Amidon powdered-iron toroid cores. See Table 1 for winding details. FB—Ferrite bead for 40-200MHz (Mouser 542-FB43-110).

reactance: 75 kΩ at about 4 MHz. The two RF stages are therefore stagger-tuned to cover the range of 4 to 15 MHz. This might seem awkward, but it works. Signal level and selectivity are further enhanced by the RF source-follower stage between the first and second RF amplifiers.

In addition, the installation of a six-position rotary switch with six values of antenna-coupling capacitance between the antenna and the top end of the first tuned circuit has dramatically improved gain of the first RF amplifier. I have found that 1 pF is about right for most frequencies. As much as 15 pF is appropriate for 15 MHz.

Keep in mind that a quarter-wavelength of wire has a feed-point impedance approaching 50 Ω. It is necessary to keep the antenna impedance well above that—higher is better until signal level begins to drop. In practice, it's easy to tell how much is too much with this receiver: The signal level drops and the beat note shifts slightly. The crystal oscillator also serves as an input port for the VFO when it's used.

The regenerative second IF amplifier stage is not a "gate-leak" detector. I have not had good results with JFET gate-leak detectors, and I have tried several configurations. I tried connecting the primary winding of a bifilar RF transformer between the JFET drain and the drain voltage supply—well bypassed, of course—with the secondary driving a 1N34A diode. Very weak signals were the result. Then it occurred to me that I had shunted the primary winding of the transformer to ground (sort of) because the secondary bottom end was tied to ground. Those two windings are capacitively coupled. Therefore, I decided to venture a little further and drive a diode bridge with the transformer secondary. That would free up the bottom end of the primary. It worked. I then had a better regenerative receiver.

I put the feedback or "tickler" winding in series with the bifilar transformer at the bottom end of the primary winding. My initial reason for this was to eliminate or reduce the erratic regeneration control that

Table 1—Coil Construction

Switch Position	*Value*	*Detail*
0	42 µH	57 turns AWG # 24 On Amidon TI06-2 core
1	21 µH	51 turns AWG # 24 On Amidon T94-2 core
2	11 µH	48 turns AWG # 24 On Amidon T80-6 core
3	5 µH	33 turns AWG # 24 On Amidon T68-6 core
4	2.2 µH	23 turns AWG # 24 On Amidon T50-6 core
5	0.94 µH	15 turns AWG # 24 On Amidon T44-6 core
6	0.38 µH	11 turns AWG # 24 On Amidon T37-6 core
7	700 kΩ	Resistor (untuned)

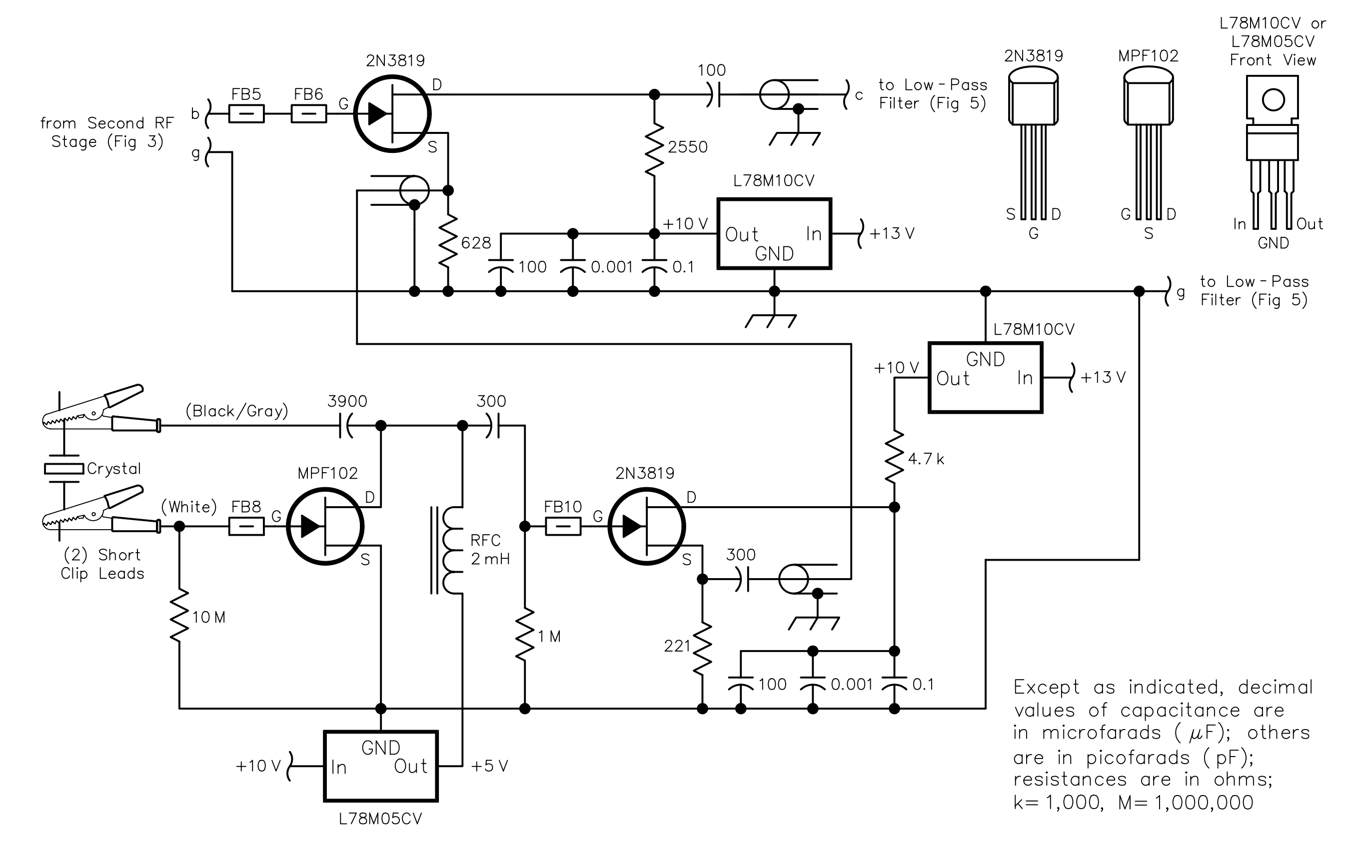

Fig 4—Schematic diagram of crystal oscillator, oscillator-follower and mixer stages.

FB5—Ferrite bead for 40-200 MHz (Mouser 542-FB43-110)

FB6, 8, 10—Ferrite bead for 200 MHz and above (Mouser 542-FB64-110)

always seems to result from connecting a variable capacitor or potentiometer from the JFET drain to chassis ground. Once I had done that, I was able to control regeneration with a potentiometer across the tickler. It has occurred to me that I have approximated a current source by putting the tickler coil at the cold end of the RF coupling transformer. Regeneration control by potentiometer is not particularly quiet, but it is repeatable. Because I installed a vernier regeneration control that is both quiet and smooth, I can adjust regeneration until the bandwidth is narrow.

In addition, "throttle" capacitors are becoming difficult to find, and the variable capacitors that can be found tend to be old, dirty and noisy. New "pots" are readily available. I should point out that the 250-Ω COARSE regeneration control consists of two 500-Ω pots on a common shaft, wired in parallel. That's the only way I could get a 250-Ω pot that is not wire-wound.

I have seen a schematic diagram for a regenerative receiver with a regenerative RF amplifier driving a semiconductor diode, but it did not include an RF coupling transformer between the amplifier and the diode (or crystal and cat whisker in this case). It's on page 74 of *Vacuum Tubes in Wireless Communication* by Elmer Bucher.[1] It is attributed to an engineer named Franklin who worked for Marconi. I have no idea how well it worked.

I also had an opportunity during the development of my regenerative superhet to test the idea that a tickler coil with a few turns close to the tuned-circuit coil works better than more turns farther away. I just happened to have a small, thin-wall cardboard tube that (with the two turns of tickler winding in place and coated with Krylon) would just slip inside the acrylic form for the second IF tuned coil. I tried regeneration control with the tickler coil almost all the way out of the coil form to all the way in. All the way in was better: Regeneration control is more positive. I then "tacked" the tickler coil form in place with a little hot glue.

The presence of an RF transformer in the drain circuit of the regenerative amplifier makes it possible to achieve regeneration with a smaller number of turns on the tickler coil. This is so because the current in that circuit can be kept at a higher level than it would be for a resistive or audio-choke load. The smaller number of turns minimizes the difference in tuned frequency from not oscillating to oscillating. That makes it easier to maintain the receiver just on the edge below oscillation where gain is high and bandwidth is narrow.

Construction

The tuned circuit or gate-circuit coil for the regenerative IF stage is "scatter-wound" on a one-inch-diameter thin-wall acrylic form (Fig 7). Scatter winding allows approximately the required inductance to be positioned within a defined one-inch winding length on the form, thereby allowing the optimum clearance between the coil and chassis steel. Better clearance means higher coil Q, which improves selectivity. This approach works well if it's not necessary to track two tuned circuits, as it is not in this case.

The bandspread-dial drive has a very light "touch." That's because the bandspread vernier drive does not drive a conventional variable capacitor, with its inherent friction. The bandspread vernier drives a floating rotor. A floating rotor, in this instance, is one half of a 2¼-inch-diameter steel fender washer mounted on a short insulating shaft (a nylon screw). The floating rotor moves between the plates of a fixed capacitor and alters the capacitance of the pair of plates as it rotates. There are no wiping contacts, so there is no noise from wiping contacts. The floating-rotor variable capacitor has a maximum capacitance of only about 30 pF. That's about right for a bandspread capacitor across an approximately 90-pF variable.

I was fortunate to have one old, very ruggedly constructed transmitting variable capacitor with a rotor wiping contact that could be removed, sanded bright and clean and reinstalled. I also thoroughly cleaned the wiping groove in the rotor shaft. It works very well, but I probably won't find any more like it.

The second IF amplifier's (Fig 7)

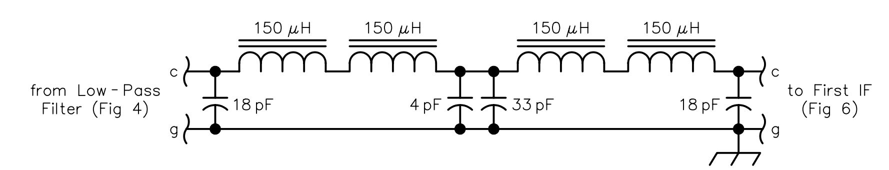

Fig 5—Schematic of mixer-output low-pass filter. Z_0 = 2900 Ω; f_c = 3100 Hz. This is a constant-k, two-section ladder filter.

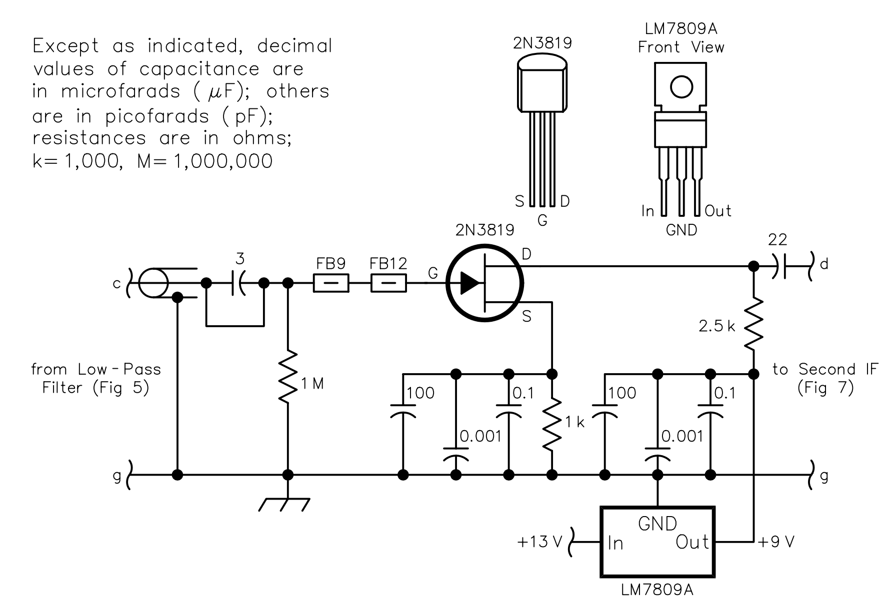

Fig 6—Schematic of first IF stage (untuned).

FB9—Ferrite bead for 40-200 MHz (Mouser 542-FB43-110)

FB12—Ferrite bead for 200 MHz and above (Mouser 542-FB64-110)

[1]Notes appear on page 35.

output transformer is bifilar wound on a wooden core. The wooden core does become warm to the touch after being "microwaved" for two minutes: It will probably be replaced with acrylic rod when I can find some.

The regenerative superhet was built in stages, starting with the power supply and associated circuits, then the audio amplifier, followed by the second IF, first IF and so on, until the first RF stage had been built. For this receiver, that approach can give misleading results. The regenerative second IF stage does not behave the same when connected to a wire antenna through a 3-pF capacitor as it does when connected to the first IF amplifier through a 22-pF capacitor. Its behavior changes again when the first IF amplifier is connected to the mixer rather than to the same antenna through the same 3-pF capacitor.

I discovered after operating the regenerative superhet for a while that its performance varied somewhat depending on which crystal was being used. Then I realized that the crystal oscillator output was getting through the mixer into the IF stages. I remedied that problem nicely by insertion of a two-section, constant-k low-pass filter between the mixer and the first IF (Fig 5).[2] The filter just begins to roll off at about 3 MHz

It became apparent after the regenerative superhet was initially completed that RF energy was getting into the LM386 stage, causing both AF oscillation and blocking at higher audio gains. The small steel-core audio transformer initially installed to solve this problem was insufficient, so I built and installed a source-follower driving a π-section, constant-k low-pass filter

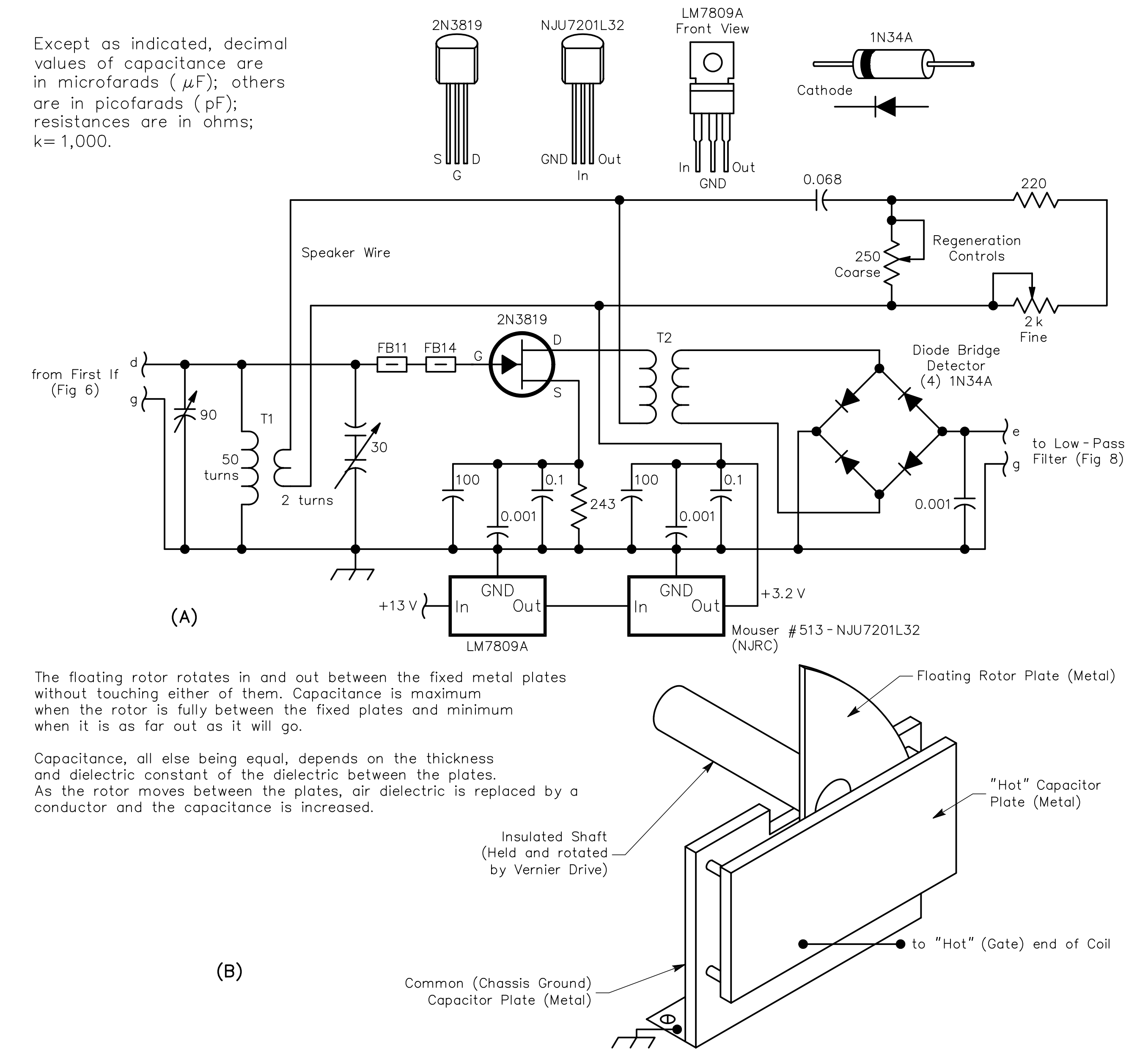

Fig 7—At (A), schematic of second IF amplifier (tunable, regenerative) and detector. Reverse the leads to the feedback winding, if necessary, to obtain oscillation. At B, details of the homebrew 30-pF capacitor with a "floating rotor."

FB11—Ferrite bead for 40-200 MHz (Mouser 542-FB43-110)

FB14—Ferrite bead for 200 MHz and above (Mouser 542-FB64-110)

T2—100 turns bifilar wound on 7/16-inch-diameter wooden dowel.

(Fig 8). That helped, but there remained audio oscillation associated with changes in the regeneration controls. I could see that RF was still entering the LM386. I then ordered and installed a 1.2-mH RF choke with a 0.1-µF bypass capacitor in the dc power lead to the LM386. I also installed a 600-µF, 25-V bypass capacitor across the 100-µF capacitor already connected from the bypass pin (pin 7) of the LM386 to ground. I then had a stable, controllable receiver. The 10-kΩ pot at the input to the LM386 stage can be "opened up" on weak signals without instability.

Another very old-fashioned thing I did was to build the power supply in a separate box with a cable from power supply to receiver (Fig 12), thereby reducing ripple and tunable hum. There is extensive use of on-board voltage regulation in the regenerative superhet. Small fixed-voltage regulators are inexpensive and they improve receiver stability. The second IF stage has two voltage regulators: The first drives the second. This allows this stage to operate at about 3 V. I had learned from a previous receiver I built that the regenerative amplifier works better at about 3 V.

The regenerative superhet circuit

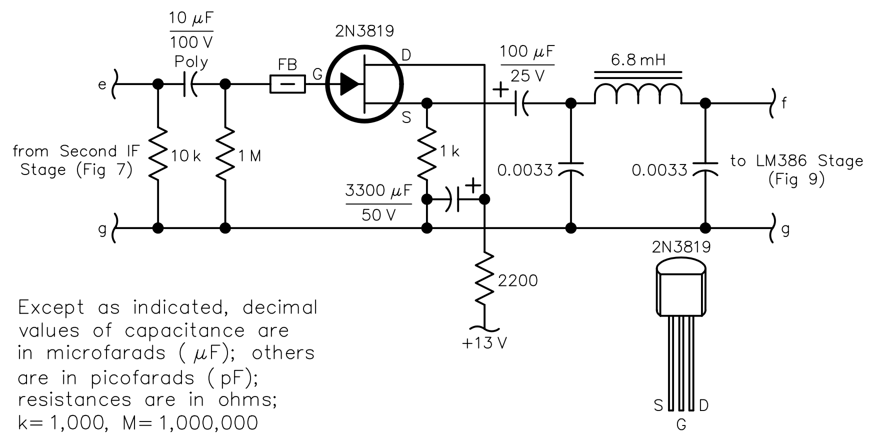

Fig 8—Schematic of the detector-follower and low-pass-filter stages. FB—Ferrite bead (Mouser 542-FB43-422)

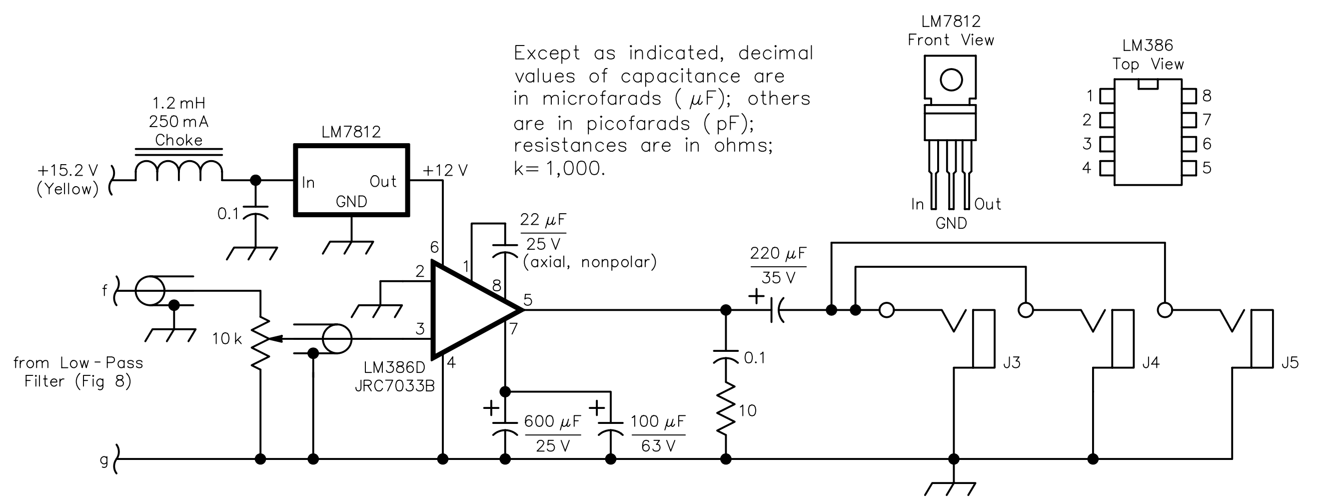

Fig 9—Schematic of the AF amplifier with a stage gain of 46 dB. The 10-kΩ potentiometer is an audio-gain control from Mouser (31VJ401). J3-J5 are phone jacks of the builder's choosing. They are wired in parallel to provide for different phone-plug sizes without adapters.

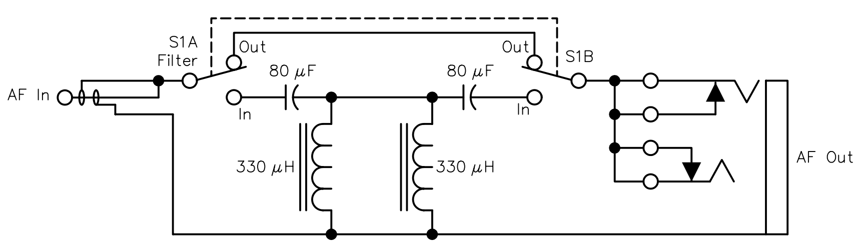

Fig 10—Schematic of the speech-enhancement filter that plugs into the LM386 output jack. A constant-k, high-pass (490-Hz cutoff) for a 4-Ω load, the design is from D. Metzger's *Electronics Pocket Handbook,* second edition (Prentice Hall Inc), p 42. The author's filter is constructed within a small aluminum box mounted to the input phone plug. S1 is one section of a 6PDT rotary switch. Each 80-µF capacitor was made by combining nonpolar 33-µF and 47-µF capacitors in parallel.

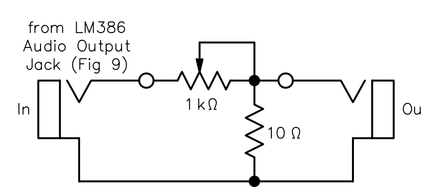

Fig 11—Schematic of the tape-recorder interface and L-pad attenuator. The output is suitable for a RadioShack CTR-66 (#14-1151) cassette tape recorder microphone jack. In use, set the attenuator control for best sound quality and minimum playback distortion (probably near 15 Ω).

boards were built on perfboard using component leads, tinned bus wire and insulated sleeves where necessary. Ferrite beads were installed on the gate leads of RF JFETs where it seemed appropriate. As a result, I have not had a problem with instability.

Most of the boards are mounted 1/2 to 3/4-inch above the galvanized steel chassis with nylon screws and spacers. Three of the boards are mounted on steel brackets made from the 18-gauge steel used for the chassis. The 18-gauge galvanized steel chassis is both an electrostatic and a magnetic shield. I have operated the regenerative superhet during a geomagnetic storm (as announced by WWV). Although signals from Europe and Asia were disturbed, I didn't hear any squealing and humming that I have heard during geomagnetic storms with a receiver having less-complete shielding. Apparently, the combination of steel and a layer of zinc is a good shield.

I began by buying a sheet of 18-gauge galvanized steel from a local supplier of ductwork for central heating and air conditioning. I then cut out a rectangular piece for the main part of the chassis, which I then bent into a channel with flanges. All ground connections are made to this main piece by leads soldered to lugs held by machine screws. There are four transverse bulkheads (penetrated by a few small holes for wires) and two end pieces. The bulkheads are fastened with sheet-metal screws parallel to the end pieces; they

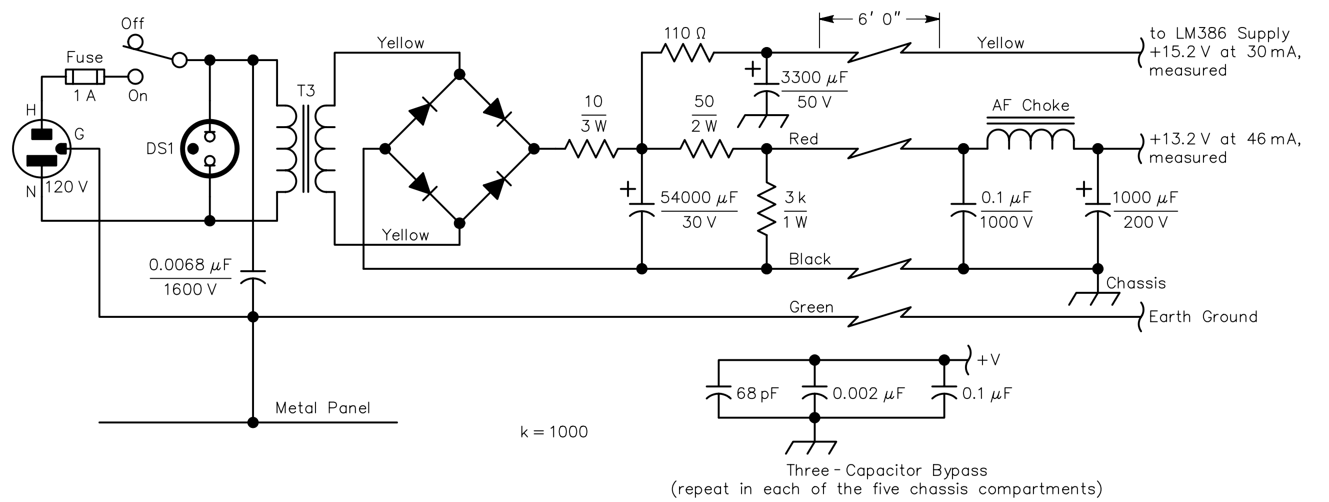

Fig 12—Schematic of the power-supply (unregulated, filtered). The 60-Hz ripple suppression is estimated at 35 dB.

DS1—120-V ac red neon lamp
T3—Power transformer 120-V primary, 12.6-V center-tapped secondary (RadioShack #273-1352A)

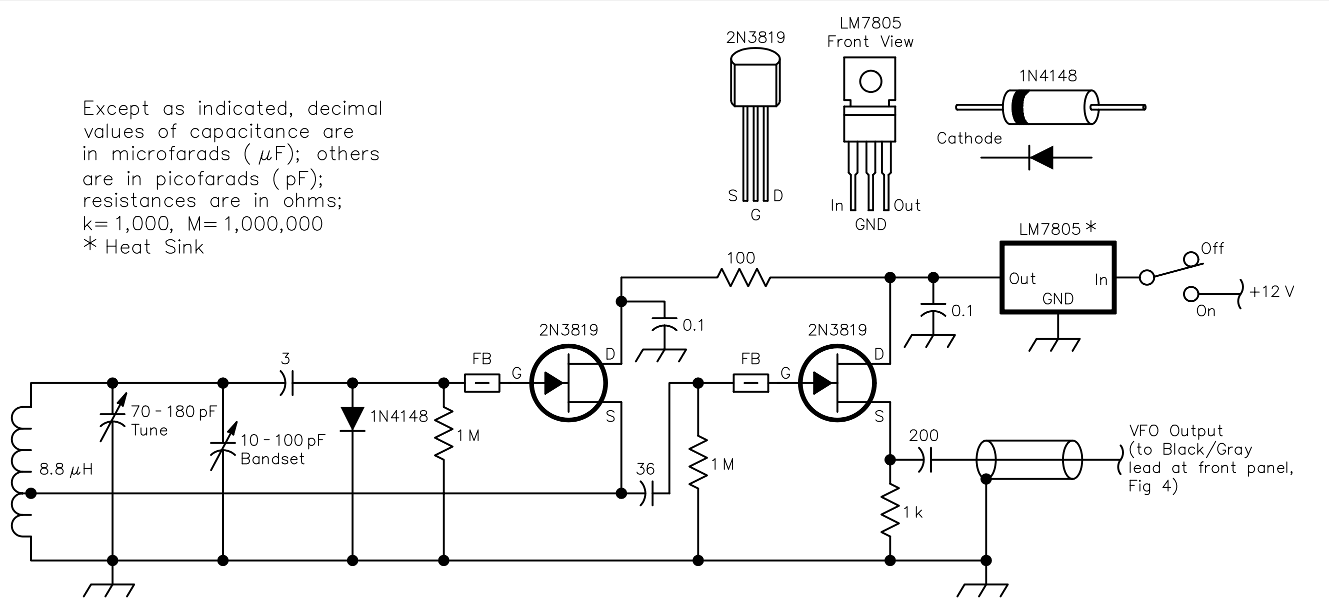

Fig 13—Schematic of the VFO and buffer. To use VFO, connect output to black/gray wire in place of a crystal. The TUNE **capacitor is 70-180 pF with a 50:1 reduction drive (WW2 surplus). The** RANGE **capacitor is 10-100 pF. The inductor is 16 turns #24 AWG, close wound on a 1-inch-diameter acrylic tube tapped 4 turns from the ground end. FB—Ferrite bead for 40-200 MHz (Mouser 542-FB43-11).**

are spaced equally along the length of the regenerative superhet. These bulkheads serve as shields, and each bulkhead is secured to the chassis or bottom plate along its periphery. The resulting chassis structure is both stiff and heavy.

When the chassis was first completed, I was somewhat disappointed because it rang like a bell when struck. I thought that would make the completed receiver microphonic. The tendency to ring disappeared as circuit boards and components were added.

I thought that a combination of the stiff, heavy steel chassis structure of bygone years and solid-state components would result in a sensitive, stable receiver. Within the limitations of the relatively simple circuitry, my expectations have been met. Keep in mind that tube radios of the past were not always completely enclosed in metal. The tubes generated heat and required ventilation. Tube radios sometimes ingested a lot of dust over several years of operation. Some solid-state radios can be completely enclosed so they remain clean inside.

Lessons Learned

There is another similarity between the regenerative superhet and early receivers: All of the active devices—except the ICs—are triodes. That design trend began with transistor radios in the 1950s. Circuit designers went back to things like triode push-pull audio stages rather than the high-gain pentode and tetrode tube stages that had been dominant for decades. Triodes don't behave well with a tuned plate, collector or source (remember the TPTG oscillator?), so recourse was made to RC coupling and more stages.

Also, when and if it's necessary to replace a JFET, there are only two types in the receiver: MPF102 and 2N3819. These little triodes are cheap and reliable, so why not use more of them? Be aware of device pin placement: Not all 2N3819s have the pin locations shown in the diagrams here.

Note that the regenerative superhet is not the first regenerative receiver I've constructed. There were several before: one vacuum-tube low-frequency receiver and one solid-state regenerative receiver that performed miserably but contributed to my understanding. Both were dismantled years ago. The "brown" radio was the immediate predecessor of the regenerative superhet, from which I learned much. Its immediate predecessor was the "trash" radio, so named by my wife because it was built on a wooden chassis and added to as experience and inspiration indicated. Trash radio had the most peculiar habit of responding to increases in the regeneration control setting with a "hang time" of up to one minute. That is, the regeneration level would increase and gradually decay back to just above where it was before it was increased.

I do not know the source of the decay or settling time. There were no long-time constants in the circuit that I could see. Trash radio also exhibited super-regeneration with an audible quench frequency. This apparently was an unintended result of an RF choke I placed after the detector.

Operation

My regenerative superhet's IF is tunable from about 1800 to about 2300 kHz. That's the lowest 500-kHz frequency band available above the standard AM broadcast band. A 500-kHz bandwidth would have been difficult to manage below the broadcast band. Calibration of the IF tuning was done in a manner suggested by *ARRL Handbook* receiver articles of the 1950s and '60s. I installed two vernier drives with no dials and then glued a heavy piece of white cardboard to the chassis around the vernier drives. Then I made and installed steel dial pointers that rotate with the vernier drives. The pointers are bent to almost touch the dial scales to minimize parallax error.

Calibration was begun by marking the 2.2-MHz point when the radio was zero beat to the signal from a 2.2-MHz crystal connected to a homemade crystal oscillator. I then continued operating the receiver with different crystals and marked the 1.82, 1.9, 2.0, 2.1 and 2.2-MHz points as I identified stations operating on or very near frequencies that corresponded to those IFs with the crystal in use. Subsequent operation has resulted in errors usually less than 20 kHz. I'm happy with it.

Keep in mind that the regenerative superhet does not have automatic gain control (AGC): Tune slowly. Reduce audio gain when you hear a strong beat note that drops in frequency as you tune. You are probably approaching a very strong carrier. Protect your ears.

Calibration of the signal-frequency amplifiers or "front end" has been done using received signals and peaking the switched inductors and variable capacitors. Optimum settings for these four controls have been entered in a table for reference. This is, of course, a rather clumsy way to tune a receiver front end. It does result, however, in good gain, and it reduces spurs, images and signals that could mix with harmonics of the crystal oscillator or VFO.

I have constructed an outboard high-pass filter (Fig 10) with a 4-Ω characteristic impedance and a cutoff of 490 Hz that plugs in between the headphone jack and headphones. This filter can be switched in and out. It improves the intelligibility of speech noticeably; I switch it out to enjoy music.

I had noticed that some shortwave stations could be received well, with good signal strength, but for some stations the speech had too much bass and was almost unintelligible. My ears are 61 years old, and they don't hear high frequencies very well. The high-pass filter helps a lot.

You may notice from the regenerative superhet schematic, Fig 1, that the antenna terminal for the receiver is a short "pigtail" with an alligator clip at the end. I did that because I have learned it's necessary to disconnect the antenna when not operating the receiver. I have—apparently from nearby lightning discharges—lost two 2N3819s in a shortwave converter I built to operate with a broadcast receiver in my garage. Shorting the antenna lead to ground with the receiver connected is not good enough. So far, disconnecting the antenna has worked okay.

Operation of the regenerative super-het continues, and I have logged some stations I had not heard before, such as the Voice of Yugoslavia and the Voice of Vietnam, along with a shore station in Malaysia. With the IF in oscillation, I have good sideband reception. The floating rotor bandspread control is very good for fine tuning SSB for maximum intelligibility. Very strong SSB signals require some detuning of the front end to avoid overload. The regenerative superhet will serve as a general-coverage receiver.

I have about 20 crystals to use with this receiver; but if I didn't, microprocessor crystals work well and can cost less than $1 each. There are two short clip leads hanging out of the front of the regenerative superhet's chassis to connect the crystals. It looks funny, but it allows me to use any available crystal, from a very large marine-radio 4050-kHz crystal I bought at a ham flea market down to small microprocessor crystals. Most of the old FT-43 crystals I have also work fine, as do several old crystals of indeterminate packaging.

I would like to mention something that I think is somewhat misunderstood: "fringe howl." True fringe howl is a rather faint but distinct howl that occurs at high gain levels just before oscillation. It tends to come and go with modulation, and it is associated with the resulting narrow bandwidth of a regenerative amplifier at high gain. It isn't a low-frequency oscillation—that's "motorboating"—which usually involves one or more audio stages. Motorboating can usually be eliminated by additional decoupling.

The regenerative superhet does have some shortcomings: There is still some reception of out-of-band signals and images. A few birdies appear as heterodynes without modulation, but they don't appear if the regenerative stage is operated just below oscillation. Skirt selectivity is poor for strong signals, but selectivity appears to be reasonably good for moderate to weak signals. The noise level is rather high, but I accept that because of the regenerative IF amplifier. The noise is regenerated along with the signal.

The regenerative superhet does have a couple of advantages over regenerative receivers using leak detectors. It does not overload on strong AM signals, and there is no tendency to lock onto a nearby strong carrier when trying to tune a weak signal. You just hear both signals together because of the poor skirt selectivity.

Embellishments

Lately, I built a simple VFO (Fig 13) to use with the regenerative superhet. I found a schematic diagram for a simple VFO on the Web that appears in several variations on more than one site. I built this VFO with two 2N3819s taken from an earlier converter that was not being used. The results have been impressive.

The VFO does not drift much. I'm sure if I used a good frequency counter over several hours, I could detect drift; but after 45 minutes, it's still tuned to the center of a weak AM station. I wound a solenoid coil on a one-inch-diameter acrylic form and secured the turns with acrylic coil sealer. I used a WW2 surplus tuning capacitor that has a 50:1 reduction drive. I mounted it parallel to the heavy-gauge aluminum front panel (it's actually screwed to the front panel for grounding) and fashioned a 1½-inch crank from yellow pine to turn the shaft. Heavy copper wire (#24 AWG) was used for the tuned-circuit wiring. My haphazard tuned-circuit calculations (I don't have a dip oscillator for the 4 to 8 MHz range) resulted in the VFO output being between 4 and 8 MHz.

I have learned, after a little experimentation, to set the regenerative superhet's **FINE** regeneration control fully counterclockwise (minimum regeneration) and tweak the **COARSE** regeneration control (just barely touching the four-inch long yellow pine "lever" that's clamped to the shaft) so that the transition between oscillating and not oscillating is somewhere within the regenerative passband—preferably near 2 MHz. I then tune just to the low (not-oscillating) side and leave it set there. Tuning is then done with the VFO after making sure both front-end RF amplifier stages are peaked on the band being tuned.

The result is a very narrow IF response—so narrow that speech intelligibility is compromised somewhat. The sensitivity also appears to be high, although that's very hard to determine. I do seem to hear weak, distant stations better than before. The stations I hear now, tuning with the VFO, are separated, not crowded together. Skirt selectivity is better. I can swing the FINE tuning control (the floating-rotor capacitor) either side of the center of an AM signal and hear the signal frequency content becoming much higher and also hear fringe howl just becoming audible. It's usually necessary to retune the IF slightly for the first 30 minutes or so after turning on the receiver to keep just below oscillation, but that was true before the VFO was constructed. Then, as a final step to improve sensitivity, the **FINE** regeneration control can be turned slowly clockwise until fringe howl is heard and then backed off slightly. The improvement in signal level as the **FINE** regeneration control is turned clockwise is enough to make a not-quite-intelligible signal intelligible.

As I write, the regenerative superhet has one peculiar behavior that needs further investigation and correction. After several hours of warm-up, with regeneration set correctly and a station tuned in, the regeneration will rapidly increase past oscillation, remain there for several minutes and then, usually, but not always, return to near its original setting. These excursions occur without any of the receiver controls being touched. I hypothesize that noise in the regenerative 2N3819 together with the small, but steady, heat build-up in the 2N3819 is the cause. I am looking toward building a second-generation regenerative IF board with an acrylic coil form for the bifilar transformer, heavy bus wire for the conducting paths, a heat sink for the 2N3819 and conformal coating on the board.

The frequency coverage of the regenerative superhet is approximately 4 to 15 MHz with crystals and about 6 to 10 MHz with the VFO. A frequency counter would be a useful addition to the regenerative superhet.

Conclusion

I have written this article to make available several possibly useful ideas to anyone who homebrews receivers:

1. Enclosure of solid-state receiver circuitry in a galvanized steel enclosure with individually shielded compartments
2. Capacitor coupling for a short antenna to a two-tuned-circuit front end
3. A tunable, high gain, selective regenerative IF amplifier driving a diode-bridge detector
4. A floating-rotor band-spread capacitor
5. VFO tuning, which together with the tunable IF, allows setting the IF for high sensitivity and narrow bandwidth, and
6. A power supply separated from the receiver by a cable of sufficient length to reduce noise pickup from the power supply.

Some of these ideas are not new; some of them may be. They can be combined to make an interesting receiver. I should also mention the very impressive homebrew receiver of W8ZR that I saw on the Web. It has a similar two-stage toroid-coil front end. I had completed the regenerative superhet before I saw his article.

Notes

[1]E. Bucher, *Vacuum Tubes in Wireless Communication*, (Bradley, Illinois: Lindsay Publications Inc); **www.lindsaybks.com/prod/otr.html**. Lindsay now prints this book, which was originally published in 1918.

[2]D. L. Metzger, *Electronics Pocket Handbook*, second edition (Englewood Cliffs, New Jersey: Prentice Hall, 1992), p 42.

Bill Young, WD5HOH, is retired following a 36-year career as a project engineer and manager with NASA in the biomedical hardware area. He was first licensed as KN5DNM in about 1953, and he has been WD5HOH (General) since about 1980. Bill holds a BSEE degree from the University of Texas (1961) and an MS degree from the University of Houston at Clear Lake in environmental management (1981). □□

HF Receiver Dynamic Range: How Much Do We Need?

We often discuss how good receivers are. Let's look at how good they need to be.

By Peter E. Chadwick, G3RZP

It was realized in the 1960s that the performance of many HF amateur—and for that matter, commercial—receivers was limited by their lack of dynamic range. Dynamic range is defined as the ability to produce an acceptable output from a weak wanted signal in the presence of large unwanted signals on possibly widely separated frequencies. Unfortunately, the term "dynamic range" has been applied to a number of different receiver parameters, so it is necessary to define it exactly here.

Dynamic Range: What Is It?

In the field of radio engineering, dynamic range is arguably one of the most confusing terms available, since it has several different meanings depending upon the context. For purposes of this article, there are several dynamic-range definitions applicable. These are:

- Limitations produced by the intermodulation in the receiver
- Effects caused by local-oscillator phase noise (reciprocal mixing)
- Spurious responses, both internal and external

As a general principle, a receiver should be designed so that its dynamic ranges, as limited by intermodulation and phase noise, are equal; that way, none of its available performance is wasted. Various real factors can modify this principle, though, and as shown later, can lead to a demand for a larger phase-noise-limited dynamic range. The limitation set by spurious responses may be the result of either discrete spurs in injection frequencies, or it can be caused by the classic receiver spurious responses such as images, harmonic mixing and so forth.

Intermodulation-limited dynamic range or ILDR, often confusingly referred to as spurious-free dynamic range or SFDR, is defined as:

$$ILDR = \frac{2}{3}\left(IP3 - NF\right)\text{dB} \qquad \text{(Eq 1)}$$

where *IP3* is the input third-order intercept point in dBm, and *NF* is the receiver's equivalent input *noise floor* in dBm—not to be confused with its *noise figure*. *ILDR* represents the range, in decibels, between the level of input signals that are strong enough to cause intermodulation equal in

Three Oaks Braydon
Swindon SN50AD England
peter.chadwick@ieee.org

level to the receiver noise floor and the noise floor itself.

The *ILDR* concept is based on simple third-order intermodulation of two strong signals. Where there are many signals intermodulating together, there would be far more products. Further, because the signals are modulated, the products have a mixture of the modulations of the individual signals on them, so the effect becomes more noise-like. That explains why the total number of signals available is important.

If it were assumed, however, that the *ILDR* needed to be such that the strongest signals would produce IM products 10 dB below the noise level measured at the antenna terminals, provided such IM products were not excessive in number, the number of signals would have little effect. To quantify these numbers, some arbitrary assumptions are made: The number of IM products [which is $0.5n(n-1)$, where n is the number of signals producing the intermodulation, see Reference 1] multiplied by twice the measurement bandwidth is to be less than 10% of the bandwidth over which the measurement is made. For example, if the bandwidth over which measurement were made were 5 MHz and the measurement bandwidth were 3 kHz, then the number of products multiplied by 6 kHz should not exceed 500 kHz. Solving the quadratic equation for n gives a maximum number of signals in the largest bin of 13.[1] The assumption is that although each intermodulation product has a bandwidth of twice the original modulation, the lack of correlation between the various signals in the largest bin means that the IM products have a negligible chance of summing in any one particular measurement's bandwidth.

The next lowest bin also needs consideration. For any given input intermodulation intercept point, signals in the next lowest bin will produce IM products 30 dB lower than those in the higher bin. Unless the number of products exceeds 1000, they will not have any effect on a performance tailored towards not producing measurable IM products from the higher bin. This requires the number of signals in the bin to be fewer than 45. The same argument means that the third bin requires less than 10^6 products or over 1400 signals within it.

Note

[1]The term "bin" in this context is a selected group of signals of a defined characteristic, for example, between defined frequency or amplitude limits. The parameter is the number of signals in a given "bin."

As far as the HF amateur bands are concerned, the largest signals are generally those in the closest international-broadcasting bands. Those are the 49 and 41-meter bands for 7 MHz, the 31 and 25-meter bands for 10 MHz and the 21 and 19-meter bands for 14 MHz. These signals are about 10-kHz wide, so the number of available signals that do not overlap within the band under consideration can be considered low enough to meet the above criteria for bin numbers.

Phase-noise-limited dynamic range (*PNDR*) is given by:

$$PNDR = N - (\alpha + 10 \log \Delta f)\,\text{dB} \qquad \text{(Eq 2)}$$

where α is the phase noise spectral density in –dBc/Hz of the local oscillator at the offset frequency under consideration. *NF* is the receiver's equivalent input noise floor in dBm, and Δf is the receiver bandwidth in hertz. *PNDR* thus represents the level of a single off-frequency signal that would increase the noise floor by 3 dB.

Spurious-free dynamic range is determined by both *ILDR* and *PNDR*, because either effect can raise the receiver's noise floor—directly in the case of internal spurious, and dependent upon the level and exact frequency of the interferer in the case of the external spurious. Because a spurious response is usually a narrow-band phenomenon, it represents a limitation in performance that is bandwidth-dependent: A narrower bandwidth would reduce the receiver's noise floor, all other factors being equal; but the spurious response would stay at the same level. Ideally, all spurs should be such that they are below the noise floor at the narrowest receiver bandwidth.

The Radio Environment

The actual dynamic range that is required for HF receivers operating in the Amateur Service has not been determined in any detail, as far as I know. Reference 2 contains some data, but it is not exhaustive. Reference 3 determines acceptable noise figures for LF-band DX operating. Reference 4 contains much the same information. Reference 5 shows some data, but is concerned more with the generality of the HF band. Reference 6 uses figures from a 1970s professional survey of the HF band. Furthermore, all these references are now rather old. Because of this lack of up-to-date information, a question arises as to how much performance is really needed. I decided to make a series of measurements.

Measurement Techniques

This is a case where simple and rather old equipment can give more meaningful results than a mass of data from a computer-controlled spectrum analyzer. For example, a "peak-hold" cannot differentiate between the signal reaching its peak and a transient. An HP-141 spectrum analyzer was used to count the number of signals of various levels present at the receiver input. (See Fig 1.) The display's center frequency was chosen for each measurement to be the lower edge of each amateur band. Then the band was chosen that had the greatest signals contained within ±1 MHz of that frequency. These were nonamateur signals, of course.

The noise from the antenna in an SSB bandwidth was measured using my station receiver (an FT-102), a calibrated signal generator and a step attenuator. Again, a computer-con-

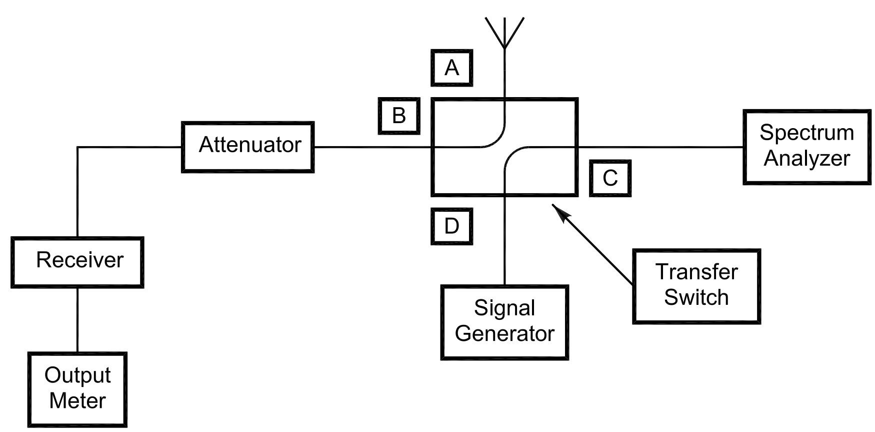

Fig 1—Measurement equipment arrangement. The transfer switch connects ports A and B at the same time as ports C and D. Alternatively, it connects A to C and B to D.

trolled system would have difficulty deciding if the signal on the channel were noise or a signal.

The band ±1 MHz relative to the amateur band was chosen on the basis that receivers of reasonable performance would almost certainly have some band-limiting filters at their inputs. The antennas were tuned, as is common amateur practice, and so provided some—but not very much—discrimination against out-of-band signals.

The antennas used in the determination were as follows:

- 10 meters, four-element monoband Yagi at 68 feet
- 15 meters, four-element monoband Yagi at 68 feet, interlaced with the 10-meter beam, separate feeders
- 20 meters, five-element monoband Yagi at 62 feet
- 30 meters,
  (1) 80 meter dipole at 60 feet, fed with open wire line and matching unit
  (2) Sloping dipole from 60 feet, sloping to west
- 40 meters
  (1) 80-meter dipole as for 30 meter
  (2) Sloping dipole from 60 feet, sloping north-northwest
  (3) Sloping dipole from 60 feet, sloping east
  (4) Sloping dipole from 60 feet, sloping south-southwest. The unused sloping dipoles were inductively tuned to act as reflectors
- 80 meters
  (1) The 80-meter dipole, as for 40 and 30
  (2) the 60 foot tower, top loaded with the beams, fed as a folded unipole
- 160 meters, the tower as for 80 meters.

Measurements were always made using the antenna that gave the largest signals. The location is rural, and calculation of the received noise levels from estimates of the capture area of the antennas, combined with the expected rural noise field strengths derived from the ITU curves, gives broad agreement with the results actually achieved. Although by no means exact measurements, the results are of the correct order of magnitude—see Reference 4.

Because the effect of limited *PNDR* and *ILDR* is to raise the perceived noise floor of the receiver, I needed some method of determining if the receiver were operating in a linear range. This was done by using an audio output meter, switching the AGC off and using the manual RF and AF-gain controls to set a reference level when the antenna was connected. By switching the attenuator to a large attenuation (60 dB or more), the effects of the receiver's internal noise floor could be determined. If the drop in output was more than 10 dB, it was considered that the receiver noise contribution was negligible. As a test for linearity, 3 dB of attenuation was switched in with the antenna connected and the output was observed to drop by 3 dB in all measurement cases. If the measurements had been limited by intermodulation, the insertion of a 3-dB loss in the antenna feed would have caused a much greater drop in output.

Results

Preliminary investigation centered on finding that part of the HF spectrum offering the largest signals to the receiver. As expected in the European environment, this was found to be on 7 MHz in the 41-meter broadcast band. Measurements to confirm this were taken in other bands, but the most demanding receiver environment was confirmed as 7 MHz. WE9V suggested in private communication that 28 MHz might be more demanding, but this was not so, basically because the higher signal levels appear always to be associated (not surprisingly) with a greater antenna noise.

Measurements were made at several times, with attempts to measure the same frequencies at similar times of day. Signals were classified into several ranges or bins by their power level and frequency. The power-level bins were –10 to –20, –20 to –30, –30 to –40, –40 to –50 and –50 to –60 dBm. The frequency bins were each 200 kHz wide, covering 7.0 ± 1 MHz. The number of signals that fell into the highest two or three power bins was particularly noted. It was interesting that on several occasions, there were signals in the top bin and none in the next bin. It was not considered worthwhile to count the exact numbers of signals in the lower-power bins, as their effect would be relatively negligible, and they would be difficult to determine from the analyzer display. The worst cases (largest signals and least antenna noises) are shown in Table 1 below.

Measurements were made on many days, and therefore successive measurements may be unrelated in time. This does give a picture of the variation in signal levels and noise floor with time.

Results Analysis: Intermodulation Requirements

From these results, it is possible to derive the minimum *ILDR* that the receiver needs in order to avoid intermodulation problems. This approach assumes a worst case because it makes the assumption that the products will fall on a wanted frequency. Another pessimism is to assume that even if only one signal were counted in the top bin, the IMD was being caused by *two* signals of the same power level. Taken together, all these assumptions produce a very high probability that reception will be intermodulation-free.

Assume that all intermodulation products are required to be 10 dB below the received noise level, and that intermodulating signal levels are in the

Table 1—Measurement results for 7 MHz

UTC	*Noise Level (dBm)*	*Number of Signals* –10 to –20 dBm	–20 to –30 dBm	–30 to –40 dBm
0200	–99	1	12	12
0615	–105	0	1	4
1445	–105	0	1	1
1500	–108	0	2	2
1545	–106	0	0	2
1645	–97	1	3	16
1715	–91	5	5	20
1745	–98	2	3	23
1815	–99	2	8	23
1945	–97	1	4	18
2000	–97	3	13	5
2045	–91	2	6	27
2050	–94	2	12	23
2145	–106	0	6	25
2200	–97	1	3	23
2230	–99	1	12	10
2255	–101	2	5	7

middle of the bin. That is, if signals exist in the bin –20 to –30 dBm, they are all assumed to be –25 dBm. Because the signals in the next lower power bin will produce IMD products 30 dB lower in power, then unless there are more than 1000 products (45 signals), it is assumed that they can be ignored. This approach predicts a worst case, insofar as there is an inherent assumption that the products will fall on a wanted frequency. A further worst case is to determine the necessary intercept-point level as if there were at least two signals in the top bin, even when only one was observed.

As an example, we will take the situation at 1645 UTC in Table 1. The received noise level is –97 dBm, so we want the noise caused by intermodulation to be 10 dB lower, or –107 dBm. The biggest received signal is in the range –20 to –30 dBm, so it is assumed that there are two signals at –25 dBm. The resultant intermodulation product then needs to be at –107 dBm, an intermodulation ratio (IMR) of 82 dB. From the "2-for-1" rule (IMD ratio decreases by 2 dB for every 1 dB decrease in power), this IMR will be achieved by a system with an input intercept point of +16 dBm.

Applying Eq 1, with the noise floor at –107 dBm, allows the *ILDR* to be derived. The receiver noise figure is derived by assuming a 3-kHz noise bandwidth. That gives a thermal noise floor of –140 dBm, and the derived noise floor is the difference between –140 dBm and a level 10 dB below the received noise from the antenna.

Table 2 shows the third-order intermodulation input intercept point, noise figure and *ILDR* that are necessary to ensure that all intermodulation products are at least 10 dB below the antenna noise. Note how much all these requirements vary with time of day.

Table 2 does assume that the added noise produced by receiver deficiencies is caused either by the noise figure of the receiver or by the intermodulation. In that case, the effective noise floor of the receiver is increased by 0.4 dB. In the case where both noise figure and intermodulation are raising the noise floor, the floor is raised by 0.8 dB.

Results Analysis: Phase-Noise Requirements

In the case of reciprocal mixing, the assumption that signals in lower bins can be ignored is invalid. The phase noise of all signals will add directly, so that 10 signals in a bin 10 dB below the strongest signals will add as much phase noise as one signal in the top bin—assuming of course that the phase-noise density is constant. For Table 3 below, the effect of any signals in the bin 10 dB below the highest level has been included.

Although it is usual to assume that phase noise of an oscillator follows the model originally developed by Leeson (ex W6QHS, now W6NL, see Reference 7) recent developments in multiple-tank oscillators have provided faster noise fall-off rates than the classic 6-dB per octave of separation from the carrier. However, many oscillators would appear to have practically reached the noise floor beyond a few megahertz of separation.

Table 3 uses the data from Table 1 to calculate the phase-noise requirements that produce oscillator noise 10 dB below the antenna noise. It assumes a phase-noise density that is flat with frequency, which is somewhat artificial and perhaps unduly pessimistic. To counterbalance this, however, the calculations ignore any effects of the generally greater number of signals in the lower-amplitude bins.

The calculation method used was to calculate the absolute power in each bin by summing the individual signal powers, and then to sum the powers of all the bins to give a *single-signal equivalent input power*. The *PNDR* was then determined as the ratio (rounded to the nearest decibel) between the single-signal equivalent input power and a level 10 dB below the noise power delivered by the antenna.

Conclusions

It is instructive to compare the various dynamic range requirements that result from the above calculations. Such as comparison is shown in Table 4.

As expected from the above discussion about the number of low-level signals affecting the *PNDR* requirements, the measurements confirm that the demands for maximum *PNDR* do not always coincide with those maximum *ILDR*. Generally speaking, *PNDR* was found to be more stringent than the *ILDR* by up to 11 dB. The

Table 2—*IP3*, *Noise Figure* and *ILDR* Requirements for 7 MHz

UTC	*Noise Level (dBm)*	*Receiver Noise Figure (dB)*	*IP3 Required (dB)*	*Dynamic Range Required (dB)*
0200	–99	31	+32	94
0615	–105	25	+20	90
1445	–105	25	+20	90
1500	–108	22	+21.5	93
1545	–106	24	+5.5	82
1645	–97	33	+36	95
1715	–91	39	+28	86
1745	–98	32	+31.5	93
1815	–99	31	+32	94
1945	–97	33	+31	92
2000	–97	33	+31	92
2045	–91	39	+28	86
2050	–94	36	+29	89
2145	–106	24	+20.5	91
2200	–97	33	+31	92
2230	–99	31	+32	94
2255	–101	29	+33	96

Table 3—Phase Noise Limited Dynamic Range Requirements

UTC	*Noise Level (dBm)*	PNDR *(dB)*
0200	–99	98
0615	–105	90
1445	–105	90
1500	–108	86
1545	–106	85
1645	–97	84
1715	–91	94
1745	–98	97
1815	–99	99
1945	–97	94
2000	–97	98
2045	–91	91
2050	–94	94
2145	–106	100
2200	–97	94
2230	–99	98
2255	–101	100

required dynamic ranges are not as high as has previously been considered to be the case, but the strong daily variations show a vital requirement for the available dynamic range to have a variable start point. Thus a variable antenna attenuator has obvious advantages, but the attenuation steps need to be much smaller than the 6 dB or even 20 dB steps provided by commercial transceivers. G3HCT has suggested that even steps as small as 1 dB can produce significant apparent changes in received signal-to-noise ratio. The disadvantage is, of course, that greater operator skill is required.

A receiver with a 10-dB noise figure on 7 MHz, with a typical input third-order intermodulation intercept point of about +11 dBm without attenuation, could apparently benefit from up to 25 dB of variable input attenuation. It would also need a *PNDR* of 100 dB at the frequency offsets in question. Obviously, the use of pre-mixer selectivity has a major effect on the performance requirements, although at 7 MHz, the proximity of the broadcast band offers little possibility of really effective filtering in conventional circuits. The attenuator is, of course, equally useful for setting the *PNDR* start point.

Valid questions are the effects of using a narrower measurement bandwidth and how far the measurements are representative of amateur station installations. Since the effect of multiple-station intermodulation is to produce a broadband noise effect, the use of a narrower bandwidth will reduce the effects proportionately, and so to a first approximation, the results are independent of receiver bandwidth. If performance is limited by the *PNDR*, the same argument will apply.

For UK amateur practice, it must be admitted that the location and antenna systems used for the measurements are atypical, being respectively quieter and larger than many. Even in comparison with the US, the installation is probably in the upper quartile in these respects. This means that the received noise is lower than for many amateurs, while the received signals will be higher. Even in comparison with the super stations, although the levels will be different, the relative levels of unwanted signals and antenna noise will be about the same, since larger antennas will tend to deliver more noise as well as larger unwanted signals. The amateur with a small antenna in a suburban garden will probably see a higher received noise level and a lower level of unwanted signal, thus easing dynamic-range problems. Thus, the conclusions are claimed to be generally applicable. Although measurements were made on 7 MHz with the antennas producing the highest signal levels, it was noticeable that the antennas producing the lower signal levels also produced lower noise floors. So, the dynamic range remained the same, although shifted along the scale.

Are our receivers too sensitive? The answer is "Probably, but . . ." There are some imponderables: On the LF bands especially, the use of separate receiving antennas producing much lower signal levels but lower levels of noise means that requirements may exist at times for the low noise-figure levels that are typically seen in modern receivers. Notice that US conditions seem a lot quieter than those in the UK. Many UK operators have commented on this, and numerous US operators have commented on how noisy and crowded the bands are in Europe.

Are our receivers adequate in terms of reciprocal mixing? Phase-noise requirements have become more pressing since the introduction of synthesized equipment; although even here, a caveat exists insofar as the limit can well be fixed by the performance of the transmitters producing the large received signals. Nevertheless, the requirement for good phase-noise performance is shown, on the whole, to exceed the requirement for intermodulation performance, mostly because *all* the unwanted off-tune signals sum directly to degrade performance, even those at lower power levels.

Do our receivers have adequate intercept points and *ILDR*? The answer is apparently "Yes, but only if you can move the dynamic range up and down to suit conditions." A not-too-distant future job at the G3RZP station is build a finely-variable step attenuator to go in the antenna line to the receiver.

Acknowledgement

Thanks to G3HCT, G3SEK, G8EUX and WE9V for their input and advice.

References

1. P. E. Chadwick, "Phase Noise, Intermodulation and Dynamic Range," *Proceedings of RF Expo*, Anaheim, California, 1986.

Table 4—Dynamic Range, Phase Noise and Noise Figure Requirements Compared

UTC	*Noise Level (dBm)*	*Receiver Noise Figure (dB)*	*IP3 Required (dB)*	*ILDR Required (dB)*	*PNDR Required (dB)*
0200	–99	31	+32	94	98
0615	–105	25	+20	90	90
1445	–105	25	+20	90	90
1500	–108	22	+21.5	93	86
1545	–106	24	+5.5	82	85
1645	–97	33	+36	95	84
1715	–91	39	+28	86	94
1745	–98	32	+31.5	93	97
1815	–99	31	+32	94	99
1945	–97	33	+31	92	94
2000	–97	33	+31	92	98
2045	–91	39	+28	86	91
2050	–94	36	+29	89	94
2145	–106	24	+20.5	91	100
2200	–97	33	+31	92	94
2230	–99	31	+32	94	98
2255	–101	29	+33	96	100

2. P. E. Chadwick G3RZP, "Dynamic Range, Phase Noise and Intermodulation," *RadComm*, May 1984, p 223.
3. John Devoldere ON4UN, *Low Band DXing*, first edition (Newington, Connecticut: ARRL, 1987), Chapter IV.
4. *Radiocommunication Handbook*, RSGB, 7th edition, figure 6.17, p 6.10.
5. U. L. Rohde, DJ2LR, "How many signals does your receiver see?" *ham radio* magazine, June 1977, p 58.
6. R. A. Barrs, "A Re-appraisal of HF Receiver Selectivity," *IERE Conference on Radio Receivers and Associated Systems*, IERE, Leeds 1981, ISBN 0 903748 45 2.
7. D. B. Leeson, "A Simple Model of a Feedback Oscillator Noise Spectrum," *Proceedings of the IEEE*, Vol 54, February 1966.

Born in 1947, the son of the late G8ON, he went to his first Field day in 1948. He obtained his license in April 1963, just before his sixteenth birthday. He joined the Marconi Co in 1964 as an apprentice, and moved widely within the radio communications industry as a design engineer, prior to joining what was Plessey (now Zarlink) Semiconductors in 1979 as a Principal Applications Engineer. He is now a Senior Principal Engineer involved with systems design of new IC's for the RF markets. He has generated over 20 patent applications, and has lost count of how many actually got as far as being issued! A Senior Member of the IEEE, he has presented or published some 27 times in the US and Europe. He has been a lecturer for several years at the Essex University RF Engineering Course, and is a member of the Industrial Advisory Board for Master's Degree in Electronic Engineering at Bristol University. He has also served on several IEE and IERE Conference Committees, and chaired two international Conferences on Frequency Control and Synthesis. He is a reviewer for IEE Electronics Letters.

He was a member of the Council of the RSGB for some years, and was President in 1993; currently, he is a member of the Technical and Publications and Licencing Advisory committees of RSGB. He has represented Amateur Radio interests at CEPT and ITU as part of the UK delegation, and is an IARU Technical Advisor. He is on DXCC Honor Roll, requirin four countries for the "No 1 position," and builds a lot of his own equipment, as well as restoring "boat anchors." Other interests include model engineering and steam railways. He is married to G4FNC, who he met at a radio club. □□

Periscopes for Microwaves: 10 GHz without Feed-Line Loss

Here's how to get 10-GHz energy to the top of your tower with no feed line!

By Paul Wade, W1GHZ

Microwave operation from mountaintops is very effective and great fun in summer. In winter, however, many mountaintops are inaccessible and more are inhospitable. More importantly, we are rarely on a mountain during short-lived propagation enhancements. We would all like to be able to operate from home, but many of us don't have superior locations. My house is surrounded by trees and my tower barely reaches the treetops.

Some tests have shown that 10-GHz operation is possible at my location, though. I have made rain-scatter and snow-scatter contacts by pointing vertically through a skylight and other contacts by aiming a dish at the tops of trees to scatter off them. If I could get the 10-GHz signal to the top of the tower, better results should be possible.

Traditionally, we use a transmission-line feed to get signals to the antenna. Feed-line loss is a difficult problem for microwave antennas. Low-loss feed line is expensive and tends to be large in diameter. At 10 GHz, coaxial feed line larger than about a half-inch diameter will support waveguide modes that increase loss, so coax is not a good choice. Waveguide has lower loss than coax, but not good enough for a decent tower: The loss approaches 10 dB per 100 feet of WR-90 waveguide at 10 GHz.

One alternative is to mount parts of the system on the tower. Many hams have been using this approach successfully, but there are problems with weatherproofing and stability over temperature extremes. Tales of climbing a tower during a New England winter for repairs make this approach sound less attractive.

For several years now, Dick, K2RIW, has been talking about the merits of a periscope antenna system for microwaves. He convinced me to do some reading.[1] Then, I made some performance estimates for a reasonably sized system. The numbers looked good, so I decided to put a periscope system together and I found that it really works. Then, to improve the system, a better understanding was desirable.

Description

A periscope antenna system consists

161 Center Rd
Shirley, MA 01464
w1ghz@arrl.net

[1]Notes appear on page 51.

of a ground-mounted antenna pointed upwards at a reflector that redirects the beam in a desired direction. A simple version, with a dish on the ground directly under a flat 45° reflector, is shown in Fig 1. The flat reflector is often referred to as a flyswatter, and we will use that terminology. The lower antenna does not need to be under the flyswatter reflector; the reflector tilt angle can compensate for offset configurations, as shown in Fig 2. The geometry is a bit more complex, but a personal computer could easily do the calculations and accurately control the flyswatter pointing.

Periscope antenna systems have been used for fixed microwave links with good results, but are no longer allowed by the FCC for new commercial installations. The reason seems to be that most good sites are so crowded with antennas that low side lobes are required; stray reflections from edges and supports of the flyswatter reflector make it difficult to meet the requirements. However, for amateurs, antenna selection is a matter of individual choice.

The only recent publications found in major databases on periscope antennas are in Russian. In English, there is a description in the *Antenna Engineering Handbook*[1, 2] which relies on a confusing graph for explanation. After some study and working out a few examples, it dawned on me that the graph is attempting to display an equation with four variables in a two-dimensional medium.

The only amateur reference I've seen for periscope antennas is by G3RPE,[3] and W1JOT was kind enough to provide a copy. G3RPE limits his analysis to 10 GHz, thus eliminating one variable, and provides six additional graphs to illustrate some of the possible combinations. This is an improvement but it still doesn't provide much insight.

I used the G3RPE graphs and the ones in the *Antenna Engineering Handbook* to work out estimates for a number of possibilities. It appeared that the gain of a periscope antenna system could be within a few decibels of the ground antenna, given the right combination of dimensions. Usually, the flyswatter has a larger diameter than the ground antenna. Thus, reasonable antenna gain is possible with a dish on the ground, so that feed-line loss is low. The "feed-line" loss in the flyswatter is power radiated from the ground antenna that misses the flyswatter and continues into space; this is obviously dependent on the geometry of the periscope components.

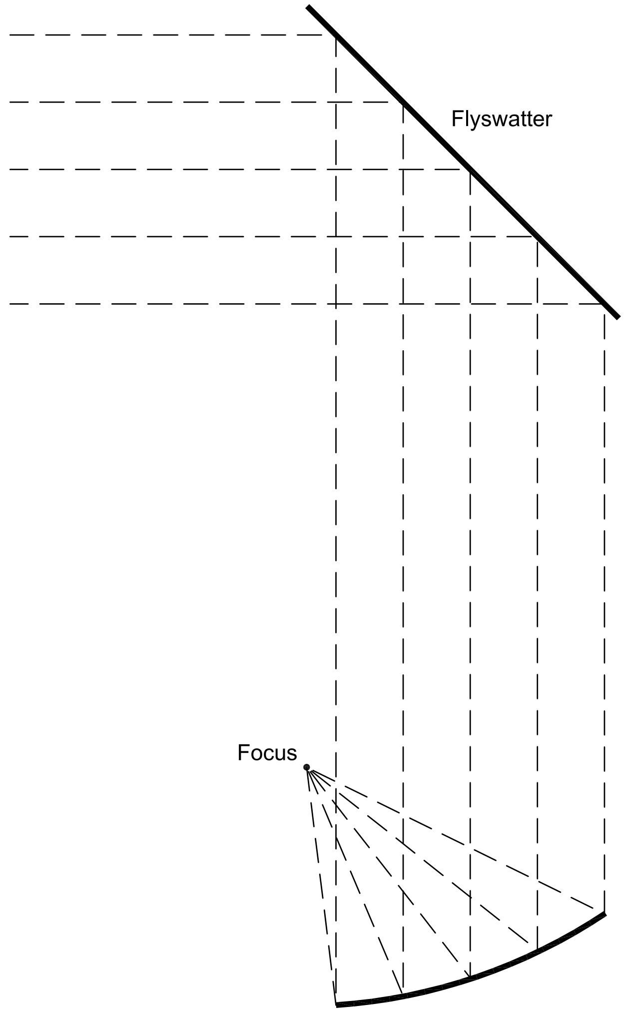

Fig 1—A vertically fed periscope antenna system with an offset-fed parabolic dish.

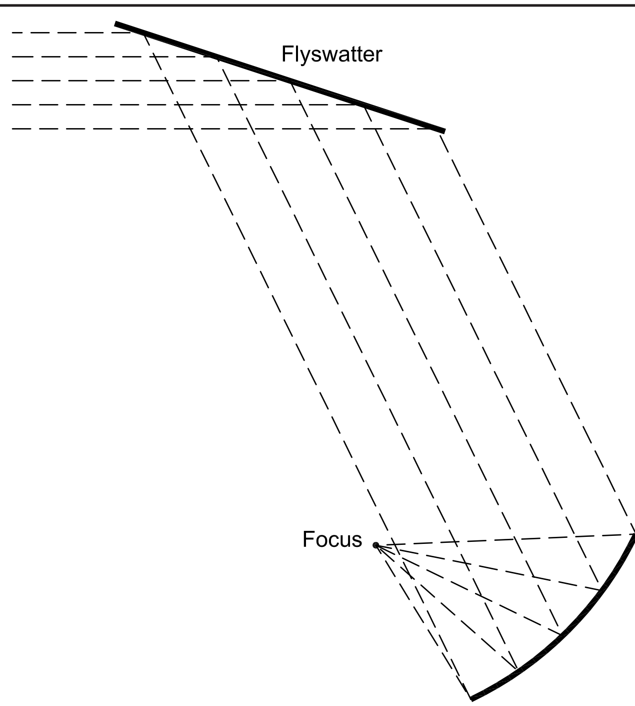

Fig 2—An offset-fed periscope antenna system with an offset-fed parabolic dish.

Fig 3—A rear view of the flyswatter assembly with the tilt sensor in place (white box on the angle bar). The swivel caster that permits the actuator to swivel is mounted near the top of the mast, among several cables. As the actuator lengthens or shortens, it adjusts the angle of the flyswatter to alter the takeoff angle of the antenna beam. A rotator at the top of the mast moves the flyswatter to set the azimuth of the antenna beam.

Fig 4—The complete flyswatter assembly mounted at the bottom of a tower for tests.

Some combinations of dish, flyswatter and spacing can even provide more gain than the dish alone—like a feed line with gain!

The beamwidth of the periscope system is similar to the beamwidth of a dish with the same diameter as the flyswatter. For some combinations, this can result in a beamwidth significantly narrower than a dish with equivalent gain—a minor disadvantage for the periscope antenna.

Another minor problem with periscope antennas concerns polarization. If the flyswatter rotation is independent of the ground antenna, the polarization changes with rotation. There are several ways to compensate:

1. Rotate the ground antenna as well as the flyswatter
2. Rotate the feed polarization, or
3. Use circular polarization and accept a 3-dB loss in all directions.

For rain and snow scatter, I've found that polarization does not seem to be particularly critical.

Since the flat flyswatter is not frequency sensitive, it can be used on other microwave bands as well. The ground antenna could be a dish with feeds for multiple bands, or separate ground antennas could be used, adjusting the flyswatter angle for each band.

Construction

The first step in constructing a periscope was to find a good-sized piece of aluminum for the flyswatter. I located a 30-inch octagon left over from one of my daughter's high-school adventures (I've been assured that it came from scrap somewhere and not from a road sign). To stiffen the mounting area, I attached a heavy aluminum frying pan with a flat rim to the center of the octagon and bought a new pan for the kitchen.

I've seen commercial periscope installations with fixed flyswatters and they looked straightforward: The flyswatter is attached to the side of the tower and bolted down after adjustment. However, I've seen no example of a flyswatter that rotates and tilts, so the difficult part was figuring out the mechanics.

One approach for rotation would be to mount the flyswatter on the central mast below other antennas. The mast could pass through a central hole in the flyswatter. For a larger flyswatter, the area blocked by the tower would be small, but I wanted to do initial testing with a reasonably sized reflector. An alternative that is shown in the G3RPE article mounts the flyswatter on one side of the mast, with the ground antenna following it around the tower as it rotates.

A better approach is to mount the flyswatter on the side of the tower, with rotator and support above it, out of the RF path. Since I didn't trust an ordinary rotator in tension with the antenna weight pulling it apart, I chose the style that has the mast passing through the body of the rotator. This is attached to a very solid side bracket, available from IIX Equipment.[4] The tower causes some blockage in one direction, but not enough to prevent successful contacts.

Tilting the flyswatter is a little more difficult, but that is important for scatter propagation. For a pivot, I drilled a hole through the mast for a stainless steel rod, which passes through sleeve bearings on each side. Two pieces of aluminum angle are mounted to the frying pan with a bearing fit in each; the mast is sandwiched between them. Fig 3 is a photograph of the assembly that should make this clear. To power the tilt mechanism, K2CBA provided an old TVRO dish actuator. The trial flyswatter assembly is shown in Fig 4.

When we tested the flyswatter before raising it, we found that the tilt actuator would bind—the actuator needed to pivot as the flyswatter tilted. Another bearing was needed in place of the U-bolts around the actuator in Fig 3. A quick trip to the hardware store located a large swivel caster, normally used for moving heavy machinery, with mounting holes that matched the U-bolt holes. When the caster wheel was removed, the actuator fit in the space and was

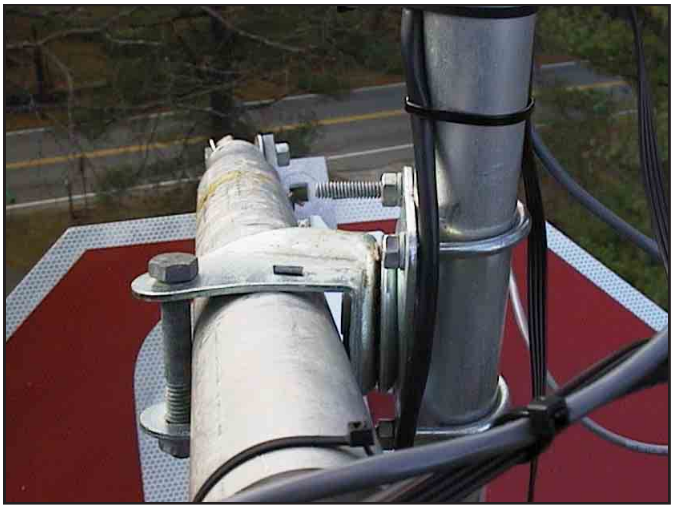

Fig 5—A close-up view from the mast end of the actuator. A heavy-duty, flange-mounted swivel caster serves as a mount and bearing for the actuator once the caster wheel is removed. The flange is secured to the mast by two U bolts.

Fig 6—The complete flyswatter assembly mounted at the top of a tower.

clamped in place by the axle bolt, as shown in Fig 5. Now the tilt operated smoothly, and we could move the assembly into position near the top of the tower, as shown in Fig 6.

On-the-Air Performance

For initial testing, I set up a 10-GHz rover system with an 18-inch DSS dish directly under the flyswatter. Separation between dish and flyswatter was about 10 meters, so the estimated gain from the curves was about 5 dB down from that of the 18-inch dish, but with the narrow beamwidth of a 30-inch dish. In addition, only crude azimuth and elevation indications were available. Clearly, this was not the optimum configuration, but it was adequate for initial testing.

The first 10-GHz tests were disappointing. Without any rain or other propagation enhancement, stations at a moderate distance were extremely weak, and closer ones were audible in all directions with no discernible peak. With trees in all directions, wet foliage was scattering and absorbing signals. After a couple of days without rain, signals weren't much better. The flyswatter does not clear the treetops; foliage has significant attenuation at 10 GHz.

Rain-scatter performance is much better. With rain predicted for the 1998 June VHF QSO party, I made a radome over the 10-GHz rover system using clear plastic garbage bags. We had several inches of heavy rain during the contest, which produced strong rain-scatter signals. I was able to work stations in four grids, with a best DX of 131 miles. I probably could have worked more if the rain hadn't stopped on Sunday morning. Most of the contacts were on CW, but AF1T, 41 miles away, was so loud that we switched to SSB. If you'd like to hear Dale's signal, there are some sound clips at **www.qsl.net/n1bwt**.

Rain-scatter signals typically have reasonably broad headings, so my crude azimuth indication was adequate. For elevation, a local beacon peaked broadly somewhat above horizontal, so I left the tilt at that setting. For normal propagation, beamwidth of the periscope antenna should be quite narrow, like any high gain antenna, so a better readout system is needed.

Since these initial tests, I have added a larger fixed dish at the base of the tower and a digital tilt indicator. With these improvements, I am able to make local 10-GHz contacts without enhancement; in addition, more-distant home stations may be contacted whenever there is any precipitation, typically in three grid squares. Fortunately, I am also able to work mountaintop stations without precipitation enhancement, since the precipitation tends to discourage the less hardy ones. To date, I have worked six grid squares, three without precipitation enhancement, on 10 GHz with the periscope antenna system.

We have noticed that rain scatter has an auroral quality, probably from random Doppler shift from raindrops falling at different speeds. Snow scatter can provide outstanding signals; if there is no wind and the snowflakes are large, the flakes fall slowly and good SSB quality is possible. Unfortunately, the northeast part of the USA had a severe drought for most of 1999 and another in 2001, so good conditions have been rare.

One last point concerns wind loading: I have never seen the flyswatter move or waver in any wind condition, even though the rotator is a cheap TV model with plastic gears. A dish of the same diameter has much more wind load than the flat reflector, and it would probably have long ago stripped the gears. For a very large flyswatter, it might be prudent to tilt it flat when not in use to further reduce wind load.

Analysis

While my periscope antenna appeared to work quite well, I really wanted to understand it better. There are two papers on periscope antenna systems referenced in the *Antenna Engineering Handbook* (see References 1 and 2), but I was not able to locate copies until several months later. The first paper, by Jakes,[5] used an analog computer for the analysis, which produced the confusing graph in *Antenna Engineering Handbook*. The second paper, by Greenquist and Orlando,[6] proved more promising, since it included not only a more detailed analysis of periscope gain, but also some measured results from actual antennas. The gain at 4 GHz is presented as a series of graphs similar to Fig 7. These curves are for a flyswatter with a square aperture, but a circle or other shape would only change the gain by a decibel or so. In addition, the true aperture is the projected aperture, viewed from the 45° angle, so that a rectangular flyswatter is needed to provide a square aperture and an ellipse is required for a round aperture. For simplicity, we will refer to the length of one side or diameter as the flyswatter aperture dimension, and not quibble about that last decibel or so.

A simple view of a periscope antenna considers it as a reflector antenna, just like a dish. The flat flyswatter reflector can be considered as a parabola with infinite focal length, so it must be fed from infinitely far away for the illuminating energy to be a true plane wave. Far-field radiation from an antenna is approximately a plane wave. Therefore, the feed dish can provide a plane wave if it is far enough away so that the flyswatter is in the far field, or Fraunhöfer region, of the dish—that is, beyond the Rayleigh distance. The gain of the periscope would be the gain of the flyswatter aperture area if the dish were able to illuminate it efficiently; a larger flyswatter would provide more gain.

However, as we shall see, the periscope antenna provides much better performance if the reflector spacing is smaller; that is, less than the Rayleigh distance of one of the reflectors. Therefore, a more complex analysis is required to calculate the gain. We must account for not only imperfect illumination of the flyswatter, but also the path loss (space attenuation) between the dish and flyswatter. Since path loss is defined between two isotropic antennas, we must also include the gain of the dish and flyswatter; both must be compensated for operation in the near field, or Fresnel region. In the Fresnel region, a large flyswatter may be illuminated with more than one Fresnel zone, and the second zone is

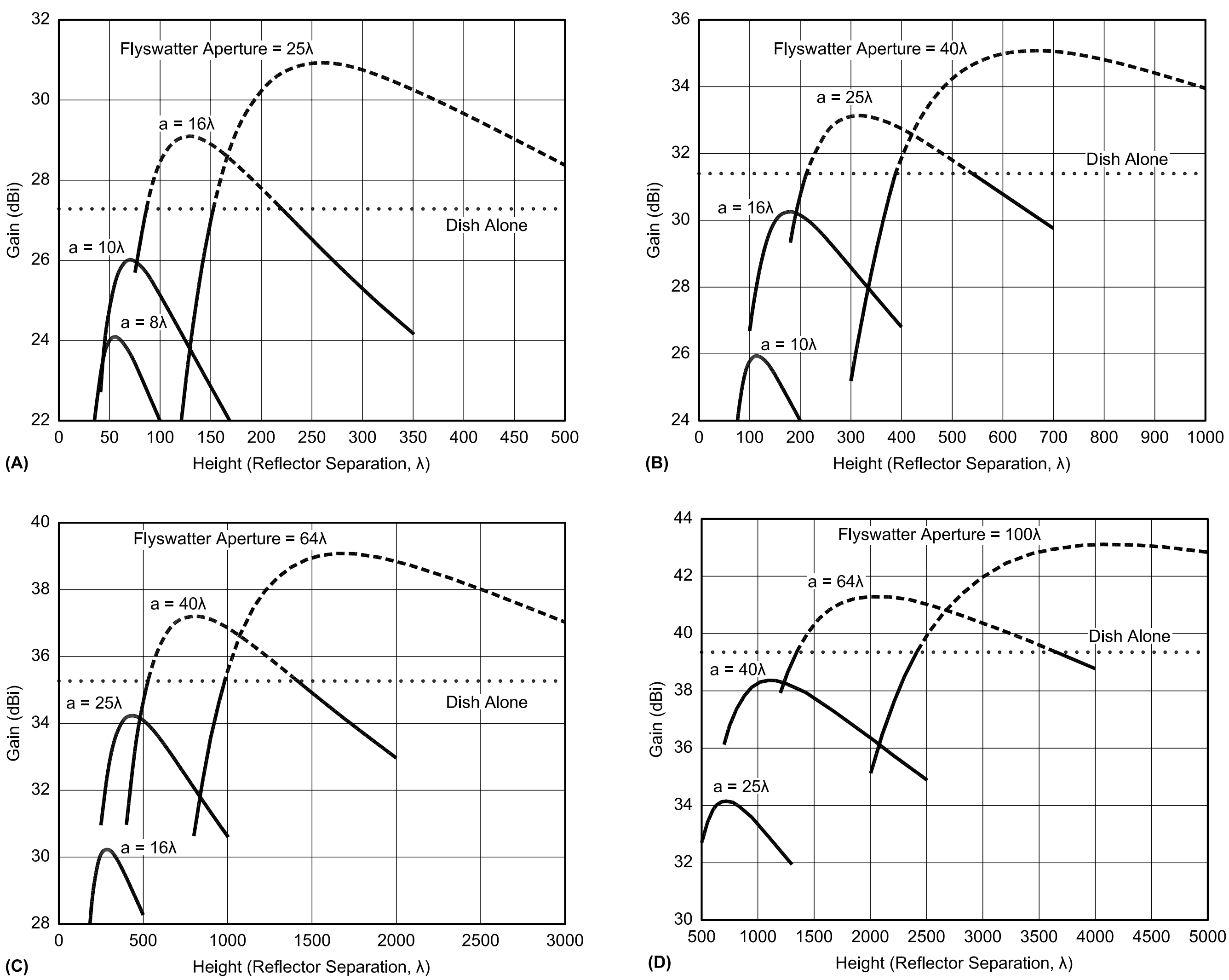

Fig 7—System-gain plots for periscope antennas fed by dishes of various diameters. At A, a 10-λ-diameter dish; at B, 16 λ; at C, 25 λ; at D, 40 λ.

out of phase with the first, causing losses. In total, five terms are necessary for the periscope gain calculation:

G1—the gain of the dish, with Fresnel correction factor

Space attenuation—the path loss between dish and flyswatter

G2—the aperture gain of the flyswatter when intercepting power from the dish, including Fresnel correction factor

Edge effect—loss of efficiency at the edge of the flyswatter due to diffraction

G3—the aperture gain of the flyswatter radiating into free space, corrected for illumination taper

The system gain of the periscope antenna is the sum total of these gains and losses.

The periscope-gain calculations involve a couple of difficult functions, so it took some work before I was able to do the calculations. One function, the Fresnel sine and cosine, I had needed previously[7] to calculate the phase center of horn antennas. The code for this was written by Matt, KB1VC. To correct for the illumination taper, a spherical Bessel function, Λ, is needed. This function proved more difficult; the paper says, "Spherical Bessel functions of the form $\Lambda_p(v)$ are tabulated." For these functions, Silver[8] refers to *Tables of Functions*[9] by Jahnke and Emde; fortunately, Byron, N1EKV, had a copy and lent it to me so that I could make and verify the calculation. Today, of course, we have personal computers, so no one uses books of tabulated functions. (Note: Spherical Bessel functions $\Lambda_p(v)$ are not the same as Bessel functions for spherical coordinates $j_n(x)$ found in modern references.[10, 11, 12])

Once I was able to calculate periscope gain and reproduce the results of Greenquist and Orlando, I wanted to understand the complex relationship between the different dimensions. The equations are far too difficult to offer any insight, so my approach was to graph the results and attempt to visualize the relationships.

The first step was to replot the curves from Greenquist and Orlando in terms of wavelengths, so they are usable at any frequency. Each curve in Fig 7 shows the periscope gain for a specific dish size as a function of flyswatter aperture and height (reflector spacing). Note that it is possible with some combinations to achieve a system gain several decibels higher than the gain of the dish alone. The curves are dotted lines where the system gain is higher than the dish alone. Best gain occurs when the flyswatter is larger

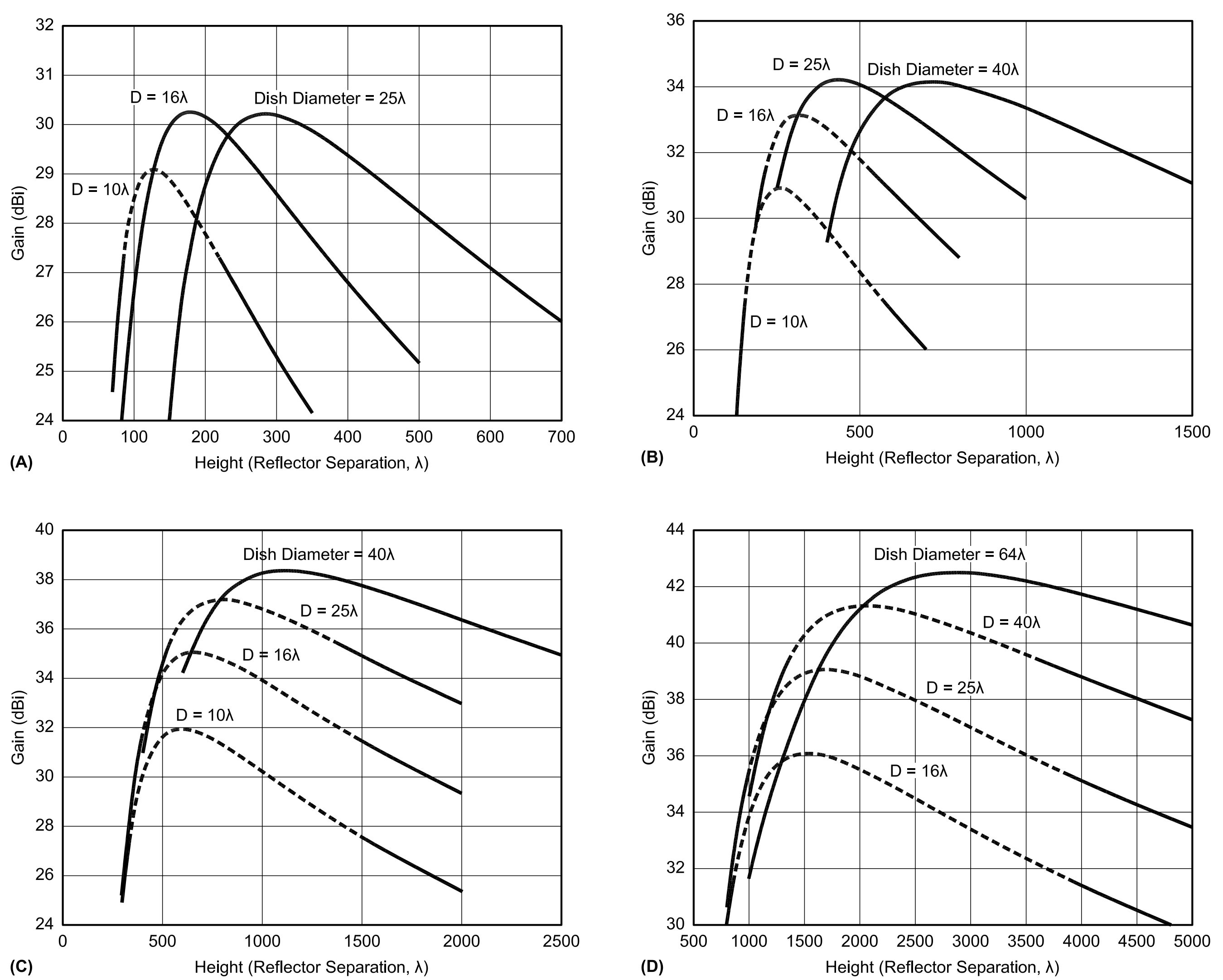

Fig 8—System-gain plots for periscope antennas with various flyswatter apertures. At A, a 16-λ aperture flyswatter; at B, 25 λ; at C, 40 λ; at D, 64 λ.

than the dish, and there appears to be an optimum height—but we can't see what produces the optimum. However, we know that path loss follows an inverse-square law: Doubling the distance increases path loss by 6 dB. To increase reflector gain by 6 dB requires a doubling of aperture diameter. Thus, we can understand why large gains require a large dish and larger flyswatter.

We can also see that large gains also require extremely large reflector spacing. Re-arranging the curves for specific flyswatter sizes (Fig 8) shows the same trend, but it doesn't really add any insight. The dotted portions of the curves again represent combinations where the system gain is higher than the gain of the dish alone.

The problem is that we are trying to display a four-dimensional problem in a two-dimensional medium. A three-dimensional graph might help, if we could reduce the problem to three dimensions. My approach is to normalize the other quantities in relation to the dish diameter, so that one axis is the ratio of flyswatter aperture to dish diameter and the gain is the effective gain of the periscope, the ratio of system gain to dish gain. The height, or reflector spacing, is normalized to the Rayleigh distance of the dish diameter D:

$$Rayleigh\ distance = \frac{2D^2}{\lambda} \qquad \text{(Eq 1)}$$

In Fig 9, we can see the effective gain, or increased gain provided by the periscope system over the dish alone, increasing as the relative flyswatter aperture increases. The 3-D plot in Fig 9A also shows that the range of optimum combinations is narrow and gain falls off quickly if we miss. The maximum effective gain shown is about 4 dB, with gain still increasing at the edge of the

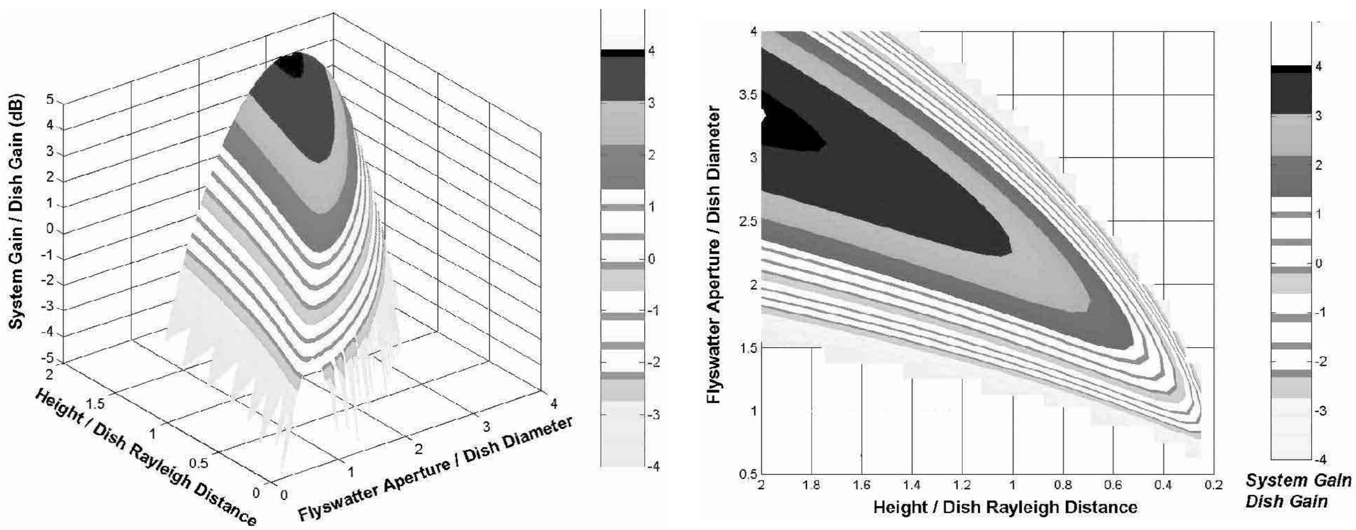

Fig 9—Normalized performance of periscope antennas for any dish size. At left is a three-dimensional representation; at right is a two-dimensional representation with the third dimension communicated by shades of gray.

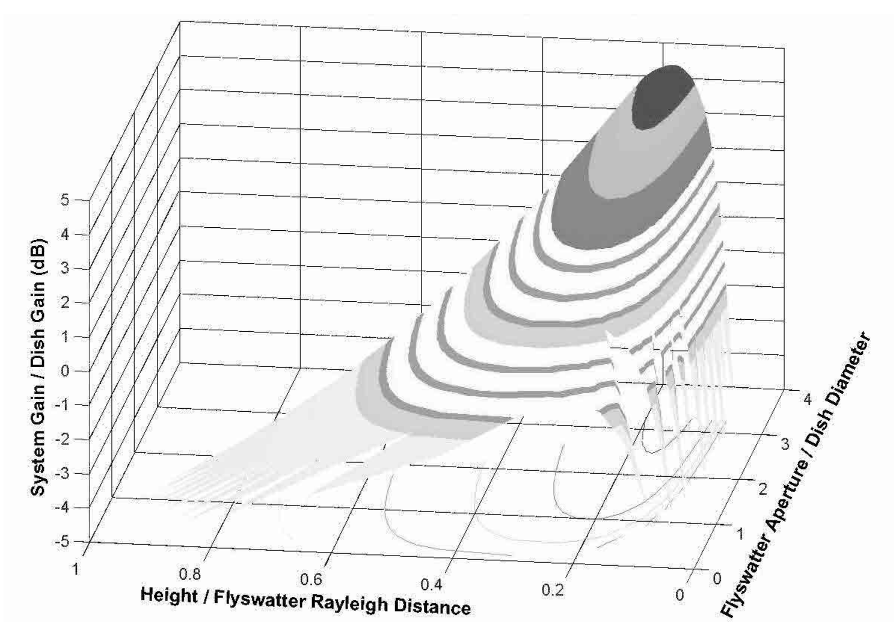

Fig 10—Normalized performance of periscope antennas based on height (reflector separation) versus flyswatter aperture.

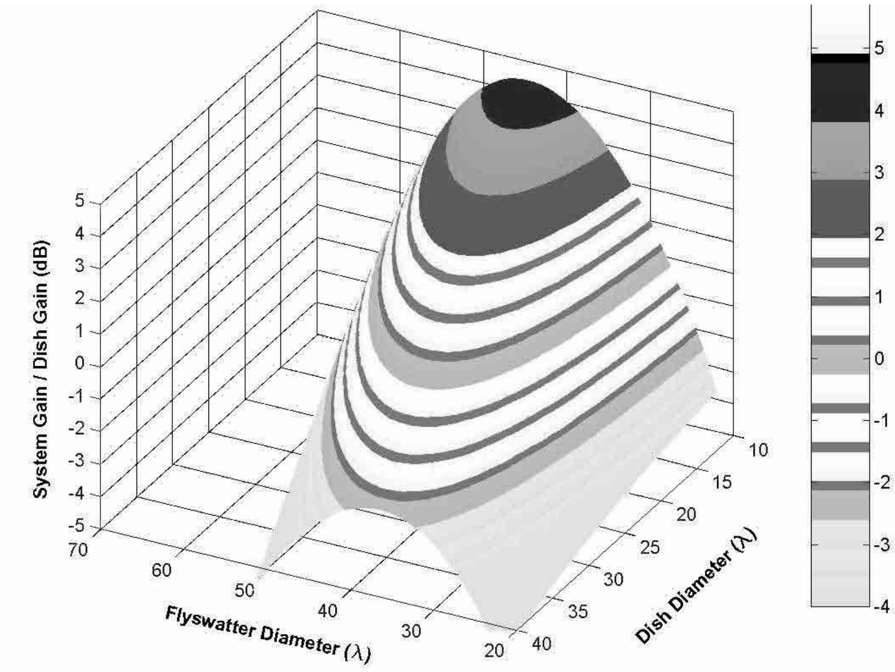

Fig 11—Periscope antenna performance with 700 λ height (reflector separation).

graph. The graph from Jakes (see Note 5) shows an asymptotic value of 6 dB as the flyswatter becomes infinitely large. Other numerical values are difficult to discern from the 3-D plot, so a 2-D version is shown in Fig 9B, looking down from the top. We must rely on shading and the gain bar to read to find effective gain values.

In Fig 9, it is apparent that the gain is not limited by the Rayleigh distance of the dish. However, if we instead normalize the height to the *flyswatter's* Rayleigh distance, using the flyswatter diameter or square side for D in the calculation, the optimum combination becomes apparent in Fig 10. The 3-D plot illustrates that the range is narrow, and the contour lines below the plot indicate the values. The contour lines for high effective gain are all in the range of 0.2 to 0.3 on the horizontal axis, the ratio of height to flyswatter's Rayleigh distance. Thus, the height for best effective gain is roughly ¼ of the flyswatter's Rayleigh distance, regardless of flyswatter size. Usually, we already have a tower of height, h, and would like to find the optimum size flyswatter aperture A:

$$A \cong \sqrt{2h\lambda} \qquad \text{(Eq 2)}$$

A flyswatter larger than this optimum size suffers excessive losses caused by the Fresnel and illumination taper effects; in the plot, this is the area to the right of the gain peak. To the left of the peak is the area where the distance is too large or the flyswatter too small, and the gain decrease is inverse-square, due to space attenuation, the path loss between the two reflectors.

Since the Rayleigh distance is a function of the square of the aperture, the relationship between the dimensions is

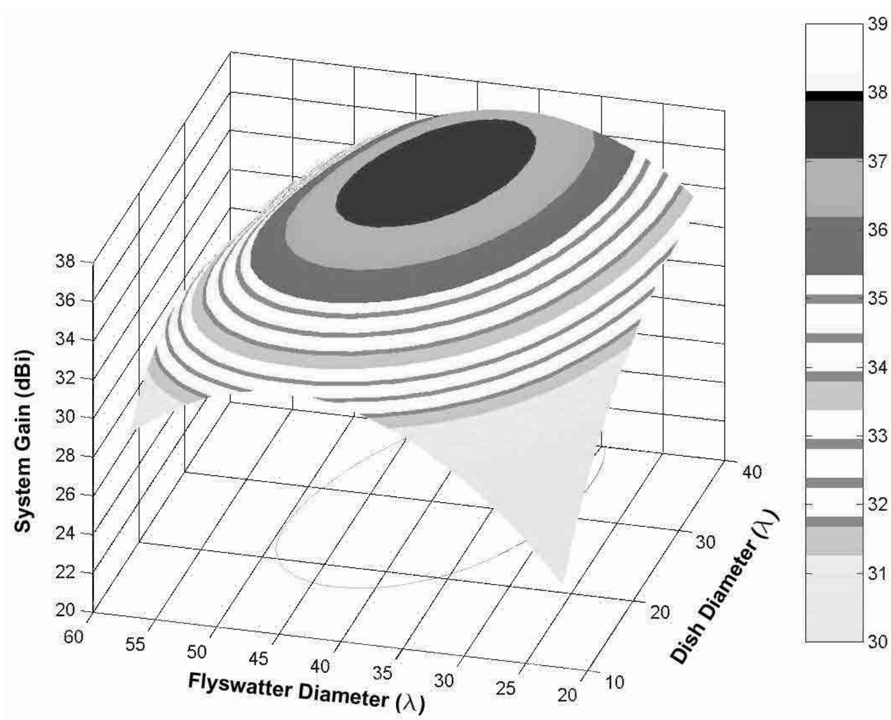

Fig 12—System gain of a periscope antenna with 700 λ height (reflector separation).

still not obvious. A realistic example should help. My periscope installation is about 20 meters high, or roughly 700 λ at 10 GHz. The effective gain for this height is plotted in Fig 11 as a function of dish and fly-swatter size. The optimum flyswatter size is roughly 40 λ, about what we would calculate using the formula above. However, the effective gain increases as dish diameter decreases (notice that this axis is reversed for better visibility). Yet we know that dish gain increases with diameter, so what is happening to the system gain? Look at Fig 12: The system gain has a broad peak with a dish diameter around 30 λ and a flyswatter aperture around 40 λ. If we can't find these exact sizes, any combination inside the contour circle below the 3-D plot will be with a couple of decibels of optimum.

We learn from Figs 11 and 12 that a smaller dish contributes only a small gain to the system, while a larger dish is too large to illuminate the fly-swatter effectively at this distance. Best system performance is a compromise between the effective gain of the periscope and the gain of the dish alone, and it must be determined for a particular height.

Reaching an intelligent compromise requires that we be able to estimate performance. The graphs included here should be adequate for rough estimates; they were created using *MATLAB*[13] software, which is powerful but a bit expensive for amateur use. However, I was able to create a Microsoft *Excel* spreadsheet that performs the periscope-performance calculations, so that you may make accurate estimates for any dimensions. You may download *periscopegain.xls* from **www.w1ghz.org**. Color versions of these graphs are also available on this Web site.

Enhancements

The original periscope trial system described above was rather small: Both the dish and the flyswatter are undersized for 20 meters of separation, resulting in the estimated 5-dB loss. One solution would be to reduce the separation, but this would elevate the bottom dish and require a "lossy" feed line. A better solution would be to increase the size of the dish and flyswatter.

I recently increased the dish size and made the installation permanent by adding a fixed, one-meter diameter, offset-fed dish at the base of the tower. The flyswatter mounting structure was designed to accommodate a flyswatter at least 3 feet wide and 4 feet high, so there is room for improvement here also. In addition, since dishes and flat reflectors aren't frequency sensitive, it would be great to use the periscope system on more than one band. The calculated periscope system gain in Fig 13 shows roughly a 3-dB improvement at 10 GHz with the 1-meter dish over the line for the previous 18-inch (~0.5-meter) dish.

Fig 13 also shows the system gain for several microwave ham bands as a function of flyswatter aperture. Clearly, a larger flyswatter than the current 0.76-meter aperture is desirable, particularly at lower frequencies. The optimum flyswatter aperture for 10 GHz is about 1.2 meters, which is manageably large. Fig 14 plots the periscope system gain versus frequency for the 1-meter dish with a 1.2-meter flyswatter as well as the current 0.76-meter one with both the one-meter dish and the original 18-inch dish. The dotted curves show the gains of the dishes alone. The current system is comparable with a 24-inch dish at 10 GHz and falls off at lower frequencies. Yet the largest combination provides performance close to a 1-meter dish—not only at 10.368 GHz, but also at 5760 and 3456 MHz. This looks like a winner! Even at 2304 MHz, the mediocre gain is comparable with a medium-sized loop Yagi.

These additional bands are almost free—only a feed horn is required. The offset dish has a huge advantage for multiband operation: The feedhorn and support are out of the beam. I envision a carousel of feed horns next to the dish, changing bands by rotating the appropriate horn into position at the focal point of the dish. Two-band operation is much simpler: A dual-band feed horn[14] will do the job.

Will the periscope work on higher bands? Of course it will, if the dish and flyswatter reflectors have surfaces that are good enough. They need to be parabolic or flat within about $\lambda/16$. As an example, I made some estimates for my system at 24 GHz. For a height of 20 meters, our formula estimates an optimum flyswatter aperture, A, of 0.7 meter, close to that of my current system, so I extended the curves of Fig 14 to include 24 GHz in Fig 15. The curve for my current combination, a 1-meter

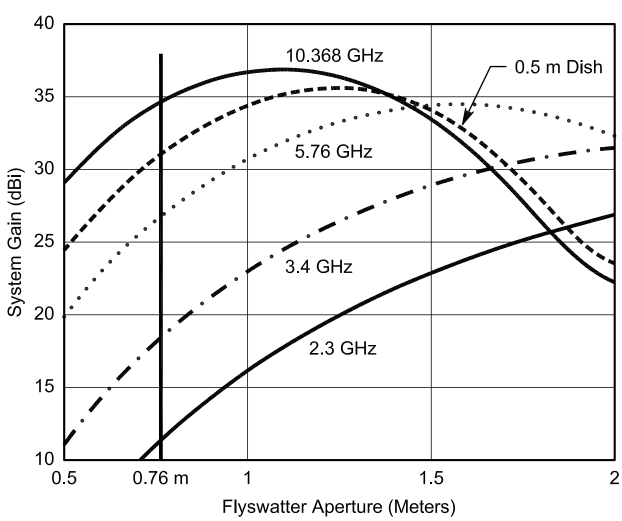

Fig 13—System gain of the W1GHZ periscope antenna (1-meter dish with flyswatter 20 meters high).

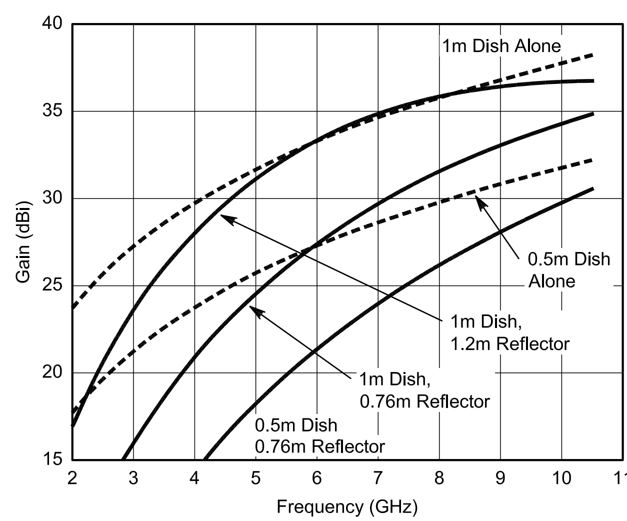

Fig 14—Gain versus frequency plot for the W1GHZ periscope antenna from 2 through 11 GHz.

dish with a 0.76-meter flyswatter, has maximum gain around 15 GHz and falls off at 24 GHz to provide less gain than at 10 GHz. My proposed larger flyswatter is even worse at 24 GHz, with low gain and very narrow beamwidth because of the large flyswatter aperture—a bad combination. However, the smaller flyswatter with a small 0.5-meter dish looks good. The gain is higher than the dish alone. Feed line without loss at 24 GHz is a real miracle!

As usual, we can't have everything and so must compromise. With the larger dish and flyswatter, I could get good performance on 10 GHz as well as 5760 and 3456 MHz. With the smaller dish and flyswatter, I could have 10 GHz and 24 GHz but not much gain on the lower bands. Since my biggest obstacle is foliage, I would probably do better at lower frequencies. However, a more complex alternative might be to use the smaller flyswatter with both dishes, moving and tilting the flyswatter to change bands.

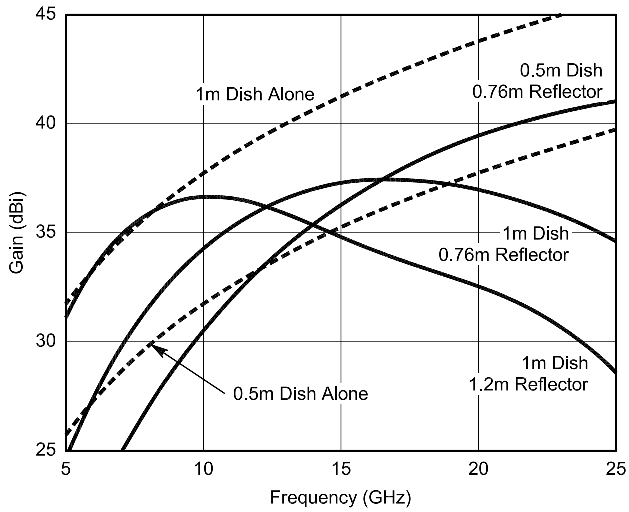

Fig 15—Gain versus frequency plot for the W1GHZ periscope antenna from 5 through 25 GHz.

Conclusion

The periscope antenna system has enabled me to achieve better microwave results from my home than I could before. Without it, I can't get out of my own backyard if the weather is good. The system works well on rain and snow scatter; in many areas, rain is easier to find than altitude. The periscope is worth considering as an alternative to high feed-line losses or tower mounted systems.

I don't believe I have explored the full potential of this antenna, so I urge you to try it and report the results. The analysis and graphs shown here should enable you to understand periscope antenna operation and allow you to design one with confidence.

Notes

[1]H. Jasik, *Antenna Engineering Handbook,* First Edition (McGraw-Hill, 1961), pp 13-5 to 13-8.

[2]R.C. Johnson, *Antenna Engineering Handbook,* Third Edition (McGraw-Hill, 1993), pp 17-24, 25.

[3]D. Evans, G3RPE, "Observations on the Flyswatter Antenna," *Radio Communication,* Aug 1977, pp 596-599.

[4]IIX Equipment Ltd, 4421 W 87th St, Hometown, IL 60456; tel 708-423-0605; **www.w9iix.com**.

[5]W. C. Jakes, Jr, "A Theoretical Study of an Antenna-Reflector Problem," *Proceedings of the IRE*, Feb 1953, pp 272-274.

[6]R. E. Greenquist and A. J. Orlando, "An Analysis of Passive Reflector Antenna Systems," *Proceedings of the IRE*, July 1954, pp 1173-1178.

[7]P. Wade, N1BWT, and M. Reilly, KB1VC, "Metal Lens Antennas for 10 GHz," *Proceedings of the 18th Eastern VHF/UHF Conference of the Eastern VHF/UHF Society,* (Newington, Connecticut: ARRL, 1992), pp 71-78.

[8]S. Silver, *Microwave Antenna Theory and Design*, (McGraw-Hill, 1949), p 194.

[9]E. Hahnke and F. Emde, *Tables of Functions: with Formulae and Curves*, (Mineola, New York: Dover, 1945), p 128, 180-189.

[10]C. D. Hodgman, S. M. Selby, R. C. Weast, *Mathematical Tables from Handbook of Chemistry and Physics*, 11th Edition, (Boca Raton, Florida: Chemical Rubber Publishing, 1959), p 287.

[11]M. Abromowitz and I.A. Stegun, *Handbook of Mathematical Functions*, (Dover, 1972).

[12]W. H. Press, S. A. Teukolsky, W. T. Vetterling, B. P. Flannery, *Numerical Recipes in C: The Art of Scientific Computing*, Second Edition, (Cambridge, United Kingdom: Cambridge University Press, 1992), pp 251-252.

[13]The Mathworks Inc, 3 Apple Hill Dr, Natick, MA 01760-2098; tel 508-647-7000, fax 508-647-7001; E-mail **info@mathworks.com**; **www.mathworks.com**.

[14]P. Wade, N1BWT, "Dual-band Feedhorn for the DSS Offset Dish," *Proceedings of the 23rd Eastern VHF/UHF Conference of the Eastern VHF/UHF Society,* (ARRL, 1997), pp 107-110. □□

A Low-Loss VHF/UHF Bias Tee

A simple circuit lets your transmission line do double duty.

By Tom Cefalo Jr, W1EX

When I became interested in satellite communications, I decided to operate the popular 2-m/70-cm mode. To reduce the system noise overall, low-noise amplifiers were installed at the antennas. To avoid running additional cables from the station up to the antennas to power and control the low-noise amplifiers, I decided to use the RF coaxial cable as the medium to carry out this task. This method provides a low-resistance path and eliminates additional cabling.

To perform this function, a device called a dc injector—more commonly known as a "bias tee"—is required. A bias tee allows dc power to be superimposed onto a transmission line without altering the RF characteristics, thereby allowing both signals to share a single cable. This article describes a low-loss bias tee that has been optimized for each band.

51 Oak St
Winchester, MA 01890
Tdcef@110.net

Theory of Operation

Fig 1 shows a typical bias tee and the component values for the two bands of operation. The bias tee has three ports: a dc port, an RF port and a RF+dc port. The operation of the circuit is very simple. The series capacitor provides a dc block to stop the dc voltage from appearing at the RF port. This capacitor must have low-loss characteristics so it can safely pass the transmitted RF power. In addition to this, the capacitor's self-resonant frequency must be above the desired band of operation. To meet these requirements, a ceramic-chip capacitor was selected. These capacitors have low dissipation factors, little series inductance, high breakdown voltages and those with larger packages will safely transfer the transmitted power.

The RF choke has a dual role. First, it provides a means to inject dc power onto the center conductor of the coaxial cable. Second, it presents high impedance to the RF signal. This provides isolation between the RF signal and the dc port. In other words, it prevents the RF from flowing through the dc port. As a general rule of thumb, the inductive reactance should be at least 10 times the system impedance (the characteristic impedance of the coaxial transmission line). However, the self-resonant frequency of the inductor must be above the band of operation. The inductor must also be able to pass the dc current without altering its characteristics. The inductance value must be carefully selected. If the above inductor criteria are not met, the performance of the bias tee will be greatly degraded.

With an RF signal applied to the RF port and a dc voltage applied to the dc port, the output port will contain both of these signals. The coaxial transmission line conveys both of the components. The dc return path is the shield of the coaxial transmission line.

Fig 2 shows a typical bias-tee installation. Notice that the bias tee at the antenna end is installed with the RF port connected to the antenna. The dc voltage is blocked from reaching the antenna by the series capacitor. The dc voltage is extracted from the coaxial transmission line via the dc port of the bias tee, thus providing power to the low-noise amplifier.

Construction

A bias tee should be constructed in a small metal enclosure such as a Pomona box. RF path lengths should be minimized to reduce losses; therefore the connectors should be placed on the narrow ends of the box. It is essential that N-type connectors be used, especially for UHF operation. The electrical performance (SWR and insertion loss) would suffer if SO-239 or BNC connectors were used. The feedthrough capacitor can be mounted at any convenient location on the box away from the RF. The inductor is soldered between the feedthrough capacitor and the transmission line using the wire leads to support the inductor. The windings around the ferrite core should be evenly spaced. Remember that each time the wire passes through the center of the core, it is counted as a turn.

Since the series-blocking capacitor is a chip component, it was mounted on a double-sided PC board between 50-Ω microstrip lines. The lines can be made using a sharp hobby knife to cut and remove the excess copper foil. The bottom of the PC board is a solid ground plane of copper. Table 1 lists some 50-Ω line widths for several common PC board materials. There are also several programs available on the Web to calculate a line width if a different board material is used.

It is very important to insure a good ground between the connectors and the ground plane of the PC board. Fig 3 shows one method of transition

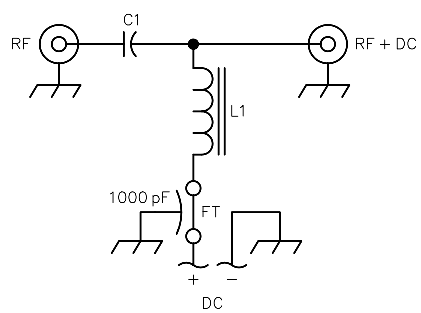

Fig 1—A schematic diagram of the bias tee.
L1—An RF choke wound on a Micrometals T25-6 ferrite core. For VHF, use 16 turns of #28 AWG wire. For UHF, use 9 turns of #28 AWG wire.
C1—Dielectric Labs chip capacitor. For VHF, 1000 pF (#C22AH102J7PXL). For UHF, 330 pF (#C22AH331JAPXL).

Table 1—Microstrip Widths for various Board Materials and Thicknesses

Board Material	*H*	*W*
Rogers 4003	0.032	0.073
GML 1000	0.030	0.071
FR4	0.031	0.055

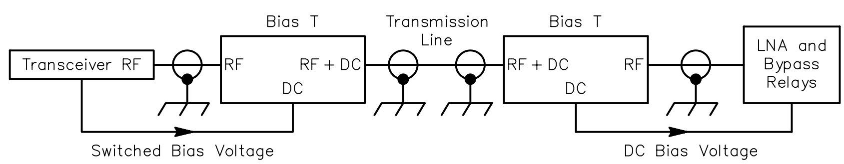

Fig 2—A block diagram of a typical station setup.

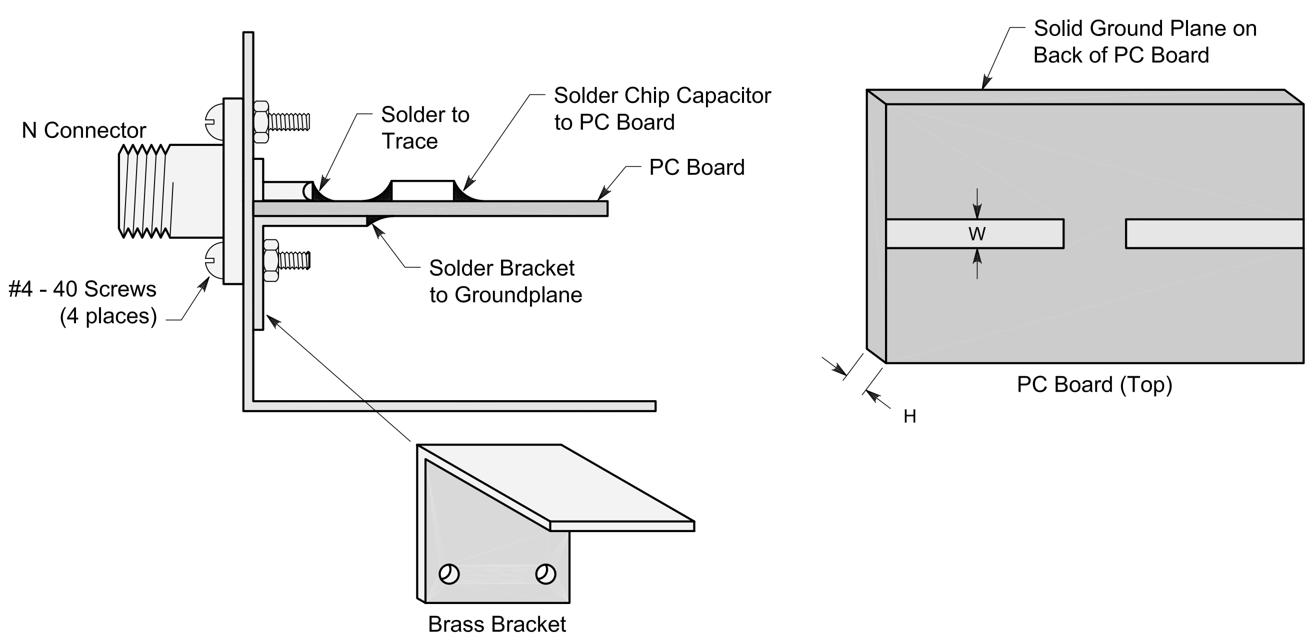

Fig 3—Construction details.

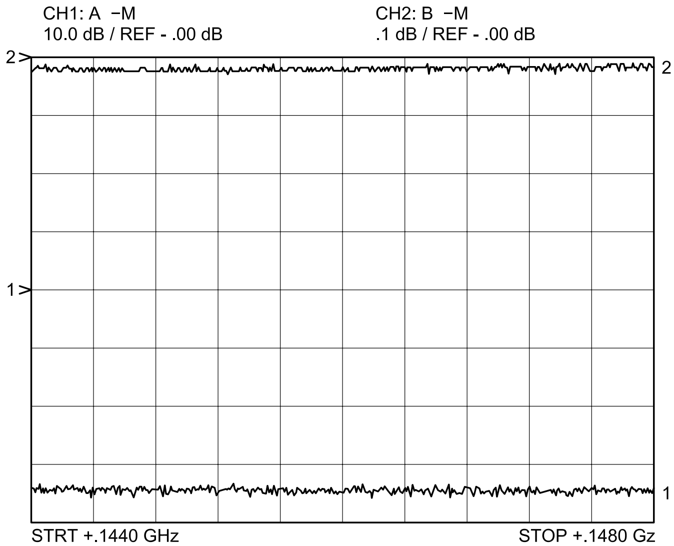

Fig 4—VHF bias tee return (1) and insertion (2) loss.

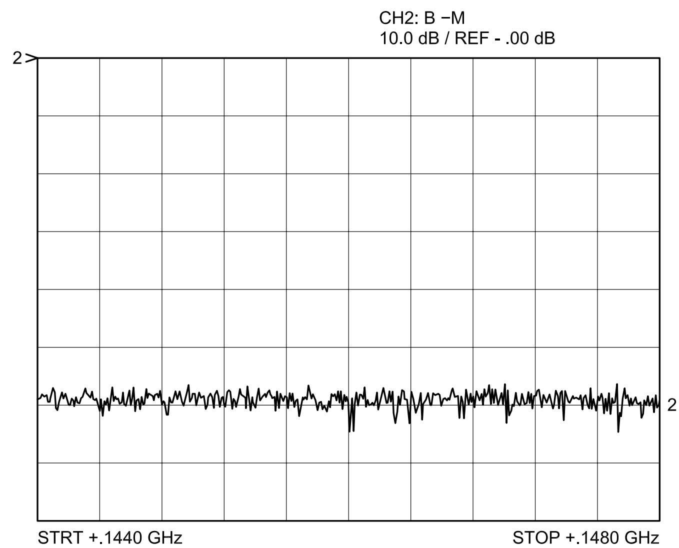

Fig 5—VHF bias tee RF-to-DC port isolation.

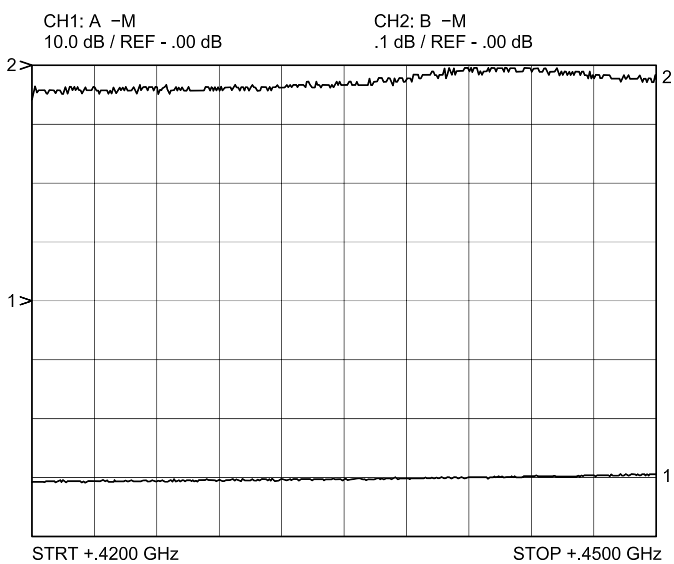

Fig 6—UHF bias tee return (1) and insertion (2) loss.

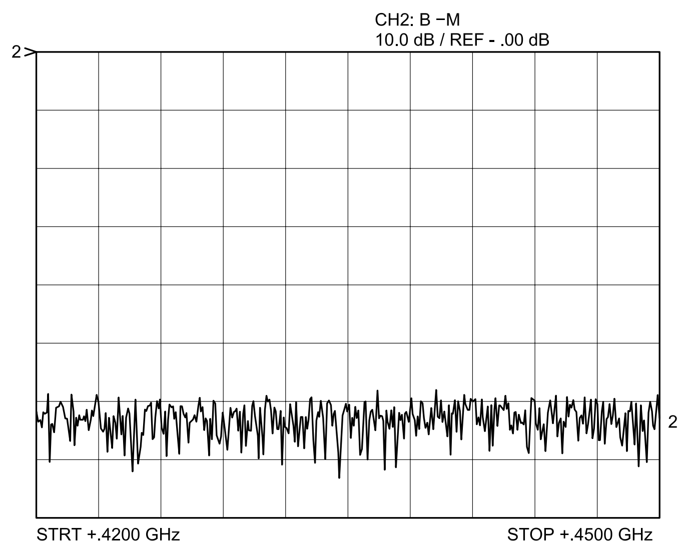

Fig 7—UHF bias tee RF-to-DC port isolation.

between the connector and the PC board. A right-angle bracket made of brass can be formed to the correct dimensions. The bracket is soldered to the ground plane and attached to the connector via the connector's two bottom mounting screws.

Measured Data

The following data were measured on an HP scalar network analyzer. Fig 4 shows the VHF bias tee's insertion loss and return loss. The average insertion loss was 0.02 dB and the minimum return loss was 35 dB, corresponding to an SWR of 1.036:1. Fig 5 shows the isolation between the RF and dc ports to be 60 dB. Figs 6 and 7 are the measured data for the UHF bias tee. The average insertion loss was 0.04 dB and the return loss was 30 dB (SWR 1.065:1). The isolation was also 60 dB.

As seen from the measured data, the bias tee has low losses, excellent SWR and isolation. The measured data were unaltered when the units were tested with a bias voltage of 28 V at 1 A. The bias tee has been operating at the 100-W level with no problems. A single bias tee could have been designed to cover both bands but the goal of low-loss characteristics would not have been achieved. □□

Tech Notes

[Tech Notes seems the ideal forum for Rudy to present some supporting documentation regarding his earlier stance on using foil conductors in antennas. Are the benefits obtained by using a thin foil element outweighed by increased edge-current losses? Read on and then decide for yourself. We are always in need of short, interesting technical articles for future Tech Notes columns. If you have something that may be of interest, please contact us.— Peter Bertini, K1ZJH, *QEX* Contributing Editor, **k1zjh@arrl.org**]

Resistance of Foil Conductors For Antennas

By Rudy Severns, N6LF

In the Nov/Dec 2000[1] issue of *QEX*, I presented an overview of conductor resistance for antennas. One of the suggestions offered was to use foil conductors to reduce resistance for a given cross-section of copper. Obviously, just using round copper wire of larger and larger diameters would be a heavy and expensive way to reduce conductor loss in low-impedance antennas. The premise was that the resistance of a round wire (which is more than a few skin depths in diameter) will be reduced by rolling it out into a foil. Several readers challenged this, stating that "The current in a foil is concentrated at the edges, and so, in effect, you don't gain anything." This illustrates a very common misconception, which I will address.

Relative Loss in Wider Foils

While it's certainly true that current densities at the edges of a foil can be much higher than in other parts, this does not mean that you cannot substantially reduce losses for the same area of copper by going from a round to a foil conductor.

I ran a very simple model using Finite Element Modeling (FEM) software,[2] which allows the loss in a given conductor of arbitrary shape to be determined at high frequencies, while accounting for eddy current effects. I chose a foil thickness of 8 mils and a frequency of 14 MHz, with a constant current of 1 A rms. The skin depth in copper at 14 MHz is about 0.7 mils, so this represents a relatively thick conductor. I then varied the width from 125 mils (1/8 inch) to 1000 mils (1 inch) and computed the losses. If it were true that all of the current would be concentrated in the edges, then making the foil wider should have little effect on the losses. However, if this view is indeed incorrect, you would expect to see the loss decrease as the foil is made wider.

The results are shown in Fig 1. The loss is normalized to 1 for a strip width of 125 mils. As we increase the width, loss decreases, but not as quickly as it would if it strictly followed the area ratio or dc resistance. It is pretty clear that the current is probably not entirely—or even largely—flowing in the edges, but there is something going on that is probably related to edge effects. Time to take a closer look!

Current Distribution in a Foil

One of the nice things about FEM CAD software is that you can graph the current density in the conductor. Fig 2 is a plot of the current density in the foil; the lines represent constant current densities. The greatest current density is indeed at the outer edge, and in fact, at the outer corners as indicated. Nonetheless, it is also clear that there is current flowing elsewhere. Because the foil is about 11 skin-depths thick, we see that there is essentially no current inside the conductor. This is due to skin effect and comes as no surprise.

Now let's look more closely at the

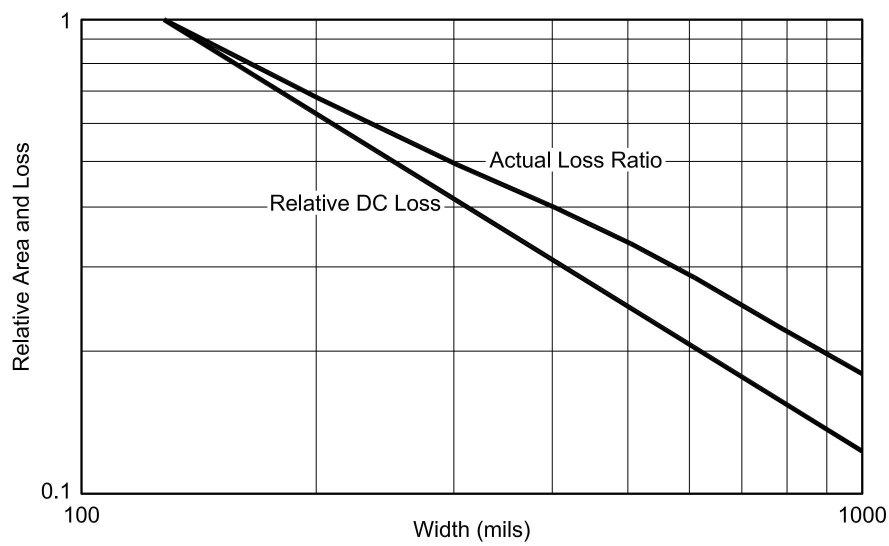

Fig 1—Comparison of dc and actual ac loss based on an increase of the 0.008-inch foil width.

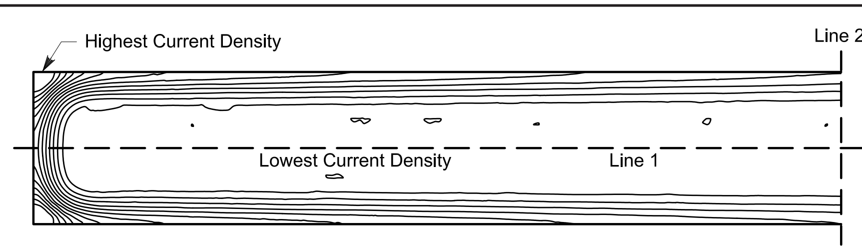

Fig 2—Current density distribution on the left half of the foil. By symmetry, the other half is a mirror image.

[1]Notes appear on page 56.

current density at the outer edge. Fig 3 is a graph of the current density along Line 1 defined in Fig 2. Sure enough, the current density at the ends is quite high, but the area of that region is relatively small so it represents only a portion of the total current in the entire conductor. There is significant current in other areas.

Fig 4 is plot of the current density along Line 2 in Fig 2, which is roughly at the middle of the foil. In line with what we know about skin effect, the current density is highest on the surface of the foil and decreases as we go inside. Yet, there is still significant current flowing on the surface of the foil away from the end edges. For this example, I chose a thick foil (11+ skin depths). Using a thinner foil would have shown that the edge effect was less pronounced, and in fact, thinner foils have less loss contributed by the edges.

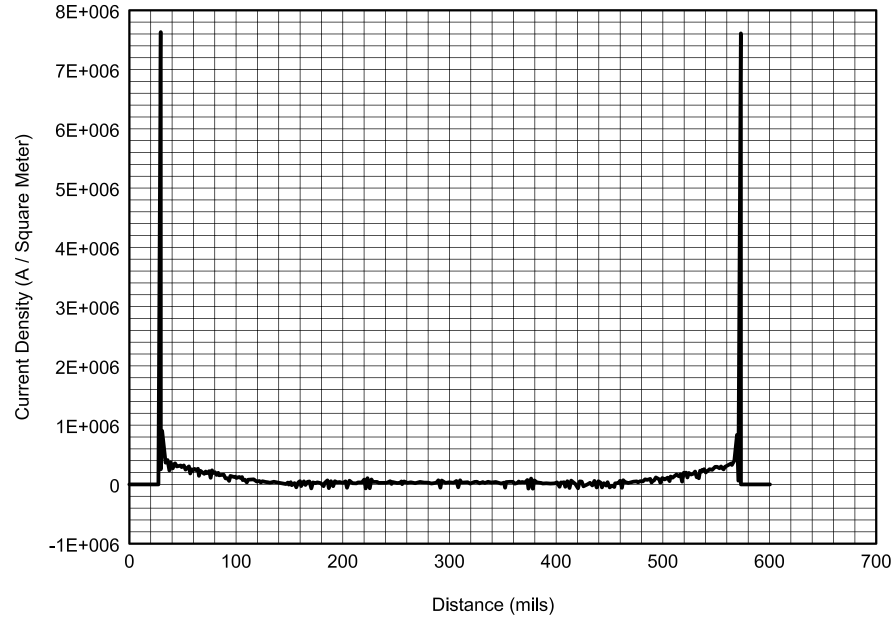

Fig 3—Current density in amperes per meter along line 1 (see Fig 2).

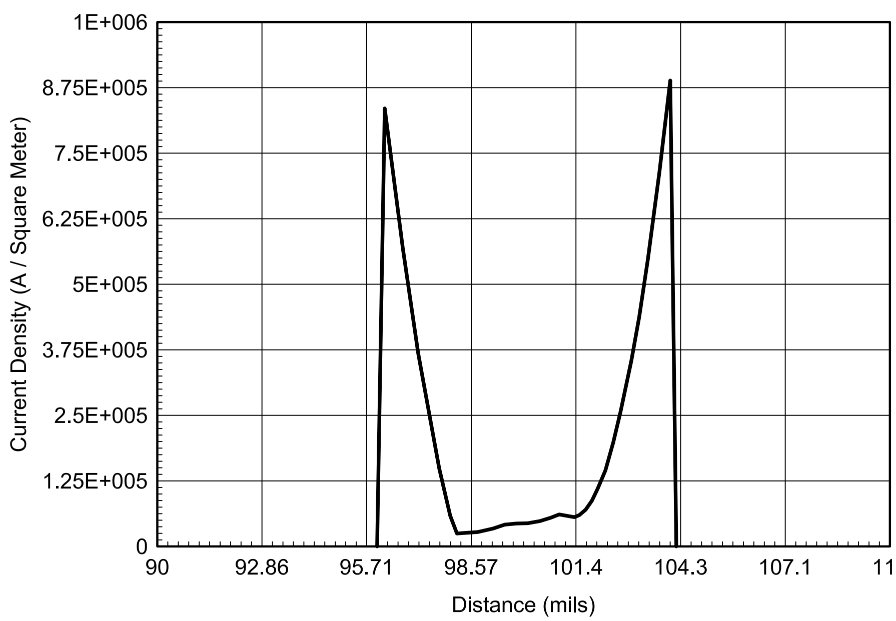

Fig 4—Current density in amperes per meter along line 2 (see Fig 2).

Summary

If a round wire is run through a roller so it flattens while keeping a constant cross-sectional area, we will discover that the HF resistance initially increases when the wire is formed into a square. It then begins to decrease as it is flattened further. As the conductor is made thinner, the resistance decreases, and when the thickness is about one skin depth, the difference between the ac and dc resistances will be small. There will also be little loss from the edges. All of this has been long known and experimentally verified in the early 20th century. Unfortunately, the idea that all the current flows in the edges is still part of our lore.

Another fact has been long known[3] but often forgotten: For a given external diameter (which is large compared to a skin depth), you can reduce the ac resistance by removing copper from the inside—that is, use a "thin-wall" tube. For a given diameter, the minimum ac resistance is reached when the wall thickness is roughly two skin depths.

Foil conductors do have disadvantages: They flutter in the wind, and very thin foils have little mechanical strength if the foil is unsupported. Several years ago, while building an antenna for my sailboat, I needed a low-loss and lightweight design to mount at the masthead. I bought some thin copper tape and applied it to a fiberglass fly-rod blank. It worked great and survived many thousands of miles of sailing across the Pacific. In effect, it was a "thin-wall" tube. Alternately, the foil could have been *inside* the fiberglass tube. Another time, losses in a stainless steel backstay antenna were reduced by bending a thin foil strip, with PVC tape on both edges, around the backstay in a U shape. This worked great. The copper tape was the conductor, and the stainless-steel backstay kept it and the mast supported.

I've noticed that the new motorized dipole being sold by Fluid Motion uses a copper-foil element inside a fiberglass tube. Reeling the foil in or out sets the length of the element. I think this shows that there is a practical use for foil conductors in some antenna installations.

Notes

[1]R. Severns, N6LF, "Conductors For HF Antennas," *QEX*, Nov/Dec 2000, pp 20-29.

[2]*Maxwell* software by Ansoft Corporation; **www.ansoft.com/products/em/max3d/index.cfm**.

[3]F. Terman, *Radio Engineers Handbook* (New York: McGraw-Hill, 1943), Fig 2, p 33. □□

RF

By Zack Lau, W1VT

Homebrewing a Main Tuning Knob

Judging from the number of posts on the Internet, many hams are interested in obtaining a high-quality main tuning knob for their SSB/CW transceivers. Many owners of the Elecraft K2 have replaced the stock tuning knob with the knob for the Yaesu FT-100. This is no surprise—accurate tuning is essential for operating these modes. Often, success is directly related to your ability to tune stations—50-Hz tuning accuracy isn't overkill. For hams that hunt rare DX, the main tuning knob is often in constant use. It's easily the most important operating control on the radio. If you have machine-shop equipment, it may be worthwhile to homebrew your own custom knob. This article will describe how to make your own tuning knob in a machine shop.

The preferred material for making knobs is brass; it is heavy and machines easily. Most operators prefer a knob with a lot of weight. People have even modified knobs by adding lead.[1] I decided to machine a polycarbonate faceplate with finger holes. It also protects the brass from corrosion. Polycarbonate is very easy to machine, which is an advantage if you have only a miniature milling machine to cut the holes.

Balance is a critical item. You do not want a knob that settles to its balance point when you let go of it. Some folks add a felt resistance pad behind an unbalanced knob to solve this problem, but it is better to start with a balanced knob and add only enough resistance to suit the operator's taste. Felt flat washers are available from Small Parts.[2] To optimize the knob's balance, I decided to install three #8-32 setscrews. Similarly, I decided to install the faceplate with three 3/8-inch-long #4-40 cap screws. Black caps screws are available from Enco.[3] All six screws are spaced at 60° intervals, to eliminate the chance of the holes colliding.

I obtained the brass via E-bay. Small pieces of brass round stock are often offered for auction. Alternatively, several companies on the Internet sell small cut pieces of brass. Plastic is a bit tougher to obtain. I would prefer a place that sells Lexan rod, but I didn't need the six-foot lengths offered by United States Plastics.[4] Instead, I cut up sheet stock into small squares that could be machined into suitable disks. This does have the advantage of giving you a fine surface finish for viewing the brass—assuming the protective paper or plastic covering provides adequate protection during machining. I wanted to accurately drill the mounting holes in the plastic sheet, so I used a four-jaw chuck mounted on a rotary table. The four-jaw chuck is better for holding square pieces than a three-jaw chuck.

I also used the four-jaw chuck to hold the brass stock. I bored out the 0.236 and 0.70-inch holes, as shown in Fig 1. The 0.236-inch hole needs to be very accurate, if one wants a good fit with the tuning shaft. Alternatively, one can get reasonably close with a 6-mm drill bit. The 0.70-inch hole is big enough to be held by the outer jaw surfaces of the three-jaw chuck. I found my three-jaw chuck reasonably accurate; a four-jaw chuck could be used for better accuracy. Holding the knob internally allows a mar free finish to be machined on all visible surfaces of the knob. Fig 2 shows these dimensions. I machined the 7° taper by tilting the headstock of my lathe. It may be easier to machine a series of steps with a form tool.

The first knobs I made had fully threaded holes for the setscrews. I don't recommend this. The threads are so long that tapping the threads becomes difficult. Instead, I recommend only tapping the last 0.4 inches of the hole. If you drill out the rest of the hole with a #19 drill bit, the enlarged hole forms a guide that insures the tap is aligned properly with the hole.

After cutting a 2-inch square of Lexan with a band saw, I mounted it on a four-jaw chuck and drilled the #4-40 mounting holes with a milling machine. The dimensions are shown in Figs 3 and 4. I used the rotary table to obtain the 120° spacing between the three holes in the faceplate. Because it has an accurate

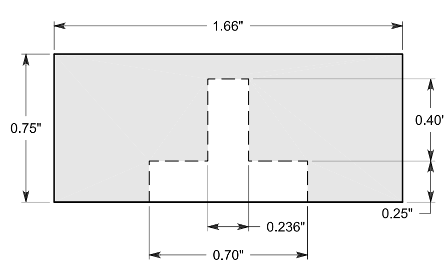

Fig 1—Dimensions for boring the holes in the brass lathe stock.

[1]Notes appear on page 59.

225 Main St
Newington, CT 06111-1494
zlau@arrl.org

hole in the center for mounting chucks, I also used it to drill the three matching holes in the brass round stock. The holes are first marked with a center drill—a stubby little drill that doesn't flex as much as normal drill bits. I then used $^{3}/_{16}$-inch drill bits with a small centering bit, stopping when the bit reached 150 mils below the surface. The centering bit provides a nice starter hole for the #33 holes, which could be quickly drilled with a drill press. Some $^{3}/_{16}$-inch bits will even cut a flat surface for the mounting screws. They have special tips designed to eliminate the need for a pilot hole.

Making the identical finger holes proved to be a bit of a challenge. If you mount the knob off center in a four jaw chuck on a lathe, a form tool can easily make one large $^{5}/_{8}$ or $^{3}/_{4}$-inch indentation. However, making three identical

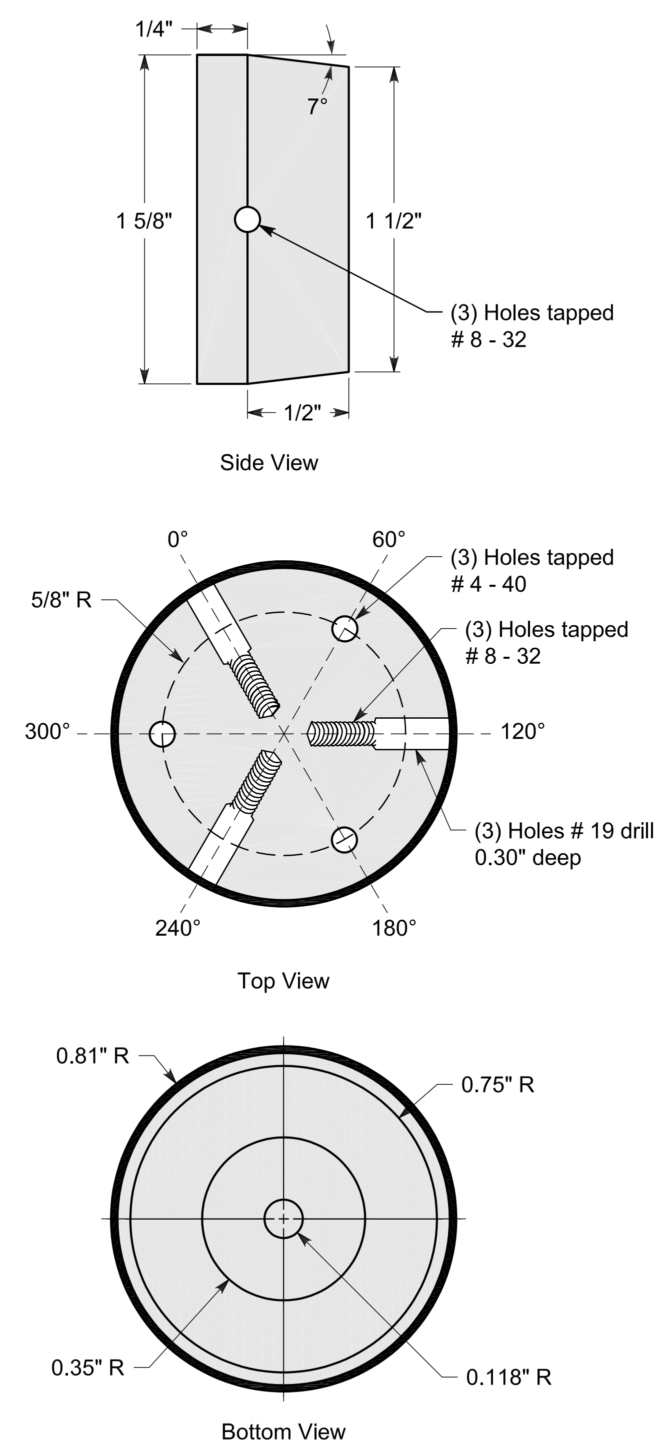

Fig 2—Dimensions for machining the brass lathe stock into a knob.

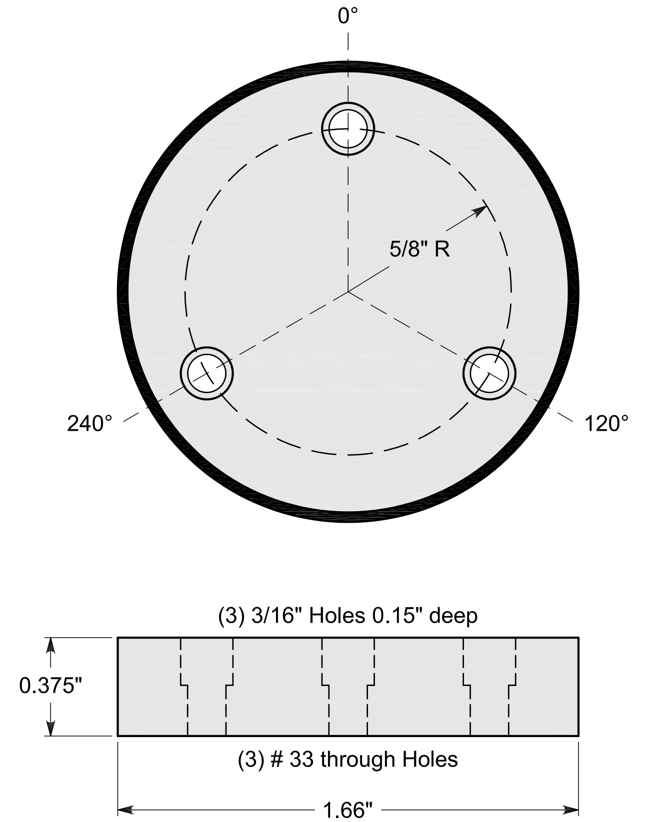

Fig 3—Dimensions of the protective polycarbonate face plate for the knob.

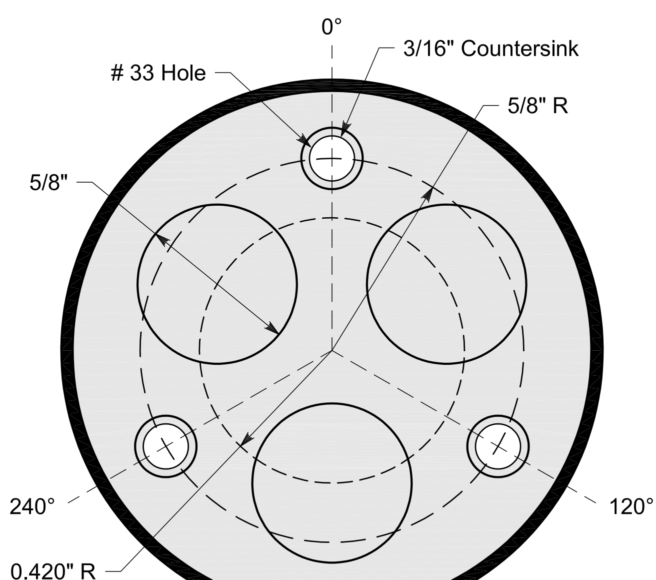

Fig 4—Dimensions for drilling finger holes in the face plate.

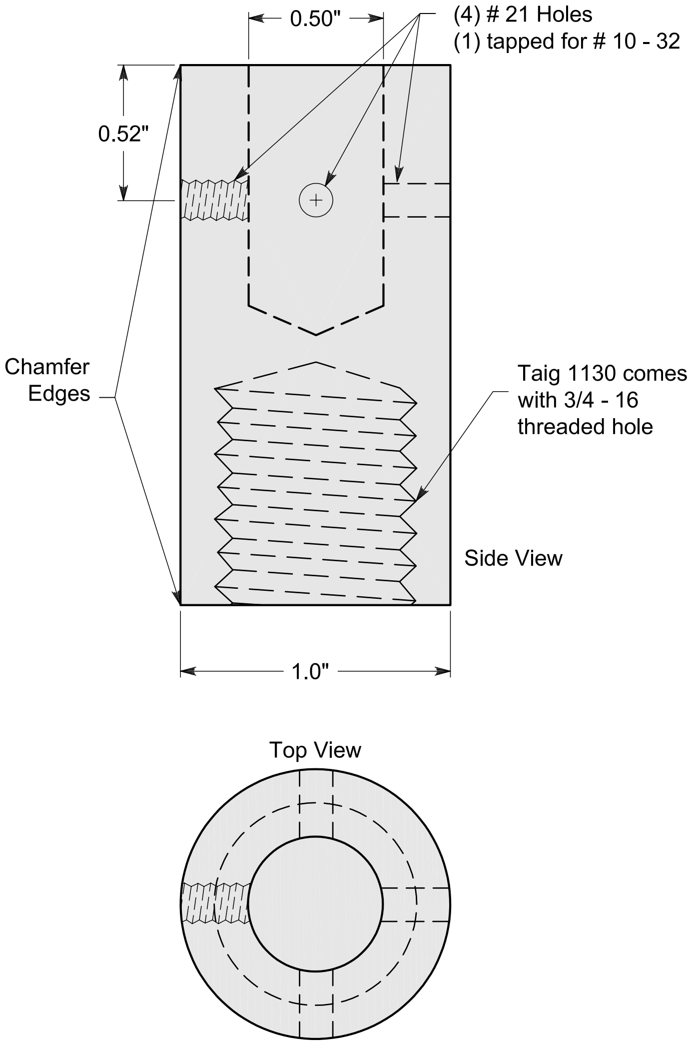

Fig 5—Making a $1/2$-inch end-mill holder out of a Taig 1130 blank arbor.

Fig 6—A photo of the finished knob.

Fig 7—An acrylic plastic knob for lightweight applications.

indentations takes quite a bit of skill. I decided that it would make more sense to use a $5/8$-inch ball end mill and a milling machine to make the holes. This is a bit large for a miniature milling machine; Sherline doesn't sell end-mill holders big enough. I machined a Taig 1130 blank arbor into a $1/2$-inch end-mill holder. It helps to have a large lathe to first drill the hole slightly undersize with a drill bit, and then bore the hole for the end mill precisely to size. Four #21 holes are drilled in pairs, each 0.52 inches from the end opposite the $3/4$-16 threaded hole, as shown in Figure 5. The most accurate pair should be used for the spindle bars. One of the remaining holes can be tapped for the #10-32 setscrew.

I used the mounting holes to attach the plastic to a faceplate, allowing the square plastic to be cut down to a circle on a lathe. I also rounded off the sharp edge into a smooth corner more acceptable to the touch (see Fig 6).

Fig 7 shows a simpler knob designed for applications where lightness is important. If a radio is used for hiking applications, it is important to minimize weight. Except for the #8-32 setscrew, the knob is made entirely out of acrylic plastic. United States Plastic sells acrylic in cubes. It is quite practical to buy a two, three or four-inch-diameter cube to obtain piece of plastic big enough to machine a tuning knob. You could make many knobs out of a four-inch cube!

I first used a band saw to cut a block at least 0.8 inches thick and 1.6 inches in diameter. I then used a lathe to cut it down to a 1.6-inch-diameter cylinder. The front and back faces were turned down, parallel to each other and at right angles to the sides. The 0.250-inch hole for the shaft was drilled at least 0.66 inches deep, but not deep enough to break through the face of the knob. A 0.70-inch diameter hole was bored 0.16 inches deep, for mounting the knob to a three-jaw chuck. This hole also provides clearance for the mounting screw of the 10-turn potentiometer used for tuning.

The acrylic cylinder is now mounted on the three-jaw chuck using the 0.70-inch hole and turned down to 1.51 inches. If the three-jaw is accurate, the cylinder will be concentric with the shaft hole. After removing the chuck from the lathe, it is mounted on a rotary table, for milling. I've had good results using a wiggler to center the knob on the milling machine. The knob is then offset by 0.390 inches to mill the three finger holes with a $5/8$-inch end mill. The holes are 120° apart and 0.300 inches deep. Opposite each hole, drill a #29 hole in the side of the knob for the setscrews. These are 0.30 inches from the back of the knob.

Notes

[1]D. F. Christensen, W8WOJ, "Another Way to Weight Knobs," Hints & Kinks, *QST*, Feb 1987, p 45.

[2]Small Parts Inc, 13980 NW 58th Ct, PO Box 4650, Miami Lakes, FL 33014-0650; tel 800-220-4242, fax 800-423-9009; e-mail **parts@smallparts.com**; **www.smallparts.com**.

[3]**www.use-enco.com**; tel 800-use-enco.

[4]United States Plastic Corp, 1390 Neubrecht Rd, Lima, OH 45801-3196; tel 800-769-1157, 800-854-5498; e-mail **techsupport@usplastic.com**; **www.usplastic.com**. □□

Out of the Box: Product Review

L/C METER IIB FROM ALMOST ALL DIGITAL ELECTRONICS (AADE)

This product review is from Cornell Drentea. He describes the latest version of a test instrument he finds very useful in his receiver, filter design and test work. Cornell can be reached at Cornell Drentea, KW7CD, 757 N Carribean, Tuscon, AZ 85748; **CDrentea@aol.com**—*Contributing Editor, Ray Mack, WD5IFS;* **rmack@arrl.org**

Today, avid experimenters and engineers alike still need to measure small inductors and capacitors despite the ever-promising digital circuits. Until recently, an L/C meter capable of measuring capacitance in the picofarad range and inductance in the nanohenry range was an expensive proposition that only large companies could afford.

Searching the Internet revealed an array of inexpensive kits and products ranging from about $14 to $250. However, none of these products had the needed range of values or accuracy. Then I came across the L/C Meter II B (see Fig 1) from Almost All Digital Electronics (AADE).

The L/C Meter II B is an offshoot of the same company's first product, the L/C Meter first produced in 1988. It has improved accuracy, an update rate that is twice as fast and offers component-matching modes.

Fig 1—The L/C Meter II B from Almost All Digital Electronics (AADE) can measure small value inductors and capacitors to a fraction of a nanohenry or a picofarad.

The L/C II B is very inexpensive considering what it does. It comes either fully assembled for $129.95 or as a kit for $99.95.

Specifications

Measuring Range:
- L: 1 nH to 100 mH
- C: 0.01 pF to 1 µF

Ranging: Automatic
Calibration: Automatic
Accuracy: 1% of reading typical
Display: 16 character intelligent display with four-digit resolution. Data shows in engineering units (ie, µH or pF)

Circuit Design

The L/C Meter II B is cleverly designed despite its simplicity. The genius of the unit is in its microprocessor, a PIC16C622 that does all the frequency counting and the complex mathematics. The manual describes the formulas used in detail. (The schematic and manual are available at **www.aade.com**.) The microprocessor uses a true 32-bit floating-point algorithm and a 2-kB ROM to perform the number crunching, data accuracy and manipulation needed. The program is interrupt-based. The processor uses an 8-MHz crystal clock, which provides the software counter reference frequency as well.

The unit calculates values using the ratio of two subsequent oscillator readings, given by the LM 311 (U1) test oscillator. The results are measured using the precision-counter function provided by the 8-MHz crystal oscillator and the PIC microcomputer. When the CX and LX switches are both in the "out" position, the test oscillator oscillates at F1. When either CX or LX are in the "in" position, the test oscillator oscillates at a new frequency, F2. The microprocessor then calculates the value of the component (CX or LX) that caused the change from F1 to F2. The test oscillator may drift a little after the initial measurement, so it is recommended that the user depresses the LX or CX switches every so often to ensure that it reads the most recent F1 frequency. This ensures continued accuracy.

The test-oscillator frequency range is very wide (20 kHz to 750 kHz). The oscillator is designed to start reliably over this entire range. For small values, the test oscillator runs at about 750 kHz, while for larger values the frequency is decreased by the L/C parts under test to about 20 kHz. The 8-MHz oscillator in my unit was 1800 Hz off from the original values when compared against a Rubidium standard with a long-term accuracy of 1×10^{-12}. However, AADE indicates that the resulting error from this shift is minimal because the two readings compensate each other.

The test oscillator is calibrated first via a relay commanded by the microprocessor, which momentarily inserts a stable, known LC value in the circuit (L1, C2A, C2B). During self-calibration, the unit measures this frequency and inserts it in the computer's formulas. Then, an unknown inductor or capacitor can be measured with accuracy. Because of the self-calibration capability, the exact values of L1 and C1 are not critical (10%). The accuracy is dependent upon C2 which is a 0.5% tolerance capacitor combination. The operator can "zero-out" any stray inductance or capacitance presented by board traces, switches and test leads by pushing the instantaneous zero button just before installing the parts to be tested and making the measurements.

Construction

The unit goes together easily. Some component lead spacings do not match the board layout, but this is not a major problem. One of the 100-kΩ resistors was 90 kΩ (within 10%) and was replaced. This also was not a major discrepancy and would have not prevented the unit from proper operation.

Assembly took about 20 minutes, with most of the time used to determine component values and install the parts on the board. The board has plated-through holes but does not have a printed overlay, so one must refer to the manual drawing for part placement. There is no specific order in which the parts must be installed, and there is plenty of room on the board. If you are like me, you only skim the manual. This did not seem to be a problem. One little problem I encountered was that the in-line switches had to be forced into the board to be installed. This wasn't mentioned in the manual. I recommend exercising care when doing this because the holes may be undersized and switch pins can bend. This may not be true on all boards.

Make sure that the R6 CONTRAST potentiometer is installed on the opposite side of the board from the other parts, otherwise it will be difficult to adjust it from under the display.

If you do everything right, the unit should be ready and operational within 20 minutes. If you experience problems, AADE offers a free "fix it" policy.

Accuracy

The manufacturer and I discussed the accuracy of the L/C Meter II B in great detail. Neil's accuracy claims are based on the published data.

I found the accuracy to be satisfactory, but somewhat elusive when compared with other instruments. Precise measurements of component values are problematic: The method used, temperature and other environmental issues, handling of stray inductance, resistance and capacitance, the test leads and many other factors cause one to wonder which instrument is right.

Even with expensive instruments, variations can be drastic. For instance, Neil indicates that he found component measurements on an HP-4275 and an HP-4276 differed by 1% to 2% for smaller values and as much as 30% for large values. My experience in comparing the L/C Meter II B against my laboratory standard (an HP-4191A impedance analyzer) has been similar, as can be seen from the test readings below. The bottom line is that the L/C Meter II B is as good, or as bad, as any expensive piece of equipment. That makes it a real value at a cost of only $100.

Unlike bridge-type instruments, accuracy of this instrument is time limited. The L/C Meter II B is more accurate when compared with reference standards, but it must be periodically forced to calibrate itself.

Operation

The most accurate measurements obtained with the L/C Meter II B are available right after a self-calibration process as the U1 oscillator can drift with time. The best readings were obtained within a minute after calibration, depending on room temperature. A 30-second update rate was found ideal when measuring very small values. Again, depressing LX or CX periodically is highly recommended for best accuracy. (This information is not in the manual.) The good news is that when the LX or CX switch has been out a while and pressed again, the unit regains accuracy.

It is possible to automate this function, and I discussed the idea with the manufacturer for future improvements. Surprisingly, recalibrating the unit every so often was not annoying. After all, the operator must contribute something to the measurement process.

Tests

A series of tests was performed with the L/C Meter II B against an older L/C Meter II and a laboratory-grade impedance analyzer, the HP-4191A. Several values of LX and CX were measured and averaged over time. The results are shown in Table 1.

Table 1—Test Results

Component	*L/C Meter II B*	*L/C Meter II*	*HP-4191A*
820 pF SM	883 pF	911 pF	845 pF
4.7 pF SM	5.21 pF	5.22 pF	5.5 pF
0.05 µF Poly	0.053 µF	0.054 µF	0.0583 µF
0.100 µH Std	0.103 µH	0.105 µH	0.116 µH

The Bottom Line

The L/C Meter II B is a good instrument for measuring small L/C values down into the nano units. Although the accuracy of the instrument is not unconditional, it is good enough for the first minute or so. Tests indicate good "traceability" down to 100 nH and 5 pF as shown in Table 1. This is remarkable at $100, if one considers that even the much more expensive units exhibit similar behavior. The L/C Meter II B is a very good value for the experimenter or the engineer who needs a reliable, accurate instrument.

Many thanks go to Robert Gillette, AC7OT, for doing the laboratory comparison tests. Additional thanks go to Randy Burcham, KD7KEQ, for donating his LC Meter II for the duration of the tests.

Manufacturer: Almost All Digital Electronics (AADE). 1412 Elm Street SE, Auburn, WA 98092; tel 253-351-9316; **www.aade.com**. L/C Meter II B: $99.95 kit, $129.95 assembled. □□

Letters to the Editor

A Homebrew Shaft Encoder (Mar/Apr 2002)

I just received the latest *QEX* and the article on optical encoders peaked my interest. Discarded computer mice can be used to get many of these parts (electrical and mechanical), and using surplus equipment is a subject I am trying to explore.

Consumer electronics are at a point that almost prevents repair, as new devices are available at such reasonable prices. An example: An "off-brand" stereo VCR with remote is $49, *brand new from a local grocery store*! A new video head would cost about $20 wholesale, plus installation; just labor at $45/hour shows its repair would not be cost effective. Broken, it is landfill fodder. What can we do with an old VCR? Lop off the line cord and pitch the rest?

Well, the tuner will receive from channel two through the cable channels and the detected audio runs through a pre-amp, producing "hi-fi" output. An LM380 amplifier and a method of tuning will make this a VHF/UHF receiver, or maybe an IF for a microwave receiver. If you have ever wanted to play with IR emitter-detector pairs, here's a free set—and a power supply, motors, switches, springs, screws and line cord.

Here's a stretch: Try a packet terminal from a text pager. What about high-voltage and microwave components from a discarded microwave oven, or re-using a TV antenna as a log-periodic antenna (which it already is!) for VHF and UHF amateur bands? Isn't that stealthy, too? And what about putting cordless phones or FRS H-Ts on 900-MHz? Do you have any discarded amplified PC speakers? Those make great AF modules for homebrew receiver projects.

There are many applications for consumer junk and I would like to volunteer to be a clearinghouse for those ideas. I will submit them for publication to *QEX* if there is any interest. Please send me any ideas, rough drafts or sketches on napkins, and I will attempt to get them in shape to be published.—*Matt Kastigar, NØEU, 28 Woodcrest Dr, Saint Louis, MO 63124-1468;* **mk2331@sbc.com**

About Monopoles and Dipoles (Mar/Apr 2002)

Tino Trainotti, LU1ACM, has written an authoritative article on vertical monopole and dipole antennas. He begins his article by showing us sketches of Hertz's (mislabeled Marconi's) dipole and spark transmitter (1887) and Marconi's monopole and spark transmitter (1896). These were untuned spark transmitters, in which the spark gap was placed directly across the antenna terminals.

Marconi's receiver, which is not discussed by LU1ACM, comprised an identical antenna with a connection to ground through a *coherer* (pronounced "co-hear-er"—*Ed.*). A coherer is a curious device: a small tube of metallic/carbon filings that lightly contact the end plugs. When shaken, this device exhibited a high resistance. Were the device subject to a voltage impulse, the filings would become "oriented" and the coherer would exhibit a low resistance. The change from high to low resistance can be detected as a click in a pair of earphones; or with a relay and a battery in the circuit, the received impulse can put a mark on an *inker* tape. The coherer then had to be tapped so that it exhibited a high resistance again, ready to receive the next voltage impulse (see Fig 1). This untuned transmitter-receiver system has been referred to as a *plain aerial system*. It is interesting to consider how this transmitter-receiver system might have worked.

First, I will review how a spark transmitter works. Early spark transmitters comprised a battery in the low-voltage circuit of a step-up transformer and an *interrupter*. When the Morse key was closed, ac current pulses at a frequency determined by the characteristics of the interrupter flowed in the primary circuit. These low-voltage impulses were stepped up to a very high voltage (5-10 kV) by the induction transformer. This high, ac-like voltage charged a "discharge capacitor." In the case of the plain aerial transmitter, this capacitor was the capacitance of the aerial system. When the voltage across the capacitor reached a potential sufficient to break down the air gap of the spark terminals, a spark was generated. This spark then connected one terminal of the discharge capacitor to ground, and the charge on the capacitor kick-started the antenna system into oscillation.[1] With the spark terminals directly connected to the terminals of the antenna, the signal radiated was determined by the $\lambda/4$ resonance response of the aerial. When the spark ceased, the aerial was connected to ground through a very high inductive reactance, so the aerial was then tuned to a very much lower frequency. The transmitted damped wave died away very quickly because the discharge capacitor was small (the capacity of the aerial system), and so the stored energy was small.

Now, let's consider the receiver. It employed an identical antenna connected to ground through a very high resistance. While waiting to receive a signal, the receiver was therefore in effect "tuned" to the $\lambda/2$ resonance response of the aerial system. This was not a very satisfactory arrangement. Unbeknownst to Marconi, his transmitter and receiver were tuned to different frequencies. If the transmit frequency were f, the receiver was in effect tuned to a frequency equal to $2f$. In spite of the rudimentary state of development in 1896, Marconi succeeded in signaling a series of tests on the Salisbury Plain over a distance of 2.8 km.

The possibility of long-distance communications should be credited to Nicola Tesla. He devised a much-improved spark transmitter (and receiver) system. His discharge capacitor and spark gap were in a primary (oscillatory) circuit, with a low inductance and a high capacitance. The capacitance of this discharge capacitor could be very large compared with the capacitance of the aerial; hence the stored energy was enormously greater. The oscillatory energy generated in this primary circuit when the spark fired was inductively coupled to the aerial circuit. The frequency response of this coupled system was determined largely by the self-impedance characteristics of the antenna, which, in effect, was base-loaded by the inductive reactance of the secondary of this oscillation/aerial transformer. In addition, since the primary circuit was tuned by changing the value of the discharge capacitor to achieve maximum aerial current. The frequency response of the coupled system was similar to that of two resonant circuits tuned to the same frequency and coupled together. There was an important difference when the spark ceased. Since the aerial was now connected to ground by the secondary of this oscillatory/aerial transformer, the induced oscillations could continue at the frequency to which the antenna system was tuned. The receiver also employed a transformer, both primary and secondary circuits were tuned and his system employed grounded antenna systems. Tesla demonstrated his wireless transmitting and receiving systems before learned audiences in 1893. His lecture notes were widely published and he patented his method of tuning in 1897.

Marconi, in later follow-on experiments, adapted the Tesla circuit for his purposes, and patented his version (as was his custom): his so-called master-tuning patent. Marconi's

1900 (English) patent was initially rejected in 1904 by reason of prior art (that of Lodge but principally of Tesla). His re-issued US patent was issued after extended litigation and finally decided by the US Supreme Court in 1943 in Tesla's favor.

Unlike Tesla and Fessenden who were real inventors, Marconi was an experimenter who tried the ideas of others, adapted the circuitry to suit his needs and patented his versions. Marconi, who had worked under Righi, had a keen eye for commercial opportunity and realized that there was a market for such telegraphic systems. It is curious that the grounded monopole antenna is often called a Marconi antenna, since Marconi did not invent the grounded antenna. Mahlon Loomis, fifteen years before Hertz, used grounded antennas to signal between two mountain peaks in Virginia; and Dolbear, Edison and Popoff used grounded antennas before Marconi.

Marconi is particularly remembered today (and just recently celebrated in December 2001) for his first transatlantic experiment on 12 December 1901. Then he claimed to have heard a signal (the Morse letter "S") on Signal Hill, New Foundland, from a sender (a curious two-stage spark transmitter) at Poldhu, Cornwall. Yet even at the time of his so-called greatest triumph there were those who said[2]—indeed there are some who still say,[3, 4] based on technical and scientific reasoning—that he misled himself and the world into believing that atmospheric noise (spherics and possibly electrostatic discharge signals generated by his bobbing antenna above Signal Hill) was in fact the Morse letter "S." Nonetheless, his claim caught the attention of the world, started a debate that continues today and prompted scientists to try and explain how this could be possible. That led to the suggestion in 1902 by Arthur Kennelly, in the USA, and Oliver Heaviside, in England, for a high altitude conducting layer (the ionosphere).—*John S. (Jack) Belrose, VE2CV, ARRL TA, 17 rue de Tadoussac, Aylmer, QC J9J 1G1, Canada;* **john.belrose@crc.ca**

References

1. J. S. Belrose, "The Sounds of a Spark Transmitter: Telegraphy and Telephony", 22 December 1994. Available online at **www.hammondmuseumofradio.org/spark.html**. See also **www.ieee.ca/millennium/radio/radio_about.html**.
2. R. A. Fessenden, "A Regular Wireless Telegraphic Service between America and Europe," *The Electrician* (London), 22 November 1907, pp 200-203.
3. J. A. Ratcliffe, "Scientists' reactions to Marconi's transatlantic radio experiments," *Proceedings of the IEE*, Vol 121, No. 9, 1974, pp 1033-1038.
4. J. S. Belrose, "A Radioscientist's Reaction to Marconi's first Transatlantic Wireless Experiment—Revisited," IEEE AP-S/URSI Meeting, Boston, Massachusetts, 8-13 July 2001.

The author responds:

I learned a lot of history from Jack and other fellows because I am interested in this matter too, especially about the experiments that were carried out in the first part of the last century. As everybody knows, Marconi was a dilettante (read amateur) and a businessman, not an academic; but he deserves the fame he reached because he created a communications empire with the help of many technicians and scientists and of course with money invested by his mother's family. As is the case today, businesspersons bring about important things using somebody else's cash. Were that not true, technical development would lag. Of course, investors are not bucking for promotions but intend to get a return on their investment. This is part of history and it is difficult to change.

I support Jack in his effort to point out the relative merits [of certain details], but unfortunately, those things are unimportant to common people. It is only important to us as amateurs, since we are not in business but are doing what we like and sharing information freely with other amateurs. Jack's comments are welcome because he has been delving into these matters for a long time. All our enthusiastic colleagues will welcome them as well, I am sure.—*Best regards, Tino Trainotti, LU1ACM;* **vtrainotti@citefa.gov.ar**

[Editor's note: We didn't make de-

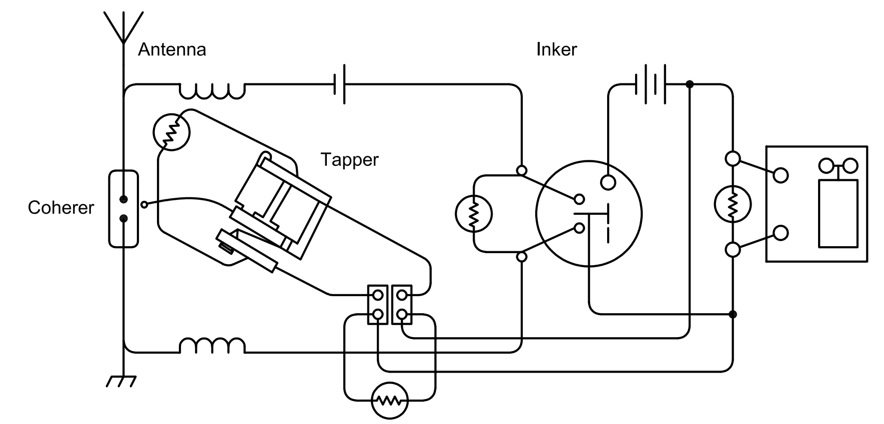

Fig 1—Marconi's plain aerial "tapper-back" coherer receiver and inking printer.

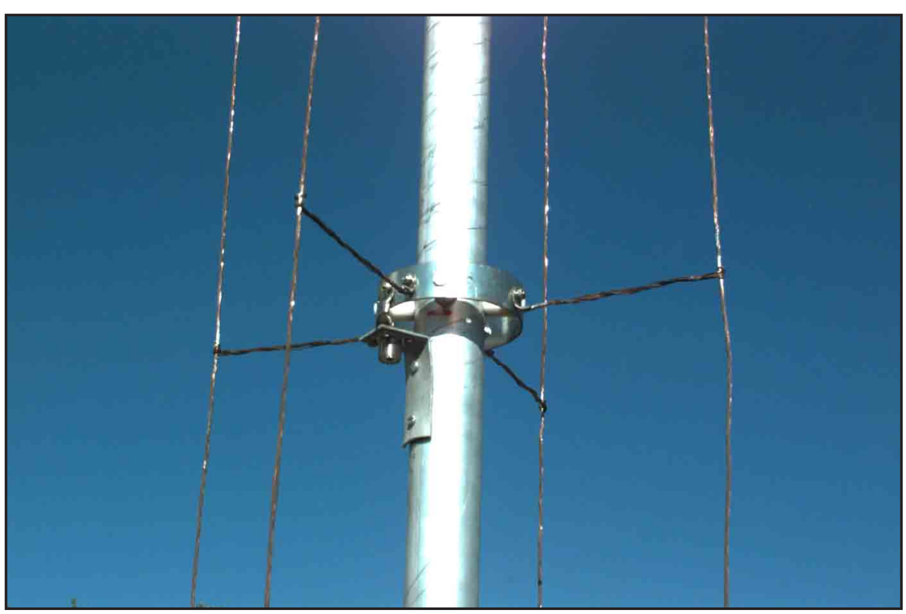

Fig 2—Details of LU1ACM's 15-meter grounded vertical dipole feedpoint.

Fig 3—Details of LU1ACM's 6-meter grounded vertical dipole feedpoint

tails of the feed-point connections of Tino's grounded dipole very clear in the last issue. The author graciously provides the needed amplification below—Doug Smith, KF6DX]

Dear Doug:

I include photos of the feed-point connections to my 15-meter (Fig 2) and 6-meter (Fig 3) vertical dipoles.

An SO-239 connector is attached at the supporting aluminum pipe with an aluminum angle bracket. The "hot" point is connected to a brass ring that runs all around the supporting pipe and is insulated with Teflon insulators. From this ring, three or four wires (depending of the number of wires in the skirt) connect to the skirt wires—and that is all!

We must be careful with the connector because if a drop of water gets between the hot and ground, the antenna impedance changes accordingly and SWR increases dramatically. Coaxial line can be attached along the supporting tube or can be put inside it.—*73, Tino* □□

Out of the Box: Book Review

THE FRIENDLY IONOSPHERE

by Crawford MacKeand WA3ZKZ/VP8CMY

Published by Tyndar Press, PO Box 236, Montchanin, DE 19710; ***www.geocities.com/tyndar_press/index.html****. First edition, paperback 6×9 inches, 126 pages with 35+ illustrations, bibliography, index. ISBN: 0-9659066-5-5 $14.95 + $3 shipping.*

This book has two sections. The first is a reasonably terse scientific description of how and why the ionosphere aids propagation at various frequencies. It deals with noise sources and the mechanisms of ionospheric reflection. The author provides both figures and mathematics to describe the physics. He also provides very comprehensive lists of references to more detailed work at the end of each chapter.

In the second section, the author describes models and experiments to prove or disprove that Marconi was actually able to span the Atlantic in 1901. He also presents a detailed analysis of the airborne and shipboard equipment used during Amelia Earhart's attempt to circle the globe. He presents data that supports the conclusion that she actually came very close to Howland Island before disappearing.

My interests don't include the detailed physical analysis of wave mechanics, but I found the historical aspects quite interesting.—*Contributing Editor, Ray Mack, WD5IFS;* **rmack@arrl.org** □□

Next Issue in QEX/Communications Quarterly

With the July/August 2002 issue, we begin another detailed look into digital transceiver design, including so-called software-defined radios (SDRs). We have several series in the works that focus on modern hardware and software design techniques. Each one is based on its author's working prototype.

Editor Doug Smith, KF6DX, has some observations on receiver dynamic range, how it is measured and some suggestions for improving measurement accuracy. He begins with theoretical considerations and follows with some practical solutions.

□□